Cardiovascular magnetic resonance imaging in patients with chronic heart failure

by

Lingyu Xu

A thesis submitted in partial fulfillment of the requirements for the degree of

Doctor of Philosophy

Department of Medicine
University of Alberta

Abstract

Heart failure (HF) is a progressive and complex syndrome with poor prognosis, characterized by a wide array of cardiac structural and functional abnormalities. Patients are typically categorized according to left ventricular ejection fraction (LVEF), with reduced ejection fraction defined as LVEF<40% (HFrEF), mid-range LVEF in the span of 40%-49% (HFmrEF) and those with heart failure with preserved LVEF≥50% (HFpEF). Since LVEF has poor prognostic value in patients with HF and presents unsatisfactory diagnostic value in patients with HFpEF, more insightful imaging biomarkers have been intensively investigated. Global longitudinal strain (GLS) conventionally measured at the endocardium has been shown to be superior to LVEF in distinguishing patients with HFpEF patients from healthy subjects and predicting adverse outcomes in patients with acute HF. However, the potential incremental value of layer-specific strain has not been investigated in patients with HF.

As HF tends to be progressive, cardiac imaging is a common surveillance strategy for patients with chronic HF and LVEF still the predominant biomarker of interest that physicians pay attention to in serial testing. Prior imaging studies of HF have often been limited to single time-points. In particular, there is a lack of literature evaluating the temporal changes in cardiac structure and function and their clinical relevance in patients with chronic HF. Notably, patients with chronic stable HF generally have a progressive course with high morbidity and mortality. Thus far, no study has investigated longitudinal cardiac changes in patients with stable HF.

While there have been advances in the treatment of HF, overall prognosis remains poor. Earlier identification of HF patients with higher risk to develop long-term adverse outcome helps physicians initiate, intensify and adjust the management strategy. The majority of the validated risk predicting models predominantly focus on clinical information including demographics,

disease history and risk factors. As cardiac imaging plays an essential role in evaluating patients with HF, it is important to incorporate valuable imaging biomarkers in the risk predicting model. To our knowledge, there has been no validated imaging predictive model in patients with HF.

Cardiac magnetic resonance (CMR) is the gold standard for non-invasive cardiac measures. Its high accuracy and reproducibility make CMR well suited for delineating epi- and endomyocardial border in order to analyze layer-specific strains, and identify temporal changes during serial testing. Furthermore, it enables us to comprehensively collect state-of-the-art information on cardiac function, volume and tissue characterization as a one-stop test.

Our studies aim to utilize CMR in patients with chronic heart failure to: 1) investigate the diagnostic and prognostic value of CMR-derived layer-specific strain; 2) evaluate the prevalence and prognostic significance of serial changes in cardiac structure and function ; 3) develop and validate comprehensive predictive models incorporating clinical and imaging data.

Preface

This thesis is an original work by Lingyu Xu. The research projects, included in this thesis, received research ethics approval from the University of Alberta and University of Calgary Research Ethics Board, Project Name "The Alberta Heart Failure Etiology and Analysis Research Team (HEART) study" which was a clinical trial with registered No. ClinicalTrials.gov NCT02052804; another dataset "Cardiac Remodeling Study" received research ethics approval from the University of Alberta, ethics NO. MS7_Pro00032356.

This work is dedicated to

My lovely parents Guoping Xu and Minhua Xu, who have dedicated every effort to loving me, educating me, helping me and cultivating me into an independent, persistent, hard-working and optimistic person which is necessary for me to love my life, enjoy the learning, and facing and addressing the challenges and difficulties in this Ph.D program.

My wonderful brother, Yuancheng Xu, who has provided substantial mental and emotional support throughout long nights of research.

My beloved daughter, Zihui (Gloria) Guo, who is a sweet heart and gives me remarkable happiness and greatly softens my anxiety and worry during this Ph.D training.

Thank you all

Acknowledgment

I would like to express my sincere gratitude to my supervisors **Dr. Ian Paterson and Dr. Richard Thompson** for their understanding, encouragement, inspiration and remarkable support throughout my Ph.D program. Their guidance has helped me in all aspects of research, including but not limited to identifying knowledge gaps, study design, image analyses, inspiration in the data analysis and drafting manuscripts.

I would like to thank my thesis committee member **Dr. Craig Butler** for his guidance and inspiration in the field of cardiac CT imaging.

I would like to thank **Drs. Ian Paterson, Richard Thompson** and **Craig Butler** who generously supported me to participate in national and international conferences to allow me to disseminate research results, expand my knowledge and interact with like-minded colleagues nationally and internationally.

I would like to thank my examining committee members **Drs. Norris and Connelly** for their insightful comments and constructive feedbacks on this thesis.

My appreciation is extended to Dr. Justin Ezekowitz for his substantial guidance and teaching on study design and manuscript writing.

My appreciation is also extended to Alberta HEART study team and its sponsor Alberta Innovates Health Solutions which allowed the collection of high-quality data forming the foundation of my thesis work.

I would also like to thank my fellow lab mates Justin Grenier for his technical help.

I would also like to thank my best friend and colleague Stanislau Hrybouski for providing tremendous technical support, encouragement and inspiration in the projects related to cardiac CT for coronary artery disease.

I would also like to thank the Sino-Li-Kashing Foundation Scholarship for allowing me to pursue my Ph.D degree at the University of Alberta.

I would like to thank graduate student association (GSA), Faculty of Graduate Studies and Research (FGSR) in University of Alberta and Canadian Institutes of Health Research (CIHR) for generously providing me travel awards for the national and international conferences.

Finally, I would also like to thank all the academic and non-academic support staff in the departments of medicine and biomedical engineering at the University of Alberta.

Thank you all

Table of contents

List of Tables

List of Figures

List of Abbreviation and Symbols

HFpEF: heart failure with preserved ejection fraction; HFmrEF: heart failure with midrange ejection fraction; HFrEF: heart failure with reduced ejection fraction; CMR: cardiovascular magnetic resonance imaging; bSSFP: balanced steady state free precession; TR: repetition time; TE: echo time; LGE: late gadolinium enhancement; BMI: body mass index; BP: blood pressure; NYHA: New York Heart Association Classification; HTN: hypertension; CAD: coronary heart disease; Af/AFL: atrial fibrillation/flutter; DM: diabetes mellitus; COPD: chronic obstructive pulmonary disease; CKD: chronic kidney disease; ACEI: Angiotensin converting enzyme inhibitor; ARB: Angiotensin II receptor blocker; NT-proBNP: N-terminal pro b-type natriuretic peptide; L(R)VEF: left(right) ventricular ejection fraction; L(R)VEDVi: left(right) ventricular end-diastolic volume indexed to ideal body surface area; L(R)VESVi: left(right) ventricular end-systolic volume indexed to ideal body surface area; LVMassi: left ventricular mass indexed to ideal body surface area; RWT: relative wall thickness; GLS_EPI: epicardial global longitudinal strain; GLS_AVE: average global longitudinal strain; GLS_ENDO: endocardial global longitudinal strain; GCS_EPI: epicardial global circumferential strain; GCS_AVE: average global circumferential strain; GCS_ENDO: endocardial global circumferential strain; GRS: global radial strain; AIC: Akaike information Criterion. NA: not applicable; MRA: mineralocorticoid antagonist; CV: cardiovascular; ED: emergency department; MAGGIC: Meta-Analysis Global Group in Chronic Heart Failure. ICD: International Classification of Diseases codes version; MNIScar: major non-ischemic scar. NRI: net reclassification improvement.

Chapter 1: Introduction

1.1 Heart failure: definition, classification, and stages

Heart failure (HF) is a complex and progressive clinical syndrome characterized by cardiac structural and functional abnormalities,[1, 2] and results either indirectly from deleterious changes to the cardiovascular system or directly from cardiomyopathic processeses.[3, 4] Clinical manifestations of HF include symptoms related to: (i) low cardiac output such as ,fatigue, and/or exercise intolerance and (ii) fluid retention such as dyspnea and/or peripheral edema. HF significantly decreases health-related quality of life, especially in the areas of physical functioning and vitality.[5]

The classification of HF is most commonly based on left ventricular ejection fraction (LVEF) including HF with preserved EF (HFpEF, LVEF ≥ 50%), HF with middle-range EF (HFmrEF, LVEF 41%-49%) and HF with reduced EF (HFrEF, LVEF ≤ 40%), respectively (Table 1.1).[2, 6] LVEF is the most widely a used imaging parameters for cardiac function and is linked to clinical demographics, comorbid conditions, and dictates response to therapies. Additionally, most clinical trials of HF select patients based on LVEF. HFrEF comprises approximately half of patients with HF and its structure is characterized by LV enlargement and ventricular wall thinning. HFpEF comprises up to 50% of HF patients, and is characterized by increased wall thickness, left atrium enlargement and diastolic dysfunction. In the GWTG-HF (Get with The Guidelines–Heart Failure) study of 39,982 patients admitted for HF, 46% had HFpEF, 8.2% had HFmrEF, and 46% had HFrEF.[7] Patients with HFpEF tend to be older and female with higher incidence of hypertension, diabetes mellitus, obesity, hyperlipidemia and atrial fibrillation. Patients with HFmrEF manifest clinical phenotypes of HFrEF or HFpEF however the prognosis resembles patients with HFpEF [8, 9].

Table 1.1 Definition of heart failure with preserved (HFpEF), mid-range (HFmrEF) and reduced ejection fraction (HFrEF) (2016 ESC Guidelines for the diagnosis and treatment of acute and chronic heart failure)[6]

Type of HF		HFrEF	HFmrEF	HFpEF
CRITERIA	1	Symptoms ± Signs[a]	Symptoms ± Signs[a]	Symptoms ± Signs[a]
	2	LVEF <40%	LVEF 40–49%	LVEF ≥50%
	3	–	1. Elevated levels of natriuretic peptides[b]; 2. At least one additional criterion: a. relevant structural heart disease (LVH and/or LAE), b. diastolic dysfunction (for details see Section 4.3.2).	1. Elevated levels of natriuretic peptides[b]; 2. At least one additional criterion: a. relevant structural heart disease (LVH and/or LAE), b. diastolic dysfunction (for details see Section 4.3.2).

BNP = B-type natriuretic peptide; HF = heart failure; HFmrEF = heart failure with mid-range ejection fraction; HFpEF = heart failure with preserved ejection fraction; HFrEF = heart failure with reduced ejection fraction; LAE = left atrial enlargement; LVEF = left ventricular ejection fraction; LVH = left ventricular hypertrophy; NT-proBNP = N-terminal pro-B type natriuretic peptide.

[a]Signs may not be present in the early stages of HF (especially in HFpEF) and in patients treated with diuretics.

[b]BNP.35 pg/ml and/or NT-proBNP.125 pg/mL.

Heart Failure is graded clinically according to the ACC/AHA HF stages and the New York Heart Association (NYHA) functional classification.[1] The former consists of four stages, including patients at risk for HF (Stage A), those with asymptomatic structural heart disease (Stage B); symptomatic HF (Stage C) and refractory HF (Stage D) (Table 1.2). Therefore, it not only emphasizes the development and progression of disease, but also emphasizes tailored management within each stage, including modifying cardiovascular risk factors at Stage A, treating structural heart disease or reversing cardiac remodeling at Stage B, and pharmacologic and non-pharmacologic therapies to improve symptoms and prognosis at Stage C and Stage D. The NYHA classification is based on exercise capacity relative to usual daily activities. (Table 1.2).

Table 1.2. Comparison of ACCF/AHA Stages of HF and NYHA Functional Classifications. From 2013 ACC/AHA Guideline for the Management of Heart Failure.[1]

ACCF/AHA Stages of HF[38]		NYHA Functional Classification[46]	
A	At high risk for HF but without structural heart disease or symptoms of HF	None	
B	Structural heart disease but without signs or symptoms of HF	I	No limitation of physical activity. Ordinary physical activity does not cause symptoms of HF.
C	Structural heart disease with prior or current symptoms of HF	I	No limitation of physical activity. Ordinary physical activity does not cause symptoms of HF.
		II	Slight limitation of physical activity. Comfortable at rest, but ordinary physical activity results in symptoms of HF.
		III	Marked limitation of physical activity. Comfortable at rest, but less than ordinary activity causes symptoms of HF.
		IV	Unable to carry on any physical activity without symptoms of HF, or symptoms of HF at rest.
D	Refractory HF requiring specialized interventions	IV	Unable to carry on any physical activity without symptoms of HF, or symptoms of HF at rest.

ACCF/ACCF indicates American College of Cardiology Foundation; AHA, American Heart Association; HF, heart failure; and NYHA, New York Heart Association.

1.2 Heart failure: epidemiology and prognosis

HF has become a significant public health issue in Canada and worldwide. HF affects an estimated 600,000 Canadians[10] and 26 million worldwide, with an estimated incidence of 1% at age 65 that approximately doubles with each decade of age thereafter.[11] Annual costs related with the management of HF have been estimated at $2.8 billion in Canada, $31 billion in the United States in 2012 with a projected increase to $70 billion in 2030.[5, 10]

Previous studies showed a 23.6 % mortality for acute HF and a 6.4% mortality for chronic HF at 1-year follow-up,[12] as well as a 19.9% and 75% mortality rate of chronic HF in a 2-year follow up and a 5-year follow up. [7, 13] A combined endpoint of mortality or HF hospitalisation within 1 year were 36 % for acute HF and 14.5 % for chronic HF.[12]

HF is a major cause of morbidity and mortality, frequent emergency room visits, and hospitalization, especially in older adults.[10] It also causes physical and emotional exhaustion in patients, an overwhelming psychological and physical burden for caregivers, and a huge financial burden for both family and the health care system.

The prognosis of HF is improving but still remains poor. Notably, HFrEF has favorable therapeutic responses to a number of pharmacotherapies including angiotensin converting

enzyme inhibitors (ACEI),[14, 15] angiotensin receptor blockers (ARB),[14, 16] β-blockades,[15, 17], mineralocorticoid antagonists and the combination of hydralazine and nitrates.[18] The application of cardiac resynchronization therapy (CRT) and implantable cardioverter-defibrillator (ICD) in advanced stage HF also improve the clinical outcome.[19] But HFrEF still has similar or slightly worse prognosis than patients with HFpEF in terms of mortality and rehospitalizations.[20, 21] The incidence of HFpEF is increasing, in part due to standardization of diagnosis, however the prognosis remains unchanged.[22] Patients with HFpEF or HFmrEF have no proven medical therapies.[7, 15, 23, 24].

Consequently, the identification of patients with early stage HF would potentially allow treatment intensification and improved health outcomes.

1.3 Heart failure: Challenges in diagnosis

The poor prognosis of HF results from ongoing challenges in early diagnosis, and management, the impact of multiple co-morbidities, and difficulties of treating the underlying etiological disease.

For diagnosis of HF, no single diagnostic test can be used for HF because it is syndrome based on a careful history and physical examination according to the Framingham or Boston criteria.[25, 26] The difficulties of early diagnosis are due to the absence of symptoms, presence of nonspecific symptoms and a lack of sensitive and specific biomarkers of HF and/or cardiac dysfunction. As HF is progressive, the delayed diagnosis potentially yields more adverse cardiac remodeling and results in worse outcome.

The evaluation of HF progression is also challenging since there is no established sensitive biomarkers for serial assessment during ambulatory follow-up visits or re-admissions to hospitals. Failure to identify disease progression prevents physicians from initiating or adjusting effective management strategies.

Co-morbidities contribute significantly to the rising HF prevalence[27] and increasing difficulties with management, with more patients characterized as older, taking more medication, having a higher burden of comorbid coronary artery disease, hypertension, diabetes mellitus, renal dysfunction, and/or chronic obstructive pulmonary disease.[28, 29] This substantially increases the complexity and difficulty with treatment, as well as the adverse effects of polypharmacy.

1.4 Cardiac imaging modalities in HF

Most patients with HF have symptoms due to impaired left ventricular (LV) function. However, it should be emphasized that several possible structural or functional reasons may exist before the development of HF and the phenotypes may range from patients with normal LV size and preserved LVEF to those with severe dilatation and/or markedly reduced EF. In most patients, abnormalities of systolic and diastolic dysfunction coexist, irrespective of EF.[1]

Cardiac imaging, as a non-invasive strategy, is a growing component of the provision of medical care for individuals with HF and plays an important role in diagnosis, monitoring and prognosis of patients with HF. Echocardiography is widely used due to availability, low cost and diagnostic quality. Echocardiography is still the foundational imaging technique in the investigation of HF. However, its relatively low resolution, acoustic window restriction, reliance on geometric assumption and operator dependence limit its performance (Figure 1.1).[30] Other cardiac imaging modalities are increasingly considered essential because of their utility in identifying underlying causes, risk stratification, and selection of therapies. In patients with HF, nuclear imaging is mainly used to assesses myocardial perfusion and viability to identify an ischemic etiology.[31] However the limited scopes of application and radiation exposure greatly limit its widespread use. In cases of heart failure, cardiac computed tomography (CT) is mainly used to assess the major coronary arteries for stenosis and calcification. [32]

Cardiac magnetic resonance imaging (CMR) provides comprehensive and state-of-the-art information on cardiac structure, function, tissue characterization and metabolism. Similar to echocardiography, it evaluates the presence and the severity of cardiac morphological and functional abnormalities. However, it is considered the gold standard imaging modality due to high reproducibility. Importantly, the relatively high temporal and spatial resolution of CMR acquisition and the volumetric evaluation without geometric assumptions provide precise measurements of cardiac anatomy and function (Figure 1.1). Thus, CMR enables clinicians to differentiate normal from pathological. For example, CMR has been shown to be more sensitive and accurate in the evaluation of cardiac remodeling due to mitral regurgitation.[33] Similarly, the right ventricle (RV) has a complex shape and its echocardiographic evaluation is limited due to restricted acoustic windows especially in obese subjects or patients with chronic obstructive pulmonary disease. CMR provides effective and precise measurements of RV function and

volume due to its high resolution and anatomical, volumetric imaging. Furthermore, CMR provides detailed information regarding the underlying HF etiology. Notably, CMR qualitatively and quantitatively evaluates myocardial tissue characteristics such as ischemic and non-ischemic fibrosis on late gadolinium enhancement imaging and T1 and T2 mapping to identify inflammation, T2* mapping for iron overload. In many cases, CMR provides definitive diagnostic information.[34] Therefore, CMR can capture comprehensive information on cardiac geometry as well as potential myocardial pathology. Moreover, the absence of ionizing radiation eliminates CMR testing without ionization exposure related damage, especially for the longitudinal assessment of HF progression or response to therapy. Last but not least, the high reproducibility of CMR examination makes CMR well suited for longitudinal monitoring of specific cardiac functional or structural parameters and decreases the sample size of patients required to achieve expected significance in clinical studies.

For prognosis, tissue characteristics derived from CMR provides unique and robust prognostic value. For instance, myocardial scar is an independent predictor of major adverse outcomes in patients with heart failure,[35, 36] myocardial infarction,[37] severe aortic stenosis,[38] Chronic Chagas Cardiomyopathy,[39] older adults,[40] and atrial fibrillation[41] Extracellular volume and native T1 mapping derived from CMR also predicts outcome in patients with HF.[42-44] Strain derived by echo and CMR have each been shown to predict outcome in cardiovascular disease.[45, 46] However, as CMR image has much higher resolution images than echocardiography, CMR is capable to delineate endocardial boarder and epicardial boarder more accurately and therefore is more suitable to measure feature tracking lay-specific strain.

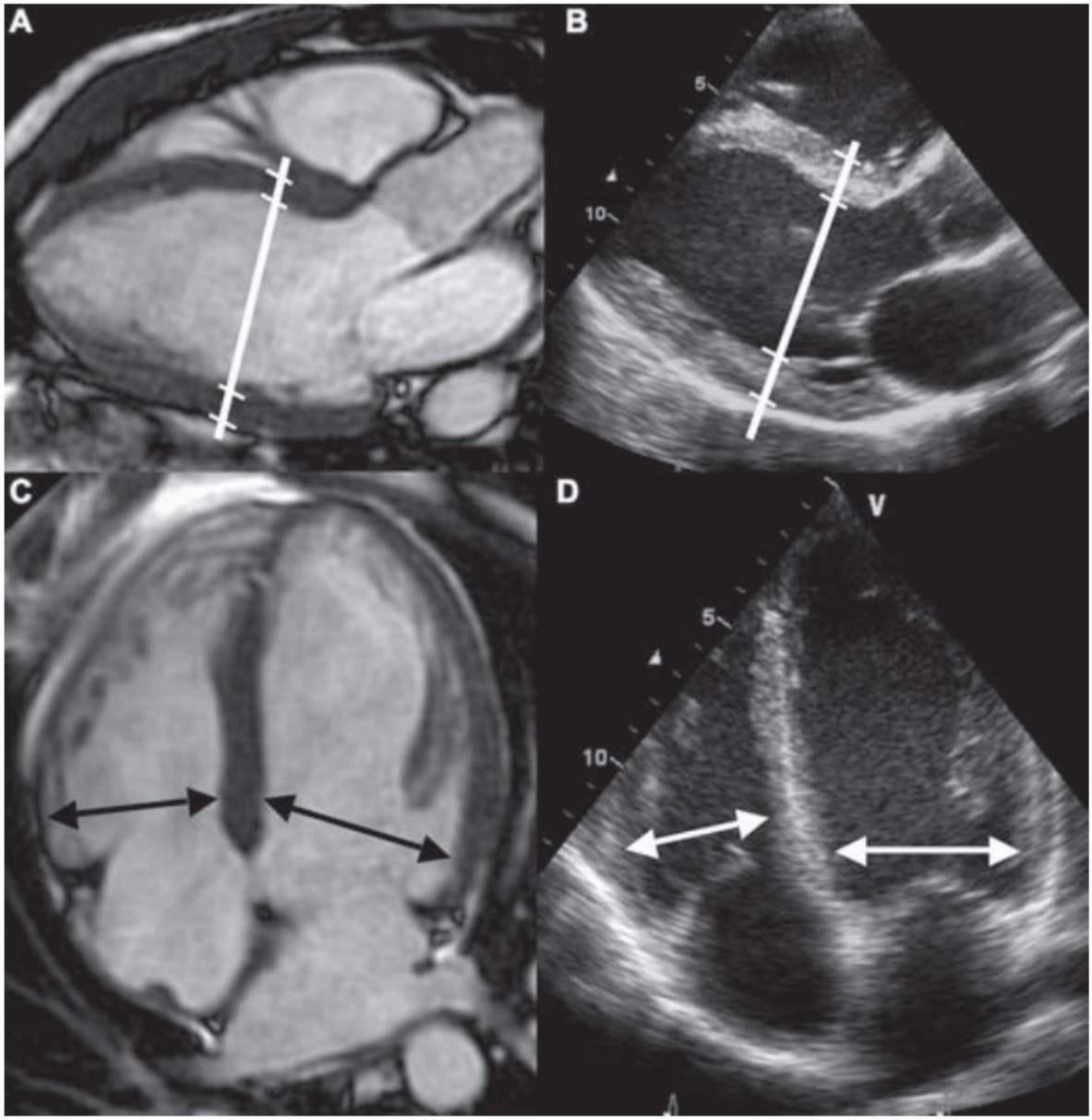

Figure 1.1 Illustrative case on methodology and intertechnique difference of cardiac measurements in an elite athletic male. Cardiac MRI: septal and wall thickness 11 mm; left ventricle (LV) long-axis internal diameter at end-diastole 66 mm; LV posterior wall thickness 12 mm; LV inflow tract diameter at end-diastole 62 mm; right ventricle (RV) inflow tract diameter at end-diastole 53 mm and echocardiography: septal and wall thickness 13 mm; LV long-axis internal diameter at end-diastole 54 mm; LV posterior wall thickness 12 mm; LV inflow tract diameter at end-diastole 49 mm; RV inflow tract diameter at end-diastole 40 mm, from Prakken et al Br J Sports Med 2012[47].

1.5 Cardiac imaging strategies for disease detection and monitoring in HF

As previously mentioned, despite ongoing advances, HF continues to be a challenging syndrome with a poor prognosis. Beyond medical history and physical examination, cardiac imaging plays a tremendously important role in the diagnosis, disease monitoring and prediction of clinical outcome. However, there are still important knowledge gaps that have not yet been addressed.

1.5.1 Imaging strategies for measuring systolic function

Many studies have investigated the diagnostic and prognostic performance of cardiac imaging in patients with HF. LVEF is the percentage change of the left ventricular volume from left ventricular end-diastole to end-systole. It is the most conventional measure of the left ventricular systolic function in routine clinical care used to evaluate cardiac function. It is also the most commonly used imaging parameter in follow-up assessments identifying disease progression or regression; LVEF is widely used to subgroups HF patients into HFpEF, HFmrEF and HFrEF, in order to assess appropriate management strategies. LVEF is also a common criterion used to recruit patients into clinical trials.

However, using LVEF to categorize the pathophysiology of HF may be misleading.[48] LVEF does not provide insight into diastolic function, therefore, it does not provide information on disease severity in patients with HFpEF. LVEF alone cannot distinguish between healthy subjects, patients at risk for HF (AHA ACC/AHA stage A and B), and patients with HFpEF (ACC/AHA stage C). Therefore, cardiac imaging detailing diastolic function or perhaps a more sensitive imaging biomarker of systolic dysfunction is necessary. Furthermore, LVEF also has poor prognostic predictive value in patients with HF.[7, 45] Similar 5 year mortality rates have been observed among patients with HFpEF, HFmrEF and HFrEF.[7] Therefore, better surrogate imaging biomarkers with better diagnostic and predictive value are preferable.

Global longitudinal strain (GLS), is an alternative measure of systolic function, and is defined as the percentage change of the length of the left ventricle from end-diastole to end-systole. GLS is often measured at the endocardium has been shown to be superior to LVEF in distinguishing HF patients from healthy subjects[49] and is also superior to LVEF in predicting adverse outcomes in patients with acute HF.[45]

However, myocardial structure and function are heterogeneous, with layer-specific fiber orientations ranging from largely circumferential at the mid-wall to more oblique at the endocardium and epicardium.[50] The potential added value of layer-specific strain has been illustrated in various cardiovascular diseases but not in patients with HF. Layer-specific strains, may have distinct value of diagnosis and prognosis from strain measured at the endocardium only. Therefore, it may be preferable to investigate layer-specific strain in HF.

1.5.2 Identification of progression and the prognosis in HF

Beyond HF symptoms and serum biomarkers, the progression of HF is conventionally assessed by the serial assessment of LVEF.[2] Notably, cancer therapy related cardiac dysfunction in patients with breast cancer is defined as an absolute decrease in LVEF>10% to a LVEF < 53%.[51] In the field of HF, serial cardiac imaging has been predominantly reported in studies post myocardial infarction,[52, 53] as well as interventional trials of pharmacotherapy,[53] valve replacement[54], revascularization,[55] and implantable electronic devices[56, 57,58]. However, a large proportion of patients with HF, i.e. those with chronic stable disease, have been underrepresented in cardiac imaging studies. Patients with chronic stable HF likely have silent disease progression at tissue, cellular and subcellular level.[59] In patients with chronic HF, no study has investigated longitudinal changes in cardiac structure, function and myocardial tissue characteristics in order to elucidate the natural history of HF.

To date, the prognostic value of a dynamic change in cardiac structure or function in patients with HF has been rarely reported. A previous study of patients with HF reported serial measurements of LVEF at a mean interval of 3.1 years and its prognostic value.[60] However, the majority of imaging studies of chronic HF have been cross-sectional and have associated prognosis with single-time point LV measurements.[45, 61, 62] Although one-time point LV measurement appears to yield important prognostic information, longitudinal cardiac changes would better reflect hemodynamic alterations in preload and afterload, and effects from neurohormonal activation.[63] Thus, incremental prognostic information may be derived from dynamic changes in cardiac structure and function.

As HF is a progressive clinical syndrome, patients tend to undergo follow-up imaging testing.[2] However, there is little data informing on the nature and relevance of temporal changes in cardiac structure and function, especially in patients with stable disease without changes to HF

therapy. As CMR is highly accurate and reproducible, and is multiparametric test, it is preferable to analyze the serial change of cardiac geometry and function using this imaging modality.

Furthermore, some patients with HF undergo serial cardiac imaging tests based on guideline and clinical needs. Longitudinal cardiac imaging assessments are still not recommended by expert opinions.[1] Serial testing may identify HF progression or response to therapy. Surveillance imaging strategies predominantly focuses on LVEF re-evaluation. Additional studies are needed to explore the value of other cardiac imaging biomarkers. Thus, it is meaningful to objectively identify the most clinically relevant cardiac imaging biomarker(s) during serial testing to aid with disease management.

1.5.3 Establishing a validated imaging risk prediction model

As patients with HF have multiple comorbidities, it is necessary to incorporate cardiovascular risk factors and other diseases in risk prediction models of outcome. Thus far, prediction models of HF have been established using demographics, concomitant diseases, cardiovascular risk factors, medication usage.[64-70] However, these clinical risk characteristics only partially contribute to or interact with HF, they do not provide specific information about cardiac structure and function which determines the presence, severity, progression or even etiology of HF. Consequently, there is the potential for remarkable additive value of incorporating the imaging biomarkers beyond the clinical information used in risk prediction models of HF.

So far, most risk prediction models of HF have included only one imaging parameter, predominantly LVEF, in addition to clinical information, which is not comprehensive enough to reflect cardiac structure and function. CMR enables multi-parametric assessment of cardiac function, volume and tissue characterization all at once. Multiple CMR-derived biomarkers have the potential to reflect different characteristics of cardiac geometry and function and more systemically predict the outcome. Therein, a methodologically solid and externally valid risk model may be incorporated in routine care to help physician better capture the overall risk to patients with HF. Furthermore, there is little information regarding externally validated risk prediction models incorporating multiparametric cardiac imaging biomarkers.

1.6 The Alberta HEART Study

The Alberta Heart Failure Etiology and Analysis Research Team (HEART) study is a multi-center (University of Alberta and University of Calgary) prospective study of patients with heart failure funded by Alberta Innovates-Health Solutions. Alberta HEART has the primary objective to define new diagnostic criteria for patients with HFpEF. Recruitment included the full spectrum of patients with HF, patients at risk for HF and healthy controls. Patients with HF included HFrEF, HFmrEF and HFpEF; patients at risk for HF were those having high-risk of developing HFpEF but no symptom of HF. These high risk features included hypertension, diabetes, atrial fibrillation; or obesity.[71] The study design is illustrated in Figure 1.2. Particularly, one of the major goals of this study was to evaluate a wider array of imaging tests to devise new criteria characterizing HFpEF. Cardiac imaging tests included CMR and echocardiography.

In all subjects, CMR scans were performed on a 1.5 T magnet (Sonata, Siemens and Avanto, Siemens) and included an assessment of: (1) atrial and ventricular volumes and function using steady state free precession (SSFP) cines, (2) myocardial tissue characterization using late gadolinium enhancement (LGE) as well as quantitative T1 and T2 imaging, (3) estimation of ventricular and vascular stiffness using SSFP, phase contrast and tagging techniques and (4) pulmonary water content.

Most CMR studies of prognosis have been single site experiences with no external validation, and the available clinical information including baseline clinical risk and serum biomarkers were not comprehensive enough to build a robust base model to test the independent predicting power of CMR measures. However, the Alberta HEART study is a multi-site study and has collected comprehensive clinical information. This high-quality multi-center data forms the basis for my thesis.

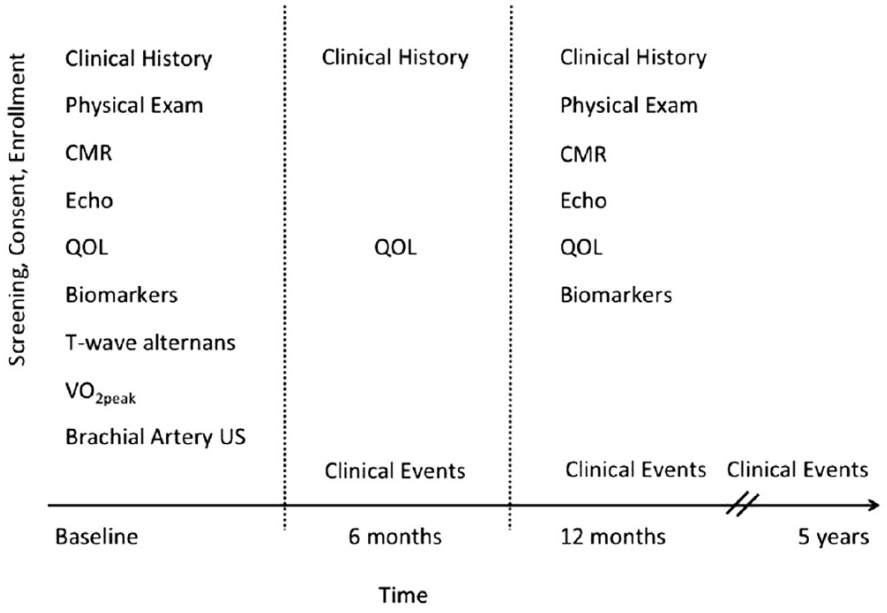

Figure 1.2 Alberta HEART study design, from Ezekowitz et al_BMC CV Disorder_2014[71].

1.7 Thesis Rationale, Hypotheses and Objectives

1.7.1 Rationale

As outlined in the previous sections, HF management is challenged by: (i) lack of early detection;(ii) limited scope of imaging assessments of HF progression; (iii) poorly characterized risk models of HF prognosis. Consequently, it is preferable to establish cardiac imaging strategies to improve early detection, determine optimal imaging biomarkers for serial testing and identify patients with HF at greatest risk of adverse outcomes. Earlier identification of disease presence or progression will pave the way for earlier intervention and may ultimately improve long-term outcomes.

1.7.2 Objectives and Hypotheses

Objective 1: to determine if global LV strains assessed at different layers of the myocardium by CMR using feature-tracking approach, would have distinct performance of diagnosis and prognosis in patients with chronic HF.

Hypothesis 1: Layer-specific global strains have superior diagnostic and predictive performance to myocardial strain measured at endocardium alone in patients with HF.

Hypothesis 1 is investigated in Chapter 2.

Objective 2: to investigate the prevalence of cardiac remodeling assessed by serial CMR assessments in patients with chronic stable HF and to evaluate prognostic value of cardiac remodeling.

Hypothesis 2: Cardiac remodeling is prevalent in patients with chronic stable heart failure; the prognostic value of cardiac remodeling by serial CMR measurement is incremental to clinical data and single-time point measurements.

Hypothesis 2 is investigated in Chapter 3.

Objective 3.1: to develop a comprehensive risk prediction model incorporating clinical information and CMR-derived measurement of cardiac structure and function;

Objective 3.2: to evaluate the applicability and validity of the model in an external cohort.

Hypothesis 3: A multiparametric imaging risk model is more robust than the risk model with clinical information alone and has excellent applicability and validity across different heart failure datasets.

Hypothesis 3 is investigated in Chapter 4.

Chapter 2: Layer-Specific Strain in Patients with Heart Failure using Cardiac MRI: Not All Layers are the Same

2.1 INTRODUCTION

Heart failure (HF) is a complex clinical syndrome with a wide array of characteristic cardiac structural and functional abnormalities. [1] Patients are typically categorized according to left ventricular ejection fraction (LVEF), with reduced ejection fraction defined as LVEF<40% (HFrEF), mid-range LVEF in the span of 40%-49% (HFmrEF) and those with heart failure with preserved LVEF≥50% (HFpEF) [2, 6]. However, LVEF has an inconsistent relationship with outcomes [7, 72] and does not distinguish those with preserved LVEF from those without cardiac disease [49]. Global longitudinal strain (GLS) provides an alternate measure of systolic dysfunction that has been shown to be superior to LVEF in distinguishing HF patients from healthy subjects [49] and predicting adverse outcomes in patients with acute heart failure [45].

However, myocardial structure and function are heterogeneous, with layer-specific fiber orientations ranging from largely circumferential at the mid-wall to more oblique at the endocardium and epicardium [50]. There is a gradient in myocardial strain across the wall, with decreasing values from endocardium to epicardium [73, 74] which makes reported values dependent on measurement layer, with endocardial values being most commonly reported [45, 49, 75, 76]. The potential added value of layer-specific strain has been illustrated in various cardiovascular diseases. In those with suspected coronary artery disease, endocardial strains were shown to be superior to epicardial strains for diagnosis [77]. Other studies of ischemic heart disease have shown the superior performance of endocardial strain for the prediction of outcomes [78, 79]. Conversely, epicardial longitudinal strain has been shown to provide incremental prognostic information for acute coronary syndrome [80] and hypertension [81], and improved diagnostic performance for myocarditis [82]. Finally, the epicardial, mid-wall and endocardial GLS were shown to have similar predictive performance in population-based cohort [83].

Layer-specific strains were recently reported in a small heart failure cohort, to characterize group and layers-specific differences. However, the reported four groups had distinct LVEF, even

between healthy control and patients with HFpEF. Therefore, it was not ideal to compare the diagnostic value between strains and LVEF [74] The aims of the current study were to compare the utility of global strains assessed at different layers of the myocardium, measured with cardiovascular magnetic resonance imaging (CMR) feature-tracking, to detect systolic dysfunction among three groups of subjects with normal LVEF and to predict outcomes in patients with HF.

2.2 METHODS

2.2.1 Study Population

The study was approved by the University of Alberta and University of Calgary Health Research Ethics Boards and all study participants provided written informed consent. We excluded those unable to provide informed consent or with a contraindication to CMR. Patient recruitment and testing has previously been reported [71]. Briefly, we recruited patients with HF and those at-risk for HF from ambulatory clinics and all subjects underwent comprehensive phenotyping that included a detailed history and physical examination, serum biomarkers and a multi-parametric CMR exam. Individuals at-risk for HF had a history of coronary artery disease, diabetes mellitus, hypertension, atrial fibrillation, and/or obesity without a diagnosis of heart failure (AHA/ACC class A and B) [71]. Heart failure patients (AHA/ACC Class C), were sub-grouped into those with preserved (HFpEF, LVEF ≥ 55%), midrange (HFmrEF, 40% ≤ LVEF < 55%) or reduced ejection fraction (HFrEF, LVEF < 40%) [2, 6]. Healthy controls were also recruited and underwent identical testing.

2.2.2 CMR Protocol

All subjects underwent a CMR examination on Siemens Sonata or Avanto 1.5 T MRI scanners (Siemens Healthcare, Erlangen, Germany) at the University of Alberta or University of Calgary sites, respectively. To quantify cardiac structure and function, the CMR exam included standard balanced steady state free precession (bSSFP) cine imaging, with 10-14 short axis slices covering the entire ventricle, as well as two-chamber, three-chamber and four-chamber long axis views. Typical acquisition parameters: Repetition time/echo time (TR/TE) 2.8/1.4 ms, 50-70 degree flip angle, 8 mm slice thickness with a 2 mm gap for short axis slices, 256 x 192 matrix, 380 x 285 mm field of view, 10 views per segment with 25 or 30 reconstructed cardiac phases over the cardiac

cycle. All cardiac images were acquired with ECG gating within an 8-12 second breath-hold per slice.

2.2.3 Image Analysis

Left and right ventricular end-diastolic volume (LVEDV, RVEDV) and end-systolic volume (LVESV, RVESV), ejection fraction (LVEF, RVEF) and left ventricular mass were measured using Syngo Argus, (Siemens Healthcare, Erlangen, Germany) or CVI42 (Circle, Calgary, Canada). Volumes and mass were normalized to body surface area, calculated using idealized weight for the given subject height [84]. Relative wall thickness (RWT) was calculated from short-axis slices as average end-diastolic wall thickness divided by average left ventricular end-diastolic diameter from two mid-ventricular short-axis slices. LV Mass/LVEDV (concentricity) was also calculated.

Strain was measured from bSSFP short and long axis cine images using a feature tracking approach based on b-spline non-rigid registration. [85] First, in-plane displacement fields were calculated from registration of all images in each cine image series to the reference end-diastolic image frame, separately for each short-axis and long-axis slice (step 1). Endocardial (red) and epicardial (green) borders (Figures 1 and 2) were manually traced only on the end-diastolic image frames by an experienced interpreter for all subjects (LX) who was blinded to clinical data and conventional CMR measures (step 2). Equally spaced contours between the endocardial and epicardial contours (blue) were automatically generated at the end-diastolic frame. Subsequently, the end-diastolic contours at all layers were automatically propagated to all image frames over the full cardiac cycle using the previously calculated feature tracking displacement fields (step 3). Strain in each slice was calculated independently for all contours as the fractional change in length of the contour from end-diastole (L_0) to end-systole (L) relative to end-diastolic length, reported as a percentage, $(L-L_0)/L_0*100$ (Lagrangian strain). [86, 87] Global longitudinal systolic strain (GLS) was calculated separately for the endocardium (GLS_ENDO), the epicardium (GLS_EPI) and the average of all contours (GLS_AVE). Peak systolic strain from all long axis slices were averaged to provide the reported global values (Figures 1, right panels). The ratio, GLS_ENDO/GLS_EPI, as well as the absolute and relative differences between GLS_ENDO and GLS_EPI were also calculated for each subject. Similarly, global circumferential systolic strains (GCS_ENDO, GCS_MID, GCS_AVE) were calculated as the average of the peak strains from two mid-ventricular short-axis slices (Figure

2). The ratio, GCS_ENDO/GCS_EPI, as well as the absolute and relative differences between GCS_ENDO and GCS_EPI were also calculated for each subject. Finally, global radial strains (GRS) were calculated separately from both long axis (GRS_LAX) and short axis slices (GRS_SAX). Contour lengths for the calculation of radial strains were measured as the distance between the endocardial and epicardial borders at end-diastole and end-systole. Radial strain for each slice was calculated as the average of regional radial strains, and GRS as the average from all slices, for short-axis (GRS_SAX) and long-axis slices (GRS_LAX).

GLS and GCS strains at all layers were also calculated using commercially available CMR feature tracking software (CVI42, Circle Cardiovascular Imaging, Calgary, Canada) in a subset of 202 subjects, for a comparison of feature tracking methodology in current study.

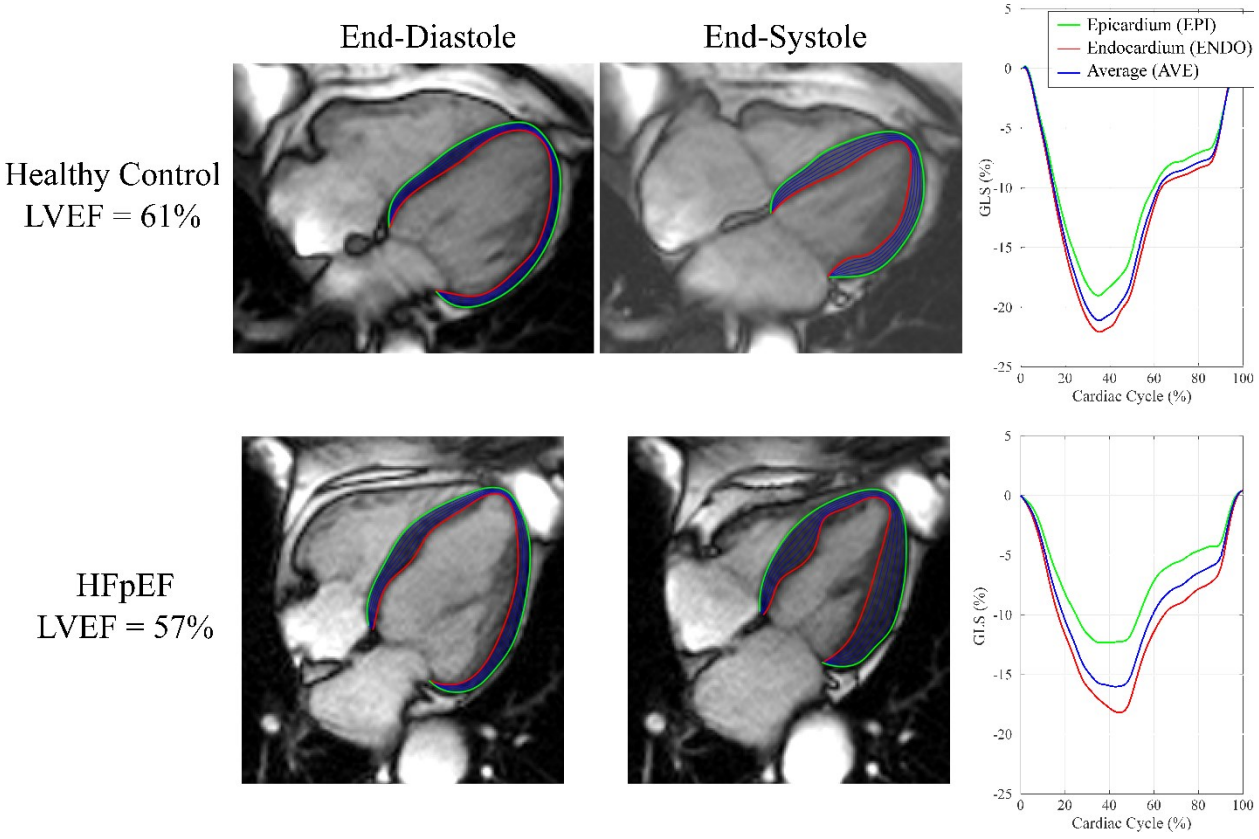

Figure 2.1. Layer-specific contours in long axis CINE images, at endocardial (red), epicardial (green) and equal spaced intramyocardial contours (blue) at end-diastole and end-systole used for the calculation of layer-specific strain. Sample tracings for a four-chamber view are shown for a health control (top) and a patient with HFpEF (bottom). Strain values at each layer over the full cardiac cycle are shown on the right. See Table 2 for abbreviations.

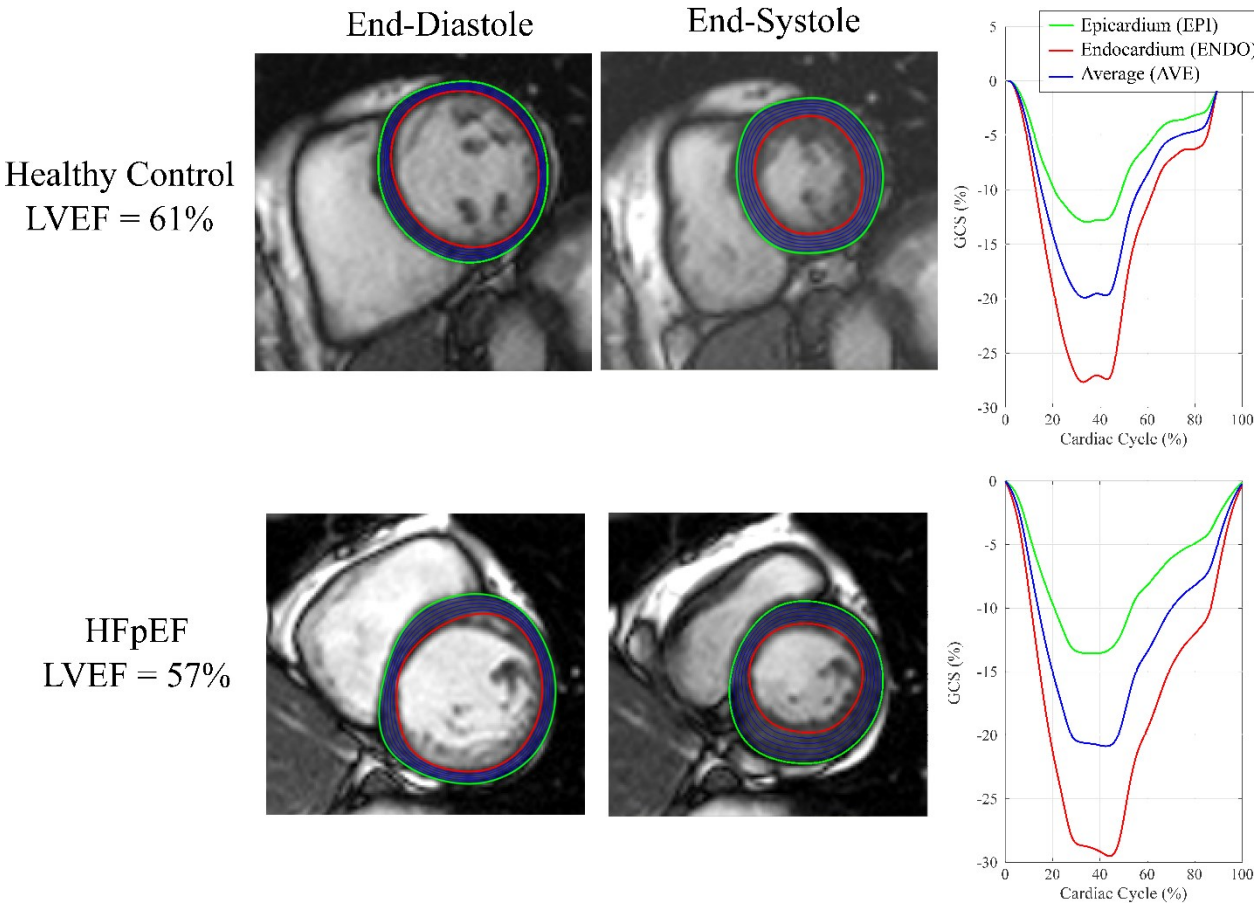

Figure 2.2. Layer-specific contours in short axis CINE images, at endocardial (red), epicardial (green) and equal spaced intramyocardial contours (blue) at end-diastole and end-systole used for the calculation of layer-specific strain. Sample tracings for a mid-ventricular short-axis view are shown for a health control (top) and a patient with HFpEF (bottom). Strain values at each layer over the full cardiac cycle are shown on the right. See Table 2 for abbreviations.

2.2.4 Statistical Approach

Continuous variables were expressed as mean±standard deviation or median (25^{th}, 75^{th} percentile), as appropriate. Categorical variables were expressed as frequency and percentage. For missing data, the data was assumed to be missing at random. Our cohort had missing values for N-terminal prohormone of b-type natriuretic peptide (NT-proBNP, 11.0% in total, including 2.3% in healthy control, 3.5% in patients at risk for HF, 5.2% for patients with HF) and creatinine

(8.6% % in total, including 3.1% in healthy control, 1.3% in patients at risk, 4.2% in patients with HF). Multiple imputation by chained equations with 50 imputed data sets was used to generate missing data based on all candidate predictors and outcomes. We averaged results from the 50 imputations [88].

Two sample t-test (or Mann-Whitney U test) or one-way analysis of variances with Bonferroni post-hoc correction (or Dunn's test) were used to compare continuous variables among groups of patients, as appropriate. Chi-square was used to compare the categorical baseline characteristics. The normal distribution of continuous variables was tested by the Shapiro-Wilk normality test. We applied logarithmic transformation to NT-proBNP and creatinine. Correlation between continuous variables was tested by Pearson correlation.

Clinical outcome was all-cause mortality over a 5-year follow-up. Univariable Cox proportional regression was performed for all demographic parameters, cardiovascular risk factors, cardiovascular disease history, concomitant diseases, and CMR-derived imaging parameters. Sex and the parameters with univariable p value<0.2, including age, systolic blood pressure, current smoker, presence of heart failure, coronary artery disease, atrial fibrillation or atrial flutter, chronic obstructive pulmonary disease, log (NT-proBNP) and log (creatinine) entered the forward selection approach based on Akaike Information Criterion (AIC) to build the optimal set of predictors as the base model for adjustment. In the multivariable Cox proportional hazard analysis conventional LV measurements, GRS, and layer-specific strains for GLS, GCS were each adjusted with the base model to test their independent association with the outcome. Additionally, the association of layer-specific strains and conventional LV measurements with clinical outcomes were quantified using the AIC values, where the lowest AIC score ($AIC_{minimum}$) indicates the best outcomes model. Each compared model included the base model and a single evaluated CMR parameter. For comparison of AIC values (between CMR parameters), $\Delta_i = AIC_i - AIC_{minimum}$ is the difference between $Model_i$ and best fit model. If $\Delta_i \leq 2$, there is substantial support for similar predictive performance of the best fit model and the i-th model; for $4 \leq \Delta_i \leq 7$ there is considerably less support for *i*-th model; for $\Delta_i > 10$ there is no support for *i*-th model [89]. Finally, the incremental value of outcomes prediction by layer-specific strain over the other CMR variables was evaluated using the likelihood ratio test.

Intra-observer and inter-observer reproducibility of all strain parameters were evaluated by intra-class correlation coefficient and coefficient of variation in 20 randomly selected subjects with blinding to clinical data. Statistical analyses were performed using STATA 16.0 software (StataCorp LP, College Station, Texas). A p-value less than 0.05 was considered significant for all tests.

2.3. RESULTS

2.3.1 Demographics

From 466 subjects who underwent CMR exams, 453 subjects with analyzable images were identified: controls (n=77), at-risk (n=143), HFpEF (n=87), HFmrEF (n=88), and HFrEF (n=58). To explore whether strains can differentiate the 3 subgroups with preserved LVEF (controls, at-risk and HFpEF), only healthy controls (n=70) and patients at risk for HF (n=126) and HFpEF (n=87) with normal LVEF > 55% were included in group comparison (Table 1 & Table 2), but all patients at risk or with HF were all included in the survival analysis. Those with HFpEF were older and had higher body mass index, higher medication use, more concomitant disease and higher serum NT-proBNP, as compared to controls and those at-risk (all ps<0.001, Table 1). Among the three heart failure groups, all had similar serum creatinine and concomitant disease, however those with HFpEF were slightly older with a larger proportion of females, slightly higher body mass index, and lower rate of beta blocker use (all ps<0.05) and those with HFrEF had higher level of serum NT-proBNP with lower systolic blood pressure (both ps <0.05). (Table 2.1)

2.3.2 Ventricular Structure and Function

Within the heart failure groups, there was significantly lower LVEF, lower strains and larger ventricular mass and volumes from HFpEF to HFmrEF and to HFrEF groups, respectively (Table 2, all ps<0.001). Within the preserved LVEF groups (controls, at-risk and HFpEF), LVEF was statically identical between healthy controls and patients with HFpEF (median 63% vs 63%, p=0.84) and slightly lower than patients at risk for HF (median 66%, both ps<0.05 with post-hoc correction). All circumferential strain components, as well as LV and RV volume were similar in all three groups. GLS_ENDO was also similar in all preserved LVEF groups, and thus also did

not identify systolic dysfunction in patients with HFpEF. However, GLS_EPI was the only strain measurement distinguishing all three groups with preserved LVEF in post-hoc analysis, with incrementally reduced systolic function (-16.5±2.4% vs. -15.5±2.7% vs. -14.1±3.0%, $p<0.001$) from controls, to those at-risk to HFpEF. Both LV Massi and LV Mass/LVEDV also had significant stepwise increase from controls, to those at-risk to HFpEF. Other parameters also identified systolic dysfunction in the HFpEF group, with significantly reduced values versus controls and at-risk groups but no difference between the latter two groups, including GLS_AVE and GRS (Table 2). HFpHF patients also had significantly larger differences (absolute and relative) between endocardial and epicardial strains as compared to healthy controls, for both GLS and GCS.

Comparison of LVEF and GLS_EPI values for all study subjects illustrates the significant overlap of GLS_EPI values among the three HF subgroups (grouped by LVEF), for which GLS_EPI values are generally reduced and overlapping regardless of LVEF (Figure 2.3A and 2.3B). Using the 90^{th} percentile in the control group as a cutoff for identification of systolic dysfunction, GLS_EPI identified 35/87 HFpEF patients (GLS_EPI >-11.4% cutoff in males (Fig. 2.3D), >-14.2% cutoff in females (Fig. 3F)), while GLS_ENDO identified a much smaller subgroup of 18/87 with reduced function (GLS_ENDO >-16.0% cutoff in males, >-18.7% cutoff in females). Similar scatter plots are shown for all strain components (Figure 2.4).

GLS and GCS values were significantly reduced from endocardial to epicardial layers in all groups, as shown by the ratio of strains on these layers as well as by the absolute and relative strain differences (Table 2.2). Also, the differences between endocardial and epicardial strains (absolute and relative) were significantly reduced from HFpEF to HFmrEF to HFrEF.

Table 2.1. Baseline Characteristics in the 5 Subgroups of Subjects

	Healthy control (n=70)	At risk for heart failure (n=126)	HFpEF (n=87)	p-value 1	HFmrEF (n=88)	HFrEF (n=58)	p-value 2
	Preserved Ejection Fraction						
Age, year	59(52,69)*†	65(60,72)*	73(64,81)	<0.001	70(60,75)¶	66(59,77)¶	0.005
Male	29(37.1%)	53(42.1%)	34(39.1%)	0.78	61(69.3%)	40(69.0%)	<0.001
BMI, kg/m^2	28(24,30)*†	29(25,34)*	30(28,35)	<0.001	29(26,33)¶	29(26,32)¶	0.013
Systolic BP, mmHg	128(116,140)†	137(123,151)	130(121,146)	0.070	125(115,136)¶	124(111,133)¶	0.006
Heart rate, bpm	67(60,76)	68(61,76)	64(60,76)	0.16	64(60,75)	68(60,76)	0.30
NYHA Class			2.1±0.7	N/A	1.9±0.7	2.0±0.7	0.30
CAD	0	22(17.5%)	37(42.5%)	<0.001	40(45.5%)	29(50%)	0.68
HTN	0	100(79.4%)	75(86.2%)	<0.001	56(63.6%)	37(63.8%)	0.001
Af/AFL	0	19(15.1%)	34(39.1%)	<0.001	36(40.9%)	23(39.7%)	0.98
COPD	0	8(6.4%)	18(20.1%)	<0.001	15(17.1%)	12(20.7%)	0.79
CKD	0	9(7.1%)	22(25.3%)	<0.001	17(19.3%)	11(19.0%)	0.55
Beta blocker	0	34(27.0%)	64(73.6%)	<0.001	79(89.8%)¶	54(93.1%)¶	0.001
ACEi or ARB	0	86(68.3%)	73(83.9%)	<0.001	76(83.6%)	50(86.2%)	0.88
NT-proBNP, pmol/l	5(3,10)*†	7(4,16)*	66(19,132)	<0.001	57(24,147)	104(52,253)¶§	0.003
Creatinine, mol/l	78(67,86)*	77(67,89)*	96(76,123)	<0.001	97(80,122)	93(77,110)	0.49

P-values 1 were derived from comparison among the three subgroups with preserved ejection fraction and P-values 2 for the three subgroups of patients with heart failure. Continuous variables were expressed as mean±standard deviation or median (25th, 75th percentile), as appropriate. Abbreviations: HFpEF=heart failure with preserved ejection fraction; HFmrEF=heart failure with midrange ejection fraction; HFrEF=heart failure with reduced ejection fraction; BMI=body mass index; BP=blood pressure; NYHA=New York Heart Association Classification; CAD=coronary heart disease; HTN=hypertension; Af/AFL=atrial fibrillation/flutter; DM=diabetes mellitus; COPD=chronic obstructive pulmonary disease;

CKD=Chronic kidney disease; ACEI=Angiotensin converting enzyme inhibitor; ARB=Angiotensin II receptor blocker; NT-proBNP=N-terminal pro b-type natriuretic peptide;

*significantly different from HFpEF in comparison among 3 subgroups with preserved LVEF.

†significantly different from patients at risk for heart failure in comparison among three subgroups with preserved LVEF.

¶ significantly different from HFpEF in comparison among three subgroups with heart failure.

§ significantly different from HFmrEF in comparison among three subgroups with heart failure.

Table 2.2. Cardiac Structure and Functions in the 5 Subgroups of Subjects

	Healthy control (n=70)	At risk for heart failure (n=126)	HFpEF (n=87)	p-value 1	HFmrEF (n=88)	HFrEF (n=58)	p-value 2
	Preserved Ejection Fraction						
LVEF,%	63(61,67)†	66(62,70)*	63(59,68)	0.008	48(44,52) ¶	32(25,38)¶§	<0.001
LVEDVi, ml/m^2	74(68,83)	75(65,87)	76(68,86)	0.73	100(81,114)¶	134(100,165)¶§	<0.001
LVESVi, ml/m^2	27(23,31)	25(21,31)	28(22,33)	0.16	51(40,62)¶	90(64,121)¶§	<0.001
LV Massi, g/m^2	55(49,61)*†	61(51,71)*	66(56,79)	<0.001	76(63,88)¶	91(74,110)¶§	<0.001
LV Mass/LVEDV	0.72(0.66,0.79)*†	0.80(0.70,0.91)*	0.85(0.73,0.98)	<0.001	0.79(0.66,0.88)¶	0.67(0.60,0.76)¶§	<0.001
RWT	0.31(0.27,0.34) *	0.32(0.28,0.37)*	0.34(0.29,0.40)	0.019	0.32(0.27,0.37)¶	0.28(0.24,0.32)¶§	<0.001
RVEF	58(55,64)†	62(57,67) *	60(52,64)	0.021	52(46,58)¶	49(41,56)¶§	<0.001
RVEDVi, ml/m^2	74(63,83)	75(61,88)	71(63,91)	0.74	81(67,97)¶	79(68,108)¶	0.070
RVESVi, ml/m^2	30(23,35)	28(22,35)	31(24,39)	0.27	38(28,48)¶	39(31,57)¶	<0.001
GLS_EPI,%	-16.5±2.4*†	-15.5±2.7*	-14.1±3.0	<0.001	-11.6±2.1¶	-8.2±2.2¶§	<0.001
GLS_AVE,%	19.6±2.5*	19.2±3.1*	17.9±3.3	<0.001	14.0±2.3¶	9.4±2.7¶§	<0.001
GLS_ENDO,%	-21.1±2.6	-21.2±3.4	-20.1±3.7	0.050	-15.3±2.9¶	-10.0±3.2¶§	<0.001
GLS_ENDO/GLS_EPI	1.3(1.2,1.4)*†	1.4(1.3,1.5)*	1.4(1.3,1.5)	<0.001	1.3 (1.2,1.4)¶	1.2(1.2,1.4)¶§	<0.001
Absolute GLS layer difference, %	-4.7(-5.8,-3.3)*†	-5.7(-7.4,-4.1)	-5.6(-7.5,-4.3)	<0.001	-3.5(-5.1,-2.3)¶§	-2.1(-2.7,-1.0)¶§	<0.001
Relative GLS layer difference, %	21.9(16.5,27.0)*†	27.3(20.4,32.5)*	28.9(23.4,34.4)	<0.001	25.4(16.1,29.9)¶§	17.9(13.4,25.8)¶§	<0.001
GCS_EPI,%	-11.1±2.8	-10.2±2.5	-10.2±3.4	0.072	-7.8±2.4¶	-5.7±2.2¶§	<0.001
GCS_AVE,%	19.9±3.4	19.9±3.3	19.3±4.0	0.40	13.9±3.1¶	9.3±3.1¶§	<0.001
GCS_ENDO,%	-29.9±4.7	-31.1±5.3	-29.9±6.1	0.17	-21.1±4.9¶	-13.1±4.6¶§	<0.001
GCS_ENDO/GCS_EPI	2.6(2.4,3.1)*†	3.0 (2.6,3.6)	2.9(2.4,4.0)	0.004	2.63(2.33,3.25)¶	2.31(1.90,2.85)¶§	<0.001
Absolute GCS layer difference, %	-18.8(-21.1,-16.3)†	-20.8(-24.3,-17.8)*	-19.0(-23.1,-16.1)	0.002	-13.0(-16.2,-9.8)¶	-7.5(-8.7,-5.1)¶§	<0.001

Relative GCS layer difference, %	61.8(58.4,67.5) *†	67.0(62.1,72.1)	65.4(57.8,74.8)	0.004	62.0(57.1,69.2)¶	56.8(47.4,64.9)¶§	<0.001
GRS_LAX	0.49±0.11*	0.47±0.13*	0.41±0.14	<0.001	0.28±0.09¶	0.19±0.08¶§	<0.001
GRS_SAX	0.46±0.13*	0.46±0.15*	0.39±0.15	<0.001	0.27±0.09¶	0.18±0.08¶§	<0.001

Absolute strain layer difference=endocardial strain - epicardial strain; relative strain layer difference= (endocardial strain - epicardial strain)/endocardial strain

P-values 1 were derived from comparison among the three subgroups with preserved ejection fraction and P-value 2 for the three subgroups of patients with heart failure.

*significantly different from HFpEF in comparison among three subgroups with preserved LVEF.

†significantly different from patients at risk for heart failure in comparison among three subgroups with preserved LVEF.

¶ significantly different from HFpEF in comparison among three subgroups with heart failure.

§ significantly different from HFmrEF in comparison among three subgroups with heart failure.

Continuous variables were expressed as mean±standard deviation or median (25^{th}, 75^{th} percentile), as appropriate.

Abbreviations: HFpEF=heart failure with preserved ejection fraction; HFmrEF=heart failure with midrange ejection fraction; HFrEF=heart failure with reduced ejection fraction; L(R)VEF=left(right) ventricular ejection fraction; L(R)VEDVi=left(right) ventricular end-diastolic volume indexed to ideal body surface area; L(R)VESVi=left(right) ventricular end-systolic volume indexed to ideal body surface area; LV Massi= left ventricular mass indexed to ideal body surface area; RWT=relative wall thickness; GLS_EPI=epicardial global longitudinal strain; GLS_AVE=average global longitudinal strain; GLS_ENDO=endocardial global longitudinal strain; GCS_EPI=epicardial global circumferential strain; GCS_AVE=average global circumferential strain; GCS_ENDO=endocardial global circumferential strain; GRS=global radial strain; LAX=long axis; SAX=short axis.

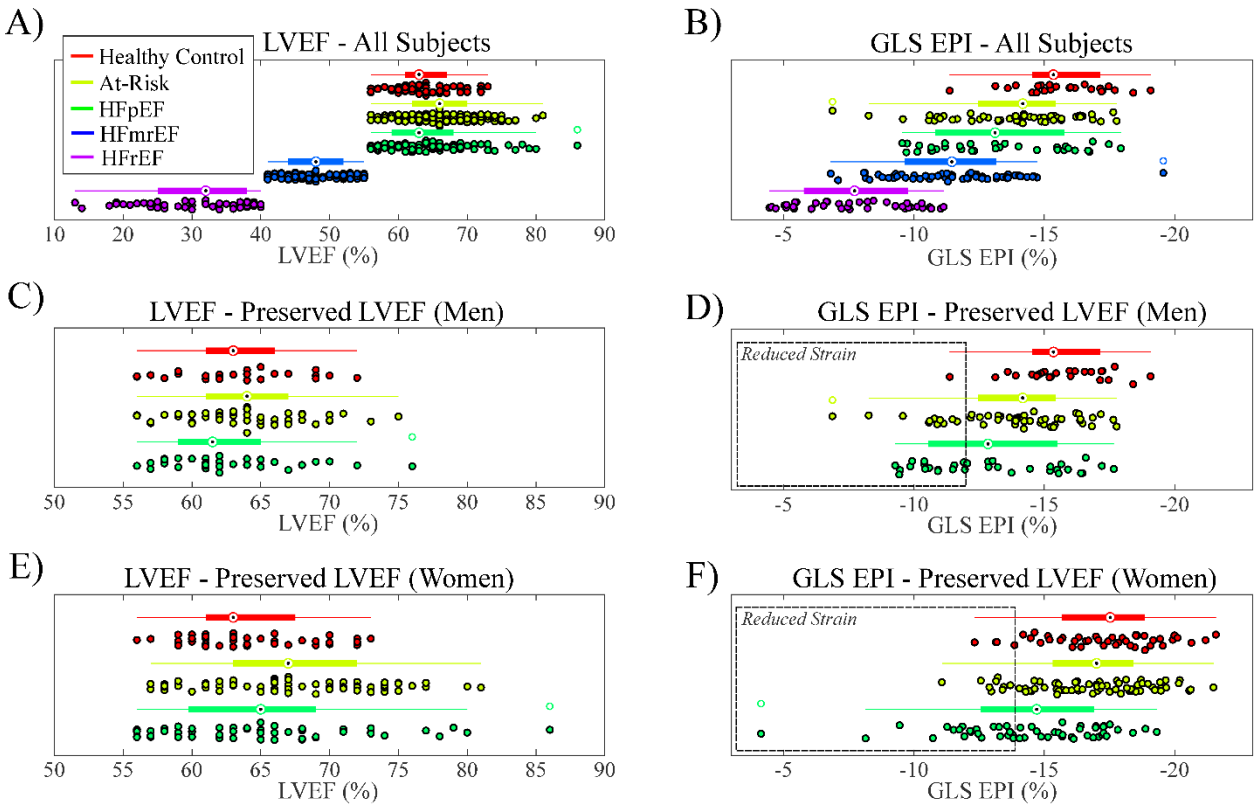

Figure 2.3. Scatter and box plots of LVEF (**A**) and GLS_EPI (**B**) in all five groups. Box plots show the median value, 25th and 75th percentiles and the full extent of the data, excluding outliers. Corresponding scatter plots are shown for LVEF (**C** and **E**) and GLS_EPI (**D** and **F**) in the preserved LVEF groups, with grouping by sex. Individuals with reduced GLS_EPI values were highlighted in the dashed boxes in **D**) (males: 11% in controls, 17% in at risk group, 32% in HFpEF) and **F**) (females: 9% in controls, 14% in at risk group, 45% in HFpEF). All subjects in the preserved LVEF groups have normal LVEF by definition. See Table 2.2 for abbreviations.

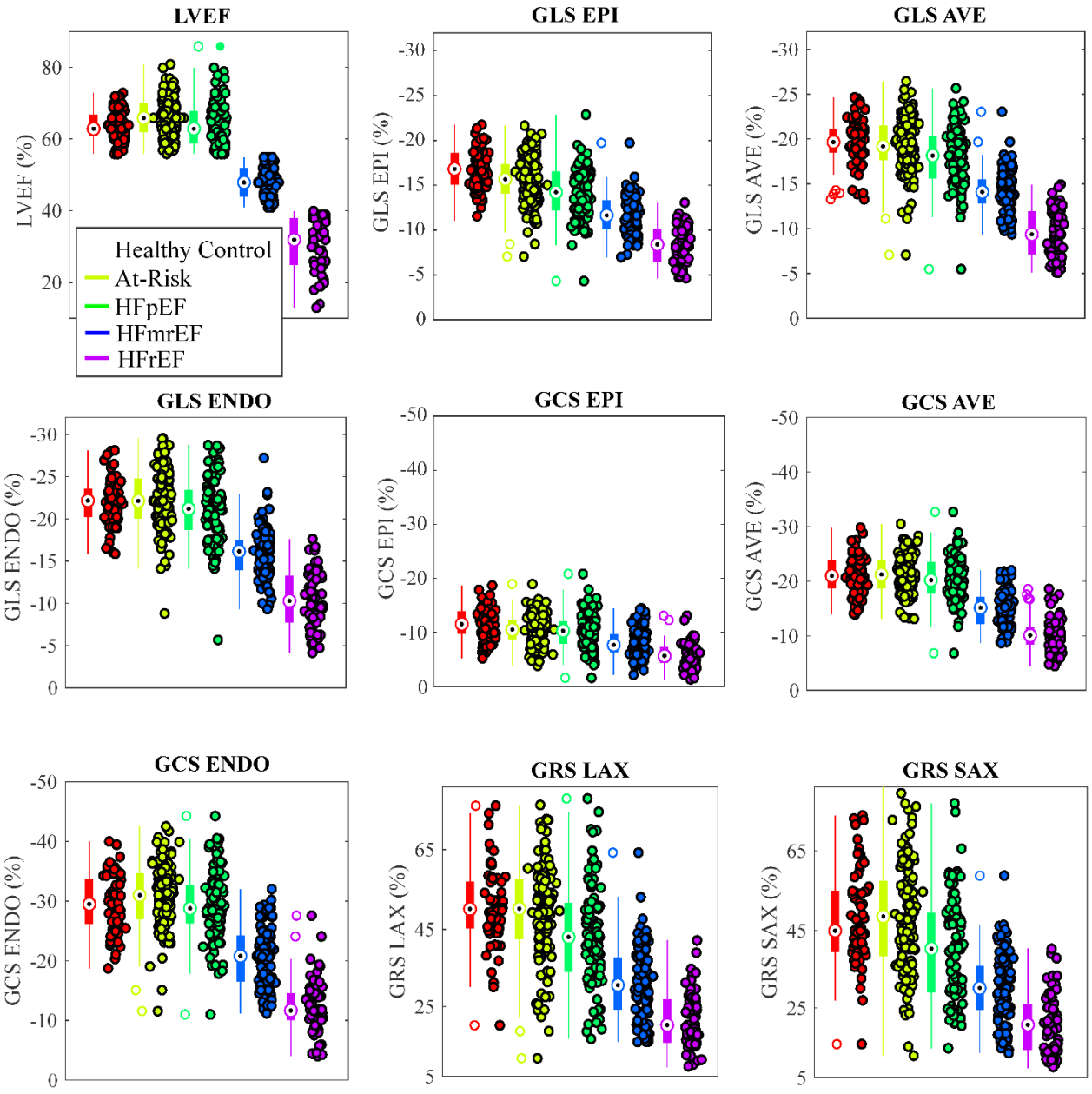

Figure 2.4. Scatter and box plots for LVEF and all strain components for all five groups. See Table 2 for abbreviations. Box plots show the median value, 25th and 75th percentiles and the full extent of the data, excluding outliers. See Table 2.2 for abbreviations.

GLS and GCS values were significantly reduced from endocardial to epicardial layers in all groups, as shown by the ratio of strains on these layers as well as by the absolute and relative strain differences (Table 2.2). Also, the differences between endocardial and epicardial strains (absolute and relative) were significantly reduced from HFpEF to HFmrEF to HFrEF.

The relationship between strain and LV structure in the preserved LVEF groups is illustrated by comparison of GRS (GRS_SAX) and LV Mass/LVEDV values in all individuals, with separate results by sex (Figure 2.5). Similar significant negative correlations were found in the HFpEF group alone (Fig. 2.5A and B), and also when including all subjects with preserved LVEF (Fig. 2.5C and D). Similar significant correlations were observed when comparing GLS_EPI and LV Mass/LVEDV (not shown).

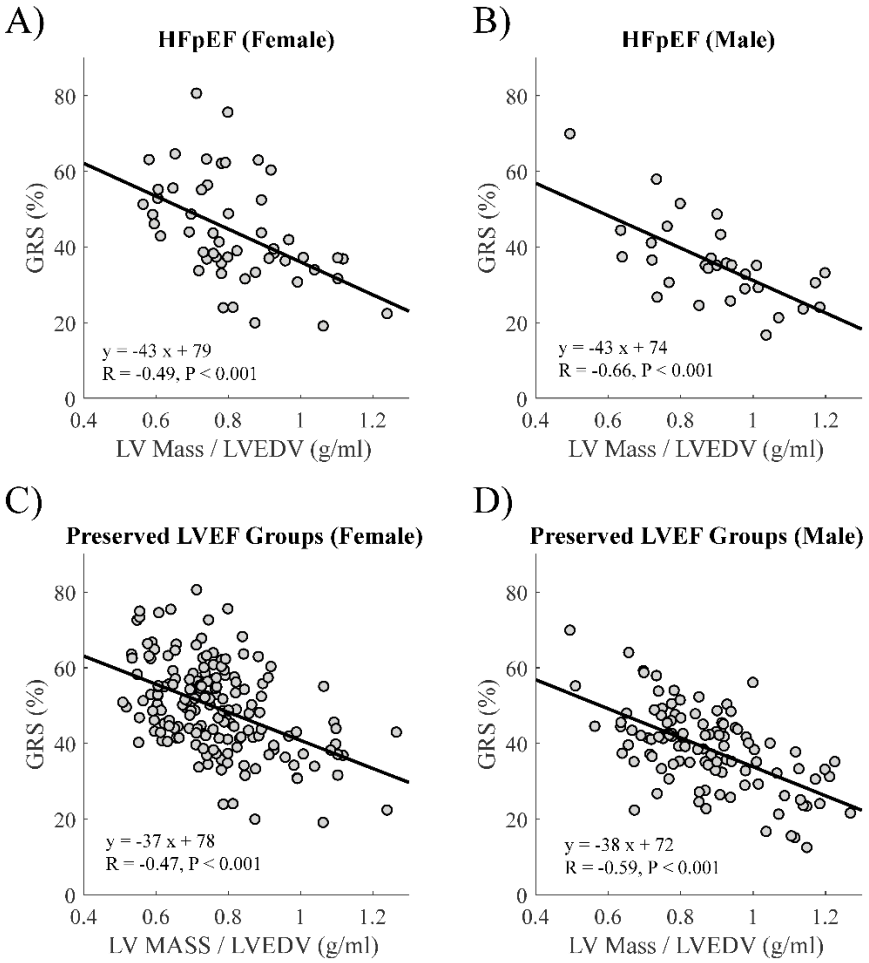

Figure 2.5. Relationship between GRS and LV Mass / LVEDV (concentricity) in HFpEF patients (**A** and **B**) and in all subjects with preserved LVEF (**C** and **D**). See Table 2.2 for abbreviations.

2.3.3 Layer-specific strain in healthy controls

Among the 77 healthy controls subjects (29 male, median age 59 years), male subjects had lower strains than females at all locations except for GCS_ENDO which were similar in men and women (Table 2.3). For both GLS and GCS, values were lowest at the epicardium with a stepwise increase from the average value in myocardium to the endocardium (all ps<0.001). The magnitude of GRS values measured from long axis (GRS_LAX) and short axis slices (GRS_SAX) were similar.

2.3.4 Clinical outcomes

During a 5-year follow-up for the at-risk and HF subgroups, there were 33 events of all-cause mortality. The base model included age and log (NT-proBNP) for multivariable analysis. After adjustment with the base model, GLS_AVE and GRS (for both LAX and SAX-derived GRS) were the only independent predictors of mortality, with adjusted hazard ratio 1.10, 1.03 and 1.03, respectively, for 1% absolute decrease of strains, all ps<0.05. However, LVEF (adjusted hazard ratio 1.22 for 10% decrease, p=0.12) and GLS_ENDO (adjusted hazard ratio 1.06 for 1% absolute decrease, p=0.15) were unable to independently predict outcome (Table 2.4). Additionally, AIC values for the layer-specific GLSs, GCSs and conventional LV measurements were compared to evaluate the relative strength of their association with clinical outcomes. GLS_AVE and GRS had the lowest AIC values, which demonstrates the strongest association with the clinical outcome (Table 2.5). For the remaining parameters, GLS_ENDO, GLS_EPI, all GCS components and conventional LV measures (LVEF, LVEDVi, LVESVi and LV Massi) had considerably less support for similar performance as GLS_AVE and GRS for outcomes prediction, with ΔAIC values of 3.5 to 6.1 [89]. The use of GLS_AVE had significant incremental value for prediction of outcomes over LVEF and GLS_ENDO (χ^2 = 5.1 and 7.4, respectively, both ps<0.05), by the likelihood ratio test. GRS both at short axis and long axis had incremental value over LVEF (χ^2 = 4.4 and 4.8, respectively, both ps<0.05).

Table 2.3. Comparison of layer-specific strain, LV mass and relative wall thickness between two sexes in healthy controls

	Male(n=29)	Female(n=48)	p-value
LVEF,%	62(59,65)	63(60,67)	0.50
GLS_EPI,%	-15.0±2.4	-17.1±2.3	<0.001
GLS_AVE,%	-18.7±2.6	-20.5±2.5	0.006
GLS_ENDO,%	-19.6±2.6	-21.4±2.7	0.005
GLS_ENDO/GLS_EPI	1.32±0.12	1.26±0.11	0.035
Absolute GLS layer difference, %	-5.0(-5.6,-3.8)	-4.2(-5.6,-3.2)	0.33
Relative GLS layer difference, %	24.2(20.1,28.0)	19.7(15.6,25.7)	0.030
GCS_EPI,%	-9.6±2.6	-11.6±2.7	0.002
GCS_AVE,%	-18.5±3.3	-20.1±3.4	0.051
GCS_ENDO,%	-28.9±4.7	-29.7±4.9	0.50
GCS_ENDO/GCS_EPI	2.97(2.61,3.47)	2.56(2.32,2.86)	0.001
Absolute GCS layer difference, %	-18.7(-21.7,-16.6)	-18.3(-20.4,-15.8)	0.29
Relative GCS layer difference, %	66.3(61.6,71.2)	61.0(56.9,65.1)	0.001
GRS_LAX	0.44±0.11	0.51±0.10	0.006
GRS_SAX	0.40±0.12	0.49±0.12	0.001
LV Massi, g/m^2	60(57,71)	52(47,57)	0.005
LV Mass/LVEDV	0.81(0.70,0.93)	0.74(0.64,0.83)	<0.001
RWT	0.34(0.30,0.37)	0.30(0.26,0.32)	<0.001

See Table 2.2 for abbreviations. Continuous variables were expressed as mean±standard deviation or median (25^{th}, 75^{th} percentile), as appropriate. P-values were derived from comparison between two sexes.

Table 2.4. Cox Proportional Hazard Regression Analysis for the Outcome of 5-Year All-Cause Mortality

	Patients with HF or at risk for HF- 376 subjects (33 events)				
	Univariable analysis			Multivariable analysis	
	HR(95% CI)	p-value	Model χ^2	HR(95% CI)	p-value
Age at MRI, per 10 year increase	2.37(1.58,3.56)	<0.001	21.5		
Male gender	0.66(0.32,1.34)	0.25	1.4		
BMI, per 1kg/m^2 increase	1.00(0.94,1.06)	0.99	0.1		
Systolic BP, per 10 mmHg increase	0.80(0.66,0.98)	0.031	0.2		
Current smoker	1.34(0.93,1.91)	0.12	2.6		
History of heart failure	6.43(1.96,21.08)	0.002	15.3		
HTN	1.07(0.48,2.38)	0.86	0.1		
CAD	2.15(1.11,4.17)	0.023	5.1		
Af/AFL	2.81(1.42,5.58)	0.003	8.6		
DM	0.81(0.39,1.70)	0.58	0.3		
COPD	1.92(0.87,4.26)	0.11	2.3		
CKD	1.20(0.50,2.91)	0.69	0.2		
Log(NT-proBNP)	1.84(1.44,2.36)	<0.001	27.5		
Log(Creatinine)	3.20(1.37,7.49)	0.007	6.2		
LVEF, per 10% decrease	1.37(1.10,1.71)	0.004	7.6	1.22 (0.95,1.58)	0.12
LVEDVi, per 10 ml/m^2 increase	1.09(1.00,1.18)	0.043	3.5	1.06(0.97,1.15)	0.19
LVESVi, per 10 ml/m^2 increase	1.11(1.02,1.20)	0.013	5.0	1.07(0.97,1.17)	0.16
LVMassi, per 10 g/m^2 increase	1.14(1.00,1.29)	0.051	3.3	1.09(0.95,1.25)	0.25
LVMass/LVEDV, per 0.1 increase	0.98(0.82,1.17)	0.82	0.1	0.92(0.81,1.03)	0.14
GLS_EPI, per 1% absolute decrease	1.11(1.04,1.18)	0.002	9.4	1.09(0.98,1.22)	0.11
GLS_AVE, per 1% absolute decrease	1.14(1.06,1.23)	<0.001	12.5	1.10(1.01,1.20)	0.023
GLS_ENDO, per 1% absolute decrease	1.10(1.04, 1.18)	0.002	9.2	1.06(0.98, 1.15)	0.15
GCS_EPI, per 1% absolute decrease	1.01(0.91,1.13)	0.83	0.1	0.99(0.90,1.10)	0.87
GCS_AVE, per 1% absolute decrease	1.05(0.99, 1.12)	0.10	2.6	1.02(0.95,1.09)	0.57
GCS_ENDO, per 1% absolute decrease	1.04(1.00,1.08)	0.044	4.0	1.02(0.98,1.06)	0.41
GRS_LAX, per 1% decrease	1.03(1.01,1.05)	0.001	12.2	1.03(1.00,1.05)	0.024
GRS_SAX, per 1% decrease	1.03(1.01,1.05)	0.002	11.9	1.03(1.00,1.05)	0.019

Base model: age+log (NT-proBNP). See Table 2.1&2.2 for abbreviations.

Table 2.5. Discrimination performance of layer-specific Strains by Akaike information Criterion (AIC) for Death at 5 Years

	AIC	ΔAIC
BM + LVEF	355.7	3.7
BM + LVEDVi	356.5	4.5
BM + LVESVi	356.4	4.4
BM + LVMassi	356.9	4.9
BM + GLS_EPI	355.5	3.5
BM + GLS_AVE	352.8	0.8
BM + GLS_ENDO	355.7	3.7
BM + GCS_EPI	358.1	6.1
BM + GCS_AVE	357.5	5.5
BM + GCS_ENDO	357.4	5.4
BM + GRS_LAX	352.3	0.3
BM + GRS_SAX	352.0	0

BM=base model, including age and log (NT-proBNP).

$\Delta AIC = AIC_i - AIC_{minimum}$ ($AIC_{minimum}=AIC_{GRS\_SAX}$). The model with lowest AIC score ($AIC_{minimum}$) indicates the best model. See Table 2.2 for abbreviations.

2.3.5 Reproducibility

The intra-observer reproducibility of all layer-specific strains was excellent; CoV values ranged from 2.7% to 5.4%, with 4.3% for GLS_EPI and 2.7% for GLS_ENDO, and ICC values ranging from 0.97 to 0.99, with 0.98 for GLS_EPI and 0.99 for GLS_ENDO. The inter-observer reproducibility of all layer-specific strains was also excellent; CoV values ranged from 4.9% to 9%, with 4.9% for GLS_EPI and 8.7% for GLS_ENDO, and ICC ranged from 0.92 to 0.98, with 0.92 for GLS_EPI and 0.98 for GLS_ENDO. Bland and Altman plots illustrate good agreement between all GLS and GCS components between the reported custom feature tracking methods and a feature tracking approach by a commercial software CVi 42 in 202 subjects (Supplemental Figure 2.1).

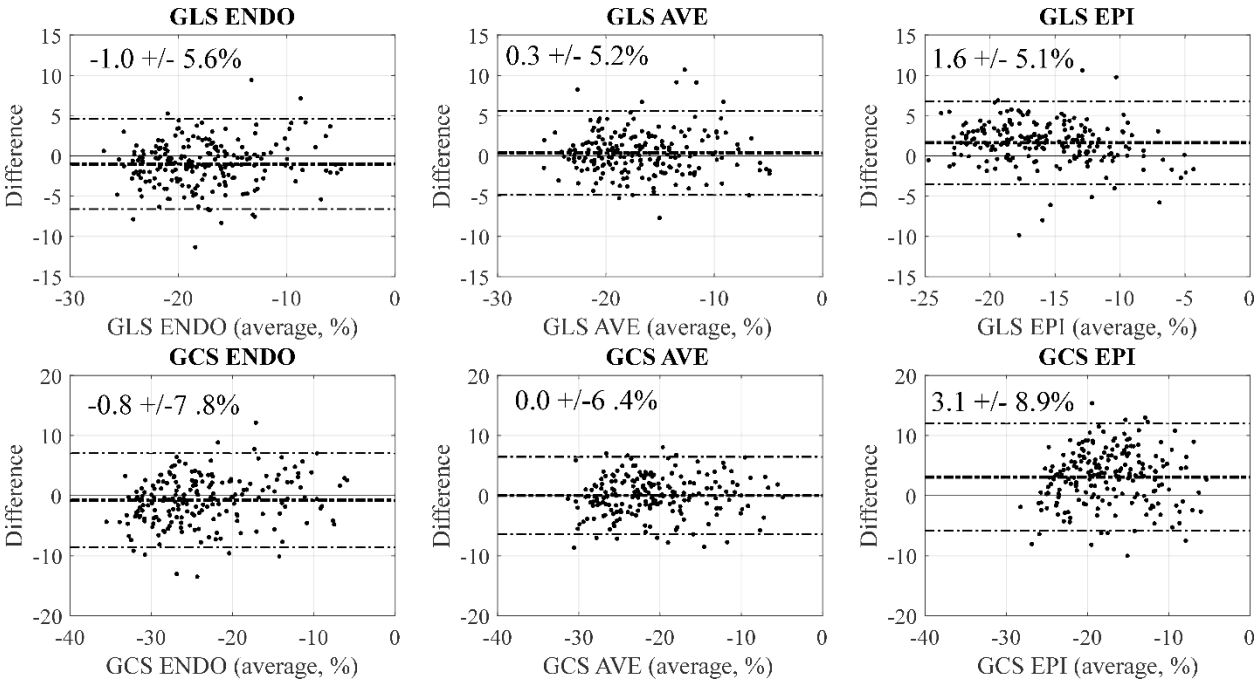

Supplemental Figure 2.1. Comparison of feature tracking software (custom software used in the current study versus CVI42) for calculation of longitudinal and circumferential strains in a subset of 202 subjects. See Table 2 for abbreviations.

2.4 DISCUSSION

The main findings of the current study are that consideration of measurement layer for global strain is necessary for optimal identification of dysfunction and outcomes prediction in heart failure. The endocardium-specific strains were shown to have poorest performance both for detection of systolic dysfunction and outcomes prediction.

Layer-Dependence of Systolic Dysfunction and Association with Remodeling in HFpEF

In subjects with preserved ejection fraction, GLS_EPI distinguished all three groups with preserved ejection fraction and identified ~40% of HFpEF patients as having reduced systolic function. In contrast, circumferential strain components at all layers and GLS_ENDO performed similarly to LVEF (i.e. values were comparable in healthy controls, those with risk factors for HF and HFpEF). Similar to recent studies in healthy subjects [74, 90, 91] and in heart failure (19), GLS and GCS values were incrementally decreased from endocardium to epicardium in all groups. In

the current study, it was also found that the difference between endocardial and epicardial strains in individuals (relative and absolute differences) were significantly higher in HFpEF as compared to healthy controls. This is in agreement with the patterns of preserved endocardial strains and reduced GLS_EPI in this heart failure group.

Additionally, indexed LV mass and LV Mass/LVEDV were significantly increased in the HFpEF group as compared to at-risk and healthy controls. Together, these findings describe a HFpEF phenotype with preserved endocardial function, paralleling LVEF, but with increased strain reduction across the wall, potentially associated with increased LV mass and concentricity (mass/volume). GRS was also significantly reduced in the HFpEF group as compared to healthy controls, and was shown to be associated with increased concentricity. A similar relationship was observed for GLS_EPI, with more impaired function in those with increased concentricity. These observed associations between strains and structure also exist in comparison of the healthy men and women, where men had larger LV mass, larger LV Mass/LVEDV, lower GLS_EPI, lower GRS and larger differences between endocardial and epicardial strains.

In the current study, the use of a higher cutoff of 55% for preserved LVEF [92, 93], as compared to the more commonly used 50%, was used to reflect the larger number of heart failure patients in the 50%-55% range but very small proportion of at-risk or control subjects in this range. A 50% cutoff would result in significantly reduced LVEF in the HFpEF group, compared to at-risk and healthy controls, and a large number of individuals that are outside of the normal range of LVEF values from the control group and literature values.

For many of the reported structural and functional parameters that distinguish HFpEF from controls, the values in the at-risk group were intermediate, between the control and HFpEF groups, with significant group differences on post-hoc analysis, suggesting early changes in these parameters may contribute to or be associated with future development of heart failure.

When comparing the three heart failure groups alone (preserved, mid-range and reduced LVEF), all CMR parameters were significantly different between all groups, with larger volumes, increased LV mass and reduced strain (all components) from HFpEF to HFrEF. The differences between endocardial and epicardial strains also followed this pattern, with reduced differences between the layers from HFpEF to HFrEF, paralleling the reduction in concentricity (mass/volume).

Heart Failure Outcomes

Among all strain components, only GLS_AVE and GRS were significantly predictive of mortality in HF patients and those at risk when including the key factors of age and NT-proBNP in the outcomes model. Both parameters had superior outcomes prediction performance as compared to commonly reported GLS_ENDO. [45, 49, 75, 76] Not surprisingly, LVEF was also not predictive of outcomes, in agreement with large studies showing that HF outcomes are independent of LVEF, being similar for HFpEF, HFmrEF and HFrEF groups. [7] Similar to our findings, a recent study of 463 patients with HFpEF showed no association between endocardial GLS and mortality or a composite of mortality or rehospitalization at 1 year. [94] While reduced GLS_ENDO has previously been shown to have incremental value over LVEF in outcomes prediction in acute heart failure, NT-proBNP, a robust and widely available predictor of mortality, [95, 96] was not included in the reported outcomes model. Case in point, in the current study, GLS_ENDO, GLS_AVE and GLS_EPI and even LVEF were all significantly predictive of outcomes in univariable analysis, but of these only GLS_AVE remained independently associated with clinical outcomes when including NT-proBNP and age in the outcomes model.

The limited improvement in endocardial-specific strain over LVEF for detection of dysfunction or prognosis might be expected given the strong relationship between volumetric function, from which LVEF is defined, and deformations of the endocardial surface. Recently, Stokke *et al* highlighted the direct relationship between endocardial strains and LVEF, and that LV wall thickness becomes a modulator of this relationship when considering average strains, measured across the wall thickness.[97] Specifically, their mathematical model showed how thicker ventricles can have reduced average strains across the wall thickness in the presence of preserved LVEF. Similarly, MacIver *et al* illustrated the mechanism by which mid-wall global strains can be reduced in the presence of normal ejection fraction as a result of increased wall thickness, based solely on geometry.[98] Similar geometric models linking wall thickness, LVEF and strains, with similar conclusions, have previously been described.[99] It is thus possible that the superior prognostic performance of GLS_AVE over endocardial strains reflects its dependence on both systolic strain and LV mass, where LV mass itself is predictive of cardiovascular outcomes. [100, 101] GRS had similar good outcomes prediction performance as compared to GLS_AVE. Like GLS_AVE, GRS directly incorporates geometric information

from the full thickness of the myocardium. Additionally, reduced GRS was shown to be associated with increased concentricity (LV mass/LVEDV), so like GLS_AVE, may integrate structural remodeling and reduced function. Global radial strains measured from short axis (GRS_SAX) or long axis (GRS_LAX) images had similar values in all groups and similar outcomes prediction performance. It is unclear why GLS_EPI was not significantly predictive of outcomes, given its sensitivity to systolic dysfunction in heart failure in the current study, and its association with structural remodeling, similar to GRS. It is possible that increased measurement variability at the epicardium has contributed to this finding. Similar to previous studies, reproducibility of endocardial strain was superior to those measured on the epicardium.[102]

It should be acknowledged that the conventional strain components, longitudinally or circumferentially, are not along the direction of fiber shortening. Fibers are helically orientated at the endocardium and epicardium.[50] It is possible that reduced strain along a single direction at the epicardium, for example, could reflect changes in fiber orientations and function across the thickness of the heart wall.[103]

Dependence on Sex

Similar to previous studies [73, 91], men were shown to have lower absolute strain values than women for most strain components, necessitating the definition of sex-specific normal values.

Study Limitations

Our study has a modest sample size and number of events for outcomes analysis, a reflection of the clinical stability of our HF cohort, which may limit the generalizability of the reported findings. However, based on the suggested 10 outcome events per predictor, our use of age, log (NT-proBNP) with each CMR parameter separately (i.e. 3 predictors in the composite model), our observed 33 events (mortality at 5 years) are sufficient. The base model, while only including age and NT-proBNP was established based on AIC forward selection including all cardiovascular risk factors and disease history with p-values <0.2 and is thus robust and representative. Also, age and NT-proBNP have previously been reported to be the strongest predictors of mortality among clinical characteristics in patients with HF or without HF. [96] An additional limitation is the generalizability of the reported findings given the heterogeneity of the underlying pathologies of

heart failure, some of which may not follow the trends reported in the current study. For example, endocardial strains have been shown to have superior prognostic performance in ischemic disease [78, 79]. Nonetheless, the overall significant findings for GLS_EPI, GLS_AVE and GRS speak to the robustness of these metrics across a wide spectrum of functional abnormalities. The calculation of average strain across the wall is limited by the relatively poor contrast within the myocardium, which may lead to errors in this strain component. This is an intrinsic limitation of CMR feature tracking with conventional cine imaging, for which the myocardium has relatively uniform signal intensity. The HFpEF group in the current study was slightly older than the healthy control and at-risk groups, which may contribute to the lower observed strains in this group, however, the relatively small expected decline in strains beyond 50 years of age [90] suggests these effects will be negligible. Age was also included as a co-factor in all statistical analyses to address potential age effects. CMR has lower availability than echocardiography for the measurement of strain. However, recent speckle tracking study of healthy subjects reported similar GLS layer-specific values to those reported in the controls in the current study [90, 91], suggesting that current echocardiographic methods are similar to CMR for layer specific stain evaluation. Also, direct comparison of strain measured with CMR feature tracking and speckle tracking echocardiography has shown good inter-technique agreement [104]. Finally, the reported findings remain to be verified in an independent validation cohort.

CONCLUSION

Global strains measured on endocardium, epicardium or average across the wall thickness are not equivalent for the identification of dysfunction or outcomes prediction in heart failure. The endocardium-specific strains were shown to have poorest all-around performance. GLS_AVE and GRS were the only CMR parameters to be significantly associated with 5-year all-cause mortality. GLS_EPI, GLS_AVE, GRS and the relative difference in endocardial and epicardial strains differentiated HFpEF patients from healthy controls, and increased LV mass and LV Mass/LVEDV were generally associated with reduced strain in those with preserved LVEF.

Chapter 3: Cardiac remodeling is prevalent in patients with chronic heart failure and predicts clinical outcomes – results from the Alberta HEART study

3.1 INTRODUCTION

Heart failure (HF) is a progressive and complex syndrome with poor prognosis.[1] Cardiac remodeling clinically manifests as a change in size, shape and function of the heart, and plays a crucial role in the development[105] and progression of HF.[106] Changes in cardiac geometry have been shown to predict outcome in pre-clinical[107] and clinical HF[108] and can be used to assess response to therapy.[16, 56, 109-112] Cardiac imaging is a common surveillance strategy for patients with HF[113] however this approach is not supported by expert opinion, principally due to concerns of cost, access and measurable impact on patient care.[114] Nevertheless, there is limited data characterizing temporal changes in cardiac structure and function and their clinical relevance in patients with chronic HF. To date, imaging studies of cardiac remodeling have largely been limited to patients with heart failure and reduced ejection fraction and are complicated by variable definitions of reverse and adverse remodeling.[115]

Cardiac magnetic resonance (CMR) is well suited for longitudinal study of remodeling due to high reproducibility of cardiac volumes and function. To date, no CMR studies have evaluated serial changes in cardiac geometry and function in patients with chronic HF.

We hypothesized that cardiac remodeling assessed longitudinally by serial CMR is common among patients with chronic HF and is predictive of clinical outcomes.

3.2 METHODS

3.2.1 Study Population

Institutional approval for this study was acquired from the Health Research Ethics Boards at the University of Alberta and University of Calgary. Written informed consent was obtained from all study participants. Recruitment and examination procedures have been previously described.[71] In

brief, patients with HF and those at-risk for HF were recruited from adult ambulatory clinics and underwent comprehensive phenotyping that included a detailed medical history and physical examination, serum biomarkers and a multi-parametric CMR exam. Individuals at-risk for HF had a history of coronary artery disease, diabetes mellitus, hypertension, atrial fibrillation, and/or obesity without a diagnosis of HF (AHA/ACC class A and B). Patients with HF (AHA/ACC Class C), were sub-grouped into those with preserved (HFpEF, LVEF ≥50%) or reduced ejection fraction (HFrEF, LVEF <50%).[1] Baseline clinical parameters were used to calculate the MAGGIC risk score[62] as a measure of HF burden. Screened patients with HF < 6 months duration or with a contraindication to magnetic resonance imaging were excluded.

3.2.2 CMR Protocol

All subjects underwent a baseline and 1-year CMR scan on Siemens Sonata or Avanto 1.5 T system (Siemens Healthcare, Erlangen, Germany). Imaging sequences included steady-state free precession (SSFP) cine imaging in long-axis and short-axis projections to determine ventricular volumes and function as well as late gadolinium enhancement (LGE) imaging with 0.15mmol/kg of gadolinium contrast to assess for the presence of myocardial scar. Typical imaging parameters for SSFP cines: repetition time/echo time 2.8ms/1.4 ms, 50-70 degree flip angle, 8 mm slice thickness with a 2 mm gap for short axis slices, 256 x 192 matrix, 380 x 285 mm field of view, 10 views per segment with 25 or 30 reconstructed cardiac phases per cardiac cycle and for LGE imaging: 380 x 285mm field of view, 256 x 173 matrix, repetition time/echo time 14.7ms/4.2ms, flip angle 25° and inversion time of 300ms. All cardiac images were acquired with ECG gating, using 8mm slice thickness and 2mm gap within 8-12 second breath-holds.

3.2.3 Image Analysis

Ventricular volumes and mass were quantified by a single interpreter (DIP) from short-axis SSFP cines using commercially available image analysis software: Syngo Argus, (Siemens Healthcare, Erlangen, Germany) or CVI42 (Circle, Calgary, Canada). Volumes and mass were normalized to body surface area. Myocardial trabeculations were included in RV and LV end-diastolic volumes and were excluded from LV mass. Left atrial volume was calculated by the area-length biplane method. Strain was measured at a mid-wall contour generated as the mid-point of endocardial and epicardial borders, both of which were traced at end-diastole and propagated to all image frames over the full cardiac cycle using the calculated feature tracking displacement fields, similar to

previous reports.[86] Strain in each slice was calculated as the fractional change of the mid-wall contour in length relative to the end-diastolic cardiac phase using customized analysis software (MATLAB 2017.a). Global circumferential systolic strain (GCS) was calculated as the average of the peak strains from two-mid-ventricular short-axis slices. Similarly, global longitudinal systolic strain (GLS) was calculated as the average of the peak strains from the three long-axis slices.

Myocardial scar quantification was measured from magnitude LGE images using commercially available software (CVI42, Circle Cardiovascular Inc., Calgary, Canada). A threshold of 5 standard deviations (SD) from the mean signal of a reference normal region of interest was used to define the scar signal.[116, 117] Total scar mass was expressed as the absolute value in grams and the relative value as a percentage of the LV mass. Furthermore, baseline myocardial scar was classified into 5 categories: no scar, ischemic scar, minor non-ischemic scar, major non-ischemic scar or no contrast given.[40]

3.2.4 Cardiac Remodeling

LV volumes and mass were remeasured in 20 patients from the overall cohort selected at random to determine intra-observer variability and coefficient of variation (CoV). Cardiac remodeling was calculated using the reference change value (RCV), a measure of test variability due to biological variation and observer reproducibility.[118] RCV = $k \times \sqrt{2} \times$ average CoV, where k=1.65 for a one-tailed test. [119] Indices of adverse remodeling were defined as a 1 year increase in LV volume, LV mass, RV volume or left atrial volume greater than RCV or a 1 year worsening of cardiac function (a decrease in LV ejection fraction (EF) or RVEF or increase in global strain) greater than RCV. Indices of reverse remodeling were defined as a 1 year reduction in LV volume, LV mass, RV volume, left atrial volume greater than RCV or a 1 year improvement in cardiac function (an increase in LVEF or RVEF or decrease in global strain) greater than RCV.

3.2.5 Clinical Outcomes

Clinical events were identified from electronic health records (International Classification of Diseases codes version 10) and direct patient contact during 4 year follow up from 1-year scan and the primary outcome was a time to first composite of all-cause mortality, cardiovascular disease related hospitalization and /or emergency department visit.

3.2.6 Statistical Approach

Continuous variables were expressed as mean ± standard deviation or median (25^{th}, 75^{th} percentile), as appropriate. Categorical variables were expressed as frequency and percentage. Missing data was assumed to be missing at random. Multiple imputation with chained equation was used to generate missing data by taking the average of 50 imputations.[88]

Chi-square testing was used to compare categorical variables at baseline and McNemar's test was used to compare medication use at baseline and 1 year. The normal distribution of continuous variables was tested by Shapiro-Wilk normality test. A logarithmic transformation was applied to N-terminal prohormone of b-type brain natriuretic peptide (NT-proBNP) and creatinine. Two sample t-test (or Mann-Whitney U test) or oneway analysis of variances with post-hoc correction (or Dunn's test) was used to compare continuous variables among groups of patients, as appropriate. Paired t-test (or Wilcoxon signed-rank test) was used to compare continuous CMR measures at baseline and 1-year.

The Kaplan-Meier method was used to plot time to clinical events. Univariable Cox proportional regression of outcome was performed in all CMR-derived imaging parameters. Positive multicollinearity of continuous variables was defined as variance inflation factor >10. In the multivariable Cox proportional hazard analysis, all non-collinear CMR parameters of interest with univariable p-value<0.2 were independently tested for their association with composite outcome after adjustment for the base model consisting of the MAGGIC score and log (NT-proBNP).[65] To further assess the association of CMR metrics with clinical outcomes, two statistical approaches were applied: Akaike Information Criterion (AIC) analysis of candidate Cox regression models and likelihood ratio test. For AIC testing, the model with lowest score indicates the best model; with a difference (ΔAIC) >10 indicating a clear advantage for the lower scoring model.[89]

A p value less than 0.05 was considered significant for all tests. Statistical analyses were performed using STATA version 16.0 software (StataCorp LP, College Station, Texas).

3.3 RESULTS

3.3.1 Clinical Findings

The study cohort comprised 262 patients (median age: 68 years, 57% male) and included 96 at-risk for HF, 97 with HFpEF, and 69 with HFrEF. Patients with HFpEF were older and had higher serum creatinine compared to those with HFrEF but otherwise had similar disease, mean MAGGIC score 19±7 vs. 17±8 respectively, p = 0.08. Only 5/262 patients had been hospitalized or visited the emergency department within 30 days of the baseline scan (Table 3.1). Medication use at 1 year for the overall cohort was similar to baseline with 80% on an angiotensin converting enzyme inhibitor or angiotensin receptor blocker, 62% on a beta blocker and 17% on a mineralocorticoid antagonist, p > 0.05 for paired comparison in each case.

3.3.2 Cardiac Magnetic Resonance parameters at baseline and 1 year

Baseline CMR findings are reported in Table 2. Late gadolinium enhancement imaging was acquired at baseline in 205/262 patients. Major non-ischemic scar was found in 14 patients, minor non-ischemic scar in 33, ischemic scar in 30 and no scar in 128.

At 1 year, right ventricular volumes decreased in all 3 patient groups (Table 3.2). Otherwise, cardiac volumes and function remained stable at 1 year in patients at risk for HF. Comparatively at 1 year, patients with HFpEF had more impaired GLS, mean -17.2% vs.-18.0% at baseline, p= 0.03, and a borderline increase in LV mass index, median 58 g/m^2 vs. 56 g/m^2 at baseline, p = 0.05. Conversely, at 1 year patients with HFrEF showed improved cardiac function with a median LVEF 46% vs. 42% at baseline, p<0.001, mean GLS -12.8% vs -11.9% at baseline, p=0.01, and median LVESV index 45 ml/m^2 vs. 55 ml/m^2 at baseline, p<0.001.

Cardiac remodeling was prevalent in all 3 patient groups (Figure 3.1, Table 3.3). Reverse remodeling of LVEDV index was observed in >30% of patients. Reverse remodeling of LVEF was also common but more prevalent in the HFrEF group, 41%, than HFpEF, 13%, and at patients at risk, 10%, p<0.001. Adverse remodeling of LV mass index was more common in the HFpEF group, 33% compared to patients with HFrEF, 17%, p=0.03.

Table 3.1. Baseline clinical characteristics of heart failure cohort

	Overall cohort (n=262)	At risk (n=96)	HFpEF (n=97)	HFrEF (n=69)	P value
Vital Statistics					
Age, years	68(61,76)	64(59,72)*	72(64,80)†	66(59,76)	<0.001
Male	150(57%)	50(52%)	52(54%)	48(70%)	0.05
BMI, kg/m^2	29.9±5.3	29.9±5.3	30.5±5.5	29.0±4.9	0.19
Systolic BP, mmHg	130(118,142)	136(120,151)*†	128(118,142)	128(116,134)	0.002
Heart rate, /min	65(60,76)	68(60,76)	64(60,72)	65(60,73)	0.58
Medical History					
HF duration, years	3(1.5,5)	NA	2.8(1.5,5)	4(2,8)	0.14
New York Heart Association class	1.9±0.7	NA	1.8±0.7	2.0±0.7	0.23
Hypertension	194(74%)	77(80%)	75(77%)	42(61%)	0.01
Diabetes mellitus	88(33%)	28(29%)	35(36%)	25(36%)	0.52
Coronary artery disease	88(34%)	20(21%)	42(43%)	26(38%)	0.009
Atrial fibrillation	83(32%)	18(19%)	38(39%)	27(39%)	0.003
Current smoker	25(10%)	10(10%)	10(10%)	5(7%)	0.75
COPD	34(13%)	5(5%)	18(19%)	11(16%)	0.02
Renal Insufficiency	31(12%)	1(1%)	17(18%)	13(19%)	<0.001
ACEI or ARB use	209(80%)	71(74%)	82(85%)	56(81%)	0.18
Beta blocker use	165(63%)	31(32%)	75(77%)	59(86%)	<0.001
MRA use	45(17%)	3(3%)	14(14%)	28(41%)	<0.001
CV hospitalization /ED visit in last 30 days	5(2%)	1(1%)	2(2%)	2(3%)	0.85
Laboratory Test					
Creatinine, umol/L	89(76,108)	81(72,92)*†	101(80,125)†	90.0(78,109)	<0.001
NT-proBNP, pmol/L	24(7,88)	7(3,18)*†	66(22,149)	43(20,122)	<0.001
MAGGIC score	16.0±6.8	12.7±4.6*†	18.7±6.7	16.7±7.6	<0.001

Continuous variables expressed as mean ± standard deviation or median (25-75th percentile) as appropriate. P value for comparison of 3 groups. * $P < 0.05$ compared to HFpEF; † $P < 0.05$ compared to HFrEF.

Abbreviations: NA = not applicable; HFpEF = heart failure with preserved ejection fraction; HFrEF = heart failure with reduced ejection fraction; BMI = body mass index; BP = blood pressure; HF = heart failure; COPD = chronic obstructive pulmonary disease; ACEI = angiotensin converting enzyme inhibitor; ARB = angiotensin II receptor blocker; MRA = mineralocorticoid antagonist; CV = cardiovascular; ED = emergency department; NT-proBNP = N-terminal pro b-type natriuretic peptide; MAGGIC = Meta-Analysis Global Group in Chronic Heart Failure.

Table 3.2. Baseline versus 1-year cardiac magnetic resonance measurements in patient groups

Variable	At risk (Baseline)	At risk (1 year)	P value	HFpEF (Baseline)	HFpEF (1 year)	P value	HFrEF (Baseline)	HFrEF (1 year)	P value
LVEF, %	64(59,70)	65(60,70)	0.08	61(55,65)	62(55,67)	0.43	42(35,45)	46(39,51)	<0.001
LVEDVi, ml/m^2	65(58,78)	68(56,77)	0.27	66(58,77)	67(56,77)	0.37	98(79,116)	87(72,111)	0.07
LVESVi, ml/m^2	24(18,31)	23(18,29)	0.06	26(20,32)	25(19,32)	0.11	55(44,72)	45(38,63)	<0.001
LV massi, g/m^2	54(45,69)	56(48,64)	0.32	56(48,67)	58(50,70)	0.05	73(61,82)	70(57,82)	0.09
LV mass/LVEDV	0.81 (0.72,0.91)	0.83 (0.75,0.90)	0.55	0.85 (0.71,0.96)	0.85 (0.75,0.99)	0.13	0.74 (0.64,0.88)	0.76 (0.66,0.87)	0.37
RVEF, %	60(55,66)	60(54,66)	0.76	57(51,62)	57(50,65)	0.29	52(45,57)	53(45,57)	0.72
RVEDVi, ml/m^2	69(55,76)	62(53,71)	<0.001	64(53,77)	62(50,75)	0.009	73(64,92)	72(54,84)	0.005
RVESVi, ml/m^2	26(20,33)	25(19,31)	0.002	28(22,35)	26(20,35)	0.01	33(27,43)	33(25,40)	0.12
LAVi, ml/m^2	37(29,48)	40(28,48)	0.99	51(36,71)	51(38,66)	0.35	53(43,63)	52(49,62)	0.44
GLS, %	-18.9±3.6	-19.1±3.1	0.34	-18.0±3.3	-17.2±4.0	0.03	-11.9±2.8	-12.8±3.9	0.01
GCS, %	-19.2±3.2	-19.1±3.6	0.66	-18.5±3.6	-18.0±4.0	0.18	-11.2±3.0	-11.9±3.2	0.03
Scar prevalence, %*	20(24%)	20(24%)	1.0	16(37%)	21(41%)	0.18	28(51%)	36(73%)	0.008
Scar mass, g	0(0,0)	0(0,0)	0.65	0(0,5.8)	0(0,6.1)	0.44	7.0(0,24.2)	8.8(0,25)	0.002
Scar %LV	0(0,0)	0(0,0)	0.36	0(0,5.3)	0(0,5.6)	0.89	6(0,16.2)	6.8(0,16)	0.01

Continuous variables expressed as mean ± SD or median (25-75th percentile), as appropriate. P-values for comparison between baseline and 1 year measurement.

*183/262 patients underwent late gadolinium enhancement imaging at both baseline and 1 year.

Abbreviations: HFpEF = heart failure with preserved ejection fraction; HFrEF = heart failure with reduced ejection fraction; LVEF = left ventricular ejection fraction; LVEDVi = left ventricular end-diastolic volume index; LVESVi = left ventricular end-systolic volume index; LV massi = left ventricular mass index; LAVi = left atrial volume index; RVEF = right ventricular ejection fraction; RVEDVi = right ventricular end-diastolic volume index; RVESVi = right ventricular end-systolic volume index; GLS = global longitudinal strain; GCS = global circumferential strain; MAGGIC = Meta-Analysis Global Group in Chronic Heart Failure.

Table 3.3. Prevalence of adverse remodeling and reverse remodeling in patient groups

Adverse remodeling								
	CoV	**RCV**	**Overall (n=262)**	**At risk (n=96)**	**HFpEF (n=97)**	**HFrEF (n=69)**	**P_1 value**	**P_2 value**
LVEF, %	0.073	17%	12(5%)	2(2%)	7(7%)	3(4%)	0.23	0.44
LVEDVi,ml/m^2	0.031	7%	70(27%)	24(25%)	28(29%)	18(26%)	0.82	0.69
LVESVi, ml/m^2	0.051	12%	54(21%)	24(25%)	23(24%)	7(10%)	0.04	0.03
LV massi, g/m^2	0.059	14%	74(28%)	30(31%)	32(33%)	12(17%)	0.06	0.03
GLS, %	0.035	8%	71(27%)	18(19%)	33(34%)	20(29%)	0.05	0.49
GCS, %	0.063	15%	45(17%)	14(15%)	20(21%)	11(16%)	0.51	0.45
RVEF, %	0.083	19%	22(8%)	4(4%)	6(6%)	12(17%)	0.006	0.02
RVEDVi, ml/m^2	0.071	17%	37(14%)	10(10%)	18(19%)	9(13%)	0.26	0.34
RVESVi, ml/m^2	0.18	41%	21(8%)	8(8%)	8(8%)	5(7%)	0.96	0.81
LAVi, ml/m^2	0.11	27%	60(23%)	26(27%)	22(23%)	12(17%)	0.34	0.41

Reverse remodeling								
	CoV	**RCV**	**Overall (n=262)**	**At risk (n=96)**	**HFpEF (n=97)**	**HFrEF (n=69)**	**P_1 value**	**P_2 value**
LVEF, %	0.073	17%	51(19%)	10(10%)	13(13%)	28(41%)	<0.001	<0.001
LVEDVi,ml/m^2	0.031	7%	97(37%)	34(35%)	35(36%)	28(41%)	0.77	0.56
LVESVi, ml/m^2	0.051	12%	108(41%)	34(35%)	41(42%)	33(48%)	0.27	0.48
LV massi, g/m^2	0.059	14%	50(19%)	17(18%)	17(18%)	16(23%)	0.60	0.37
GLS, %	0.035	8%	89(34%)	31(32%)	27(28%)	31(45%)	0.07	0.02
GCS, %	0.063	15%	64(24%)	20(21%)	19(20%)	25(36%)	0.03	0.02
RVEF, %	0.083	19%	36(14%)	8(8%)	9(9%)	19(28%)	0.001	0.002
RVEDVi, ml/m^2	0.071	17%	76(29%)	20(21%)	32(33%)	24(35%)	0.08	0.81
RVESVi, ml/m^2	0.18	41%	24(9%)	4(4%)	10(10%)	10(14%)	0.07	0.41
LAVi, ml/m^2	0.11	27%	39(15%)	15(16%)	15(15%)	9(13%)	0.88	0.66

Definitions: Reference change value = $k \times \sqrt{2} \times$ CoV, where k=1.65 for a one-tailed test. Adverse remodeling = 1-year increase in volume or mass or decrease in function (EF and GLS) greater than RCV. Reverse remodeling = 1-year decrease in volume or mass or increase in function (EF

and GLS) greater than RCV. Abbreviations: CoV = coefficient of variation; RCV = reference change value; see Table 2 for others. P_1-value for comparison of 3 groups. P_2-value for comparison of HFpEF vs. HFrEF.

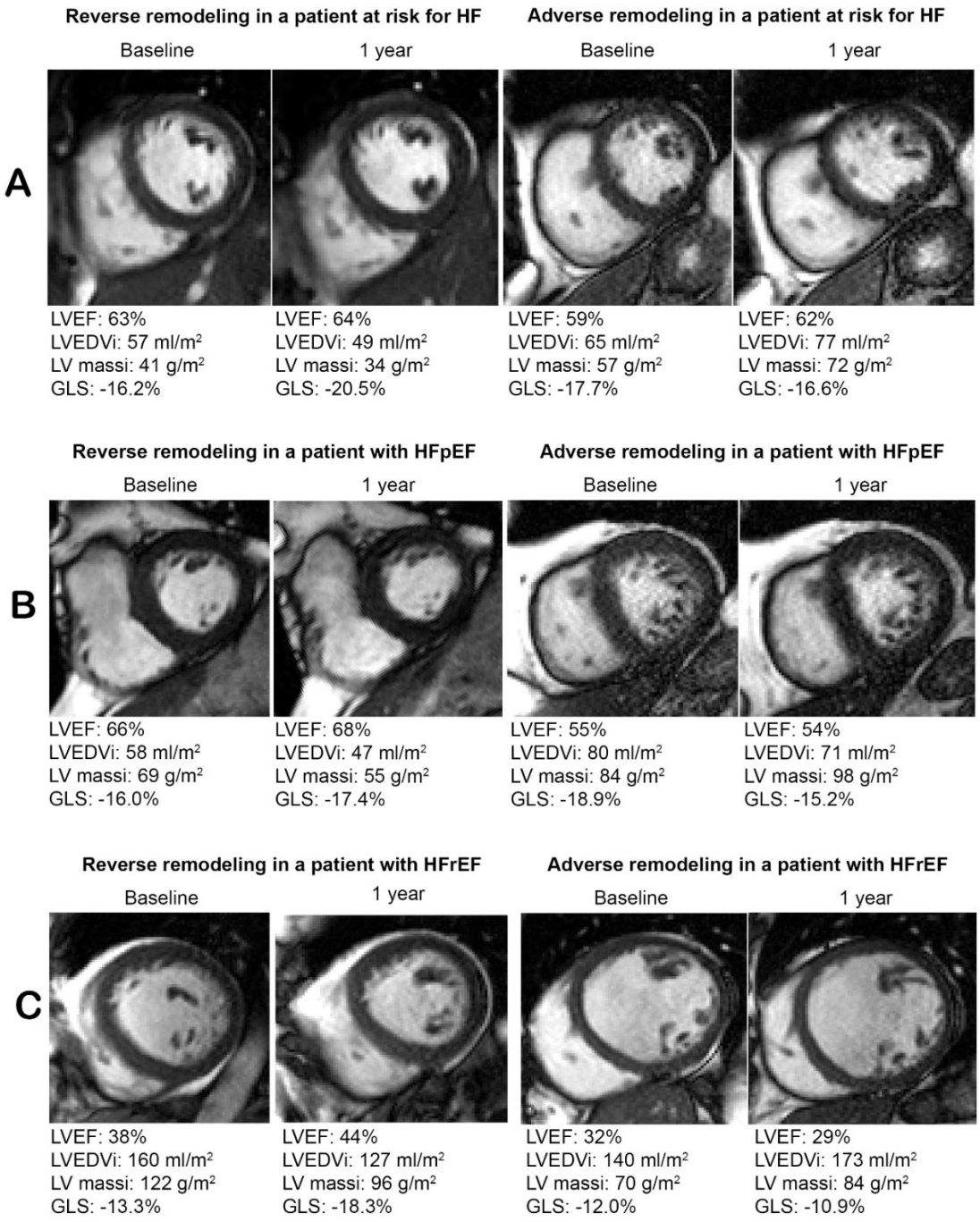

Figure 3.1. Examples of reverse remodeling and adverse remodeling for patients at risk (panel A), with HFpEF (panel B) and with HFrEF (panel C).

Abbreviations: HF = heart failure; HFpEF = heart failure with preserved ejection fraction; HFrEF = heart failure with reduced ejection fraction; LVEF = left ventricular ejection fraction; LVEDVi = left ventricular end-diastolic volume index; LV massi = left ventricular mass index; GLS = global longitudinal strain.

3.3.3 CMR predictors of outcome

In the overall cohort, after 4 years of follow-up from the 1-year scan there were 86 events including 18 deaths, 51 cardiovascular disease related hospitalizations and/or 56 related emergency department visits.

In multivariable analyses adjusting for MAGGIC score and log (NT-proBNP), the only CMR measure at baseline predictive of outcome was the presence of major non-ischemic scar, hazard ratio (HR) 2.3, 95% confidence intervals (CI) (1.1, 4.7), p = 0.021.

In terms of cardiac remodeling for the overall cohort, only % Δ LV mass index, HR 1.14, 95% CI (1.02,1.27) per 10% increase, p = 0.02, and % Δ GLS, HR 0.99, 95% CI (0.98,1.00) per 1 % increase, p = 0.04, were independently associated with outcome after adjusting for MAGGIC score and log (NT-proBNP) (Table 3.4). However, % Δ LVEF was not associated with outcome, HR 1.07, 95% CI (0.96,1.19) per 10 % increase, p = 0.24. Patients with adverse remodeling (defined as 1 year increase in LV mass index > 14% from Table 3.3), or no remodeling (1 year change in LV mass index ≤ 14%) had increased risk for clinical events compared to patients with reverse remodeling (1 year decrease in LV mass index > 14%), HR 2.9, 95% CI (1.3-6.2), p = 0.006, and HR 2.4, 95% CI (1.2-4.8), p=0.01 respectively. Similarly, in Kaplan-Meier analysis, patients with reverse remodeling of LV mass index had fewer events than those with adverse or no remodeling, log-rank p = 0.005. (Figure 3.2)

3.3.4 Discrimination performance of dynamic remodeling

To identify the incremental prognostic performance of longitudinal changes in CMR parameters, significant predictors of outcome from Table 4 were each modeled with baseline predictors. % Δ LV mass index and % Δ GLS each demonstrated added value over baseline predictors likelihood ratio test (Figure 3.3).

Table 3.4. Regression analysis of dynamic remodeling for predicting subsequent death, cardiovascular hospitalization or emergency department visit at 5 years

	Overall cohort: 262 subjects (86 events)			
	Univariable Cox analysis		Multivariable Cox analysis	
	Hazard Ratio	P value	Hazard Ratio	P value
% Δ LVEF, per 10% increase	1.09(0.97,1.22)	0.15	1.07(0.96,1.19)	0.24
% Δ LVEDVi, per 10% increase	0.98(0.86,1.12)	0.75		
% Δ LVESVi, per 10% increase	0.98 (0.90,1.07)	0.66		
% Δ LV massi, per 10% increase	1.12(1.01,1.25)	0.03	1.14(1.02,1.27)	0.02
% Δ LV mass/LVEDV, per 0.1 increase	2.87(1.22,6.77)	0.02	1.04(0.97,1.11)	0.25
% Δ RVEF, per 10% increase	0.98(0.89,1.09)	0.73		
% Δ RVEDVi, per 10% increase	0.97(0.88,1.06)	0.49		
% Δ RVESVi, per 10% increase	1.01(0.95,1.08)	0.76		
% Δ LAVi, per 10% increase	1.04(0.99,1.09)	0.15	1.05(0.99,1.10)	0.08
% Δ GLS, per 1% increase	0.99(0.99,1.00)	0.16	0.99(0.98,1.00)	0.04
% Δ GCS, per 1% increase	1.00(0.99,1.01)	0.63		
Δ Scar mass, per 10 g increase*	1.85(1.07,3.20)	0.03	1.84(1.04,3.24)	0.02
Δ Scar % LV, per 10% increase*	1.80(0.85,3.81)	0.12	1.70(0.79,3.66)	0.17

Definitions: Multivariable analyses were performed in variables with univariable P value<0.2 and were adjusted for MAGGIC score + log (NT-proBNP).

* 183/262 patients had late gadolinium enhancement imaging at both baseline and 1 year (49 events).

Abbreviations: see Table 2.

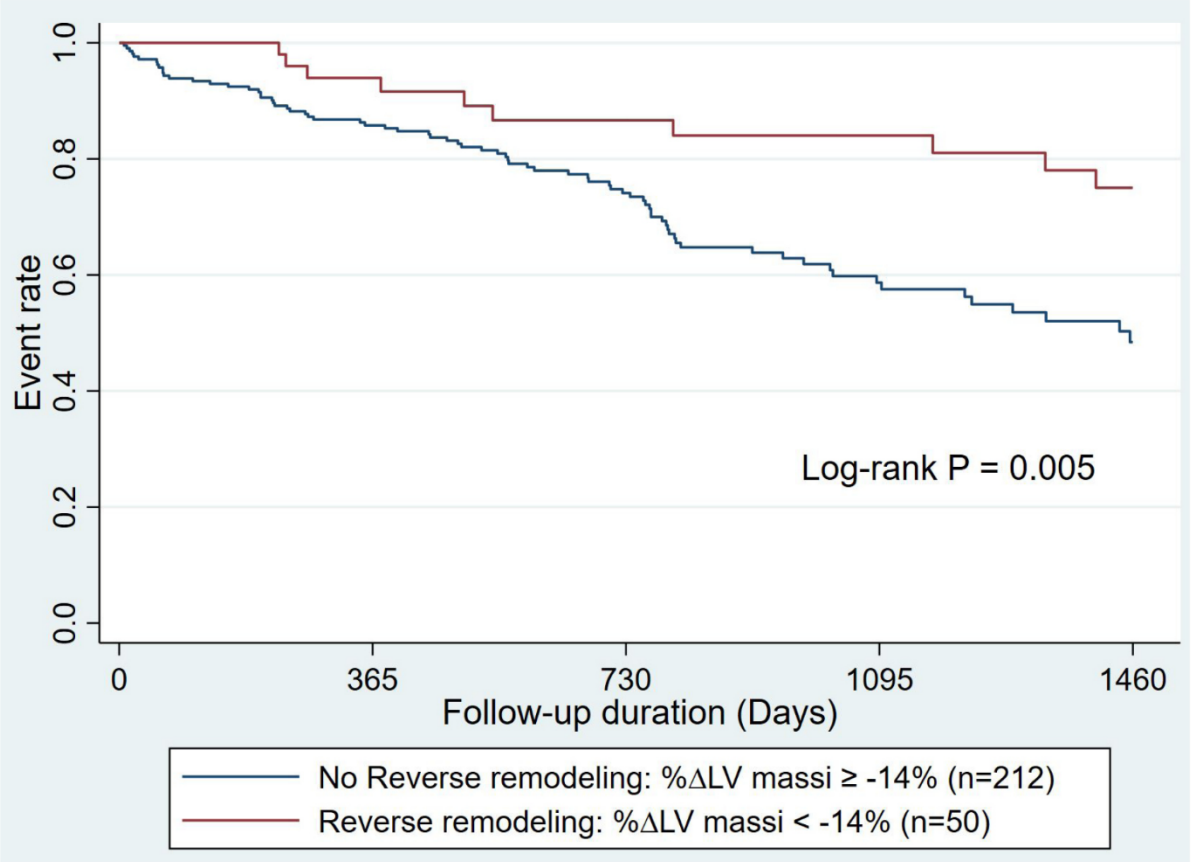

Figure 3.2. Kaplan-Meier analysis of reverse remodeling of LV mass index for predicting outcome

Definitions: Outcome = death, cardiovascular hospitalization or emergency department visit at 4 years from 1-year scan; Reverse remodeling = 1-year decrease in LV mass index greater than reference change value from Table 3.

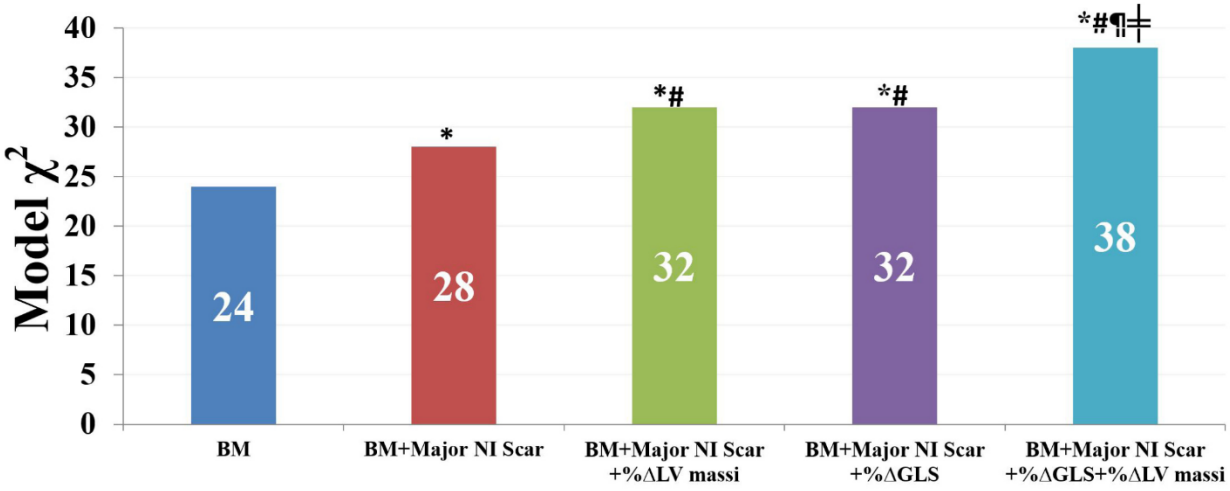

Figure 3.3. Stepwise incremental value of cardiac parameters for predicting outcome by Global model χ^2 test

Definitions: Outcome = death, cardiovascular hospitalization or emergency department visit at 4 years from 1-year scan; Base Model = MAGGIC score + log (NT-BNP). Abbreviations: BM = Base Model; GLS = global longitudinal strain. LV massi = left ventricular mass index; NI = non-ischemic.

* p value < 0.05 for comparison with Base Model by likelihood ratio test;
# p value < 0.05 for comparison with Base Model + major non-ischemic scar;
¶ p value < 0.05 for comparison with Base Model + major non-ischemic scar + % Δ LV mass index;
╪ p value < 0.05 for comparison with Base Model + major non-ischemic scar + % Δ GLS

AIC analysis showed that among all the candidate models, the optimal model with the lowest AIC score consisted of the baseline predictors, 1 year change in GLS and the presence or absence of reverse remodeling by LV mass index (Supplemental Table 3.1). This model incorporating % Δ GLS and reverse remodeling significantly improved the prediction of outcome over baseline predictors: MAGGIC score, log (NT-proBNP) and presence of major non-ischemic scar, ΔAIC ≥ 10.

Supplemental Table 3.1. Stepwise predictive performance of outcome by candidate models by Akaike information criterion

Model	Candidate sets of models	AIC	ΔAIC*i*
1	Base Model	853.2	11.9
2	Base Model + Major non-ischemic scar	852.5	11.2
3	Base Model + % Δ LV massi	850.2	8.9
5	Base Model + Reverse remodeling (LV massi)	845.8	4.5
6	Base Model + % Δ GLS	851.4	10.1
7	Base Model + Major non-ischemic scar + % Δ LV massi	850.4	9.1
8	Base Model + Major non-ischemic scar + Reverse remodeling (LV massi)	846.1	4.8
9	Base Model + Major non-ischemic scar + % Δ GLS	850.2	8.9
10	Base Model + Major non-ischemic scar+ % Δ GLS+ % Δ LV massi	846.6	5.3
11	Base Model + Major non-ischemic scar+ % Δ GLS + Reverse remodeling (LV massi)	841.3	0

Abbreviations: LV massi = left ventricular mass index; GLS = global longitudinal strain; MAGGIC score = Meta-Analysis Global Group in Chronic Heart Failure risk score.

Definitions: Base Model: MAGGIC score + log (NT-proBNP). Reverse remodeling (LV massi): a 1-year decrease in LV massi > 14%. $\Delta AIC_i = AIC_i - AIC_{minimum}$ where $AIC_{minimum}$ = Model 11.

3.4 DISCUSSION

In this prospective cohort study of patients with stable, chronic HF and those at risk, we found a high prevalence of cardiac remodeling, expressed as a change in cardiac volume, mass or function during 1 year follow-up. Reverse remodeling was common, especially in patients with HFrEF, whereas adverse remodeling predominated in patients with HFpEF. More importantly, cardiac remodeling defined as a change in LV mass index or GLS predicted long-term outcomes for these patients, even after adjustment for baseline clinical risk.

To our knowledge, this is the first study to comprehensively investigate longitudinal changes in cardiac structure and function in individuals across the entire HF spectrum. In an echo-based cohort study of patients with incident HF, Dunlay et al. found that on average patients with HFpEF had decreased LVEF and those with HFrEF had increased LVEF during 5 years of follow-up.[120] However other measures of cardiac structure and function were not reported. Notably, the reproducibility of echocardiography is suboptimal due to low resolution, restricted acoustic window, geometric assumption, and operator dependence. This variation of repeated echo measures is an important limitation of longitudinal echo-based studies of heart failure. CMR, by contrast, has become the gold standard of assessing cardiac function and volume and its high reproducibility makes it the ideal modality of identifying change on serial examinations. To date, no CMR study has explored dynamic remodeling of cardiac structure and function.

Most prior imaging studies of patients with HF have evaluated the prognostic potential of cardiac measures at a single time-point and have identified cardiac function and/or geometry as the best predictors of outcome. In cross-sectional echo studies, LV mass predicts outcome for patients with HFpEF[121, 122] however its prognostic utility in HFrEF is less well established. In our cohort after correcting for clinical risk, the only CMR measure at baseline predictive of outcome was the presence of major non-ischemic scar. Similarly, Shanbhag et al recently found that major non-ischemic scar was the best CMR predictor of adverse outcome in a well-characterized cross-sectional study of patients without HF.[40]

Longitudinal imaging studies of HF have typically evaluated changes in LV volume and/or ejection fraction and have defined LV remodeling arbitrarily using a threshold of 10 - 15%.[109, 111, 115, 123] In our study, thresholds for indices of LV remodeling were defined using reference change value, a measure of test variability, and predictors of outcome were identified through regression analyses. We did not find a change in LV volume or ejection fraction to be associated with outcome in our well-characterized cohort. However, a 1-year decrease in LV mass index of > 14% strongly predicted event free survival. Compared to other cardiac structural and functional parameters, LV mass is less susceptible to transient changes in loading conditions and is therefore a potentially more reliable interstudy measure of remodeling. Change in GLS was also identified as an important predictor of outcome in our study. To date, change in GLS has been shown to predict outcome in patients following cardiac resynchronization[56] and those

with amyloidosis.[124] The effects of drug and device therapies on LV mass and GLS in patients with chronic HF remain to be determined.

Our study results confirm that HF is a dynamic process, even in patients with chronic disease on stable medical therapy. In our overall cohort, adverse remodeling was present in 28% on LV mass index and 27% on GLS whereas reverse remodeling was present in 19% on LV mass index and 34% on GLS. Reverse remodeling of LV mass index was also strongly predictive of outcome. The utility of imaging guided care has not been evaluated in ambulatory HF. The GUIDE-IT HF trial did not find a survival advantage for patients with chronic HFrEF undergoing serial measures of NT-proBNP during a mean of 15 months follow-up.[125] However, our results suggest that serial imaging measures provide long-term (> 1 year) prognostic information. Interestingly, reverse remodeling was also prevalent in patients with HFpEF, and has the potential to yield excellent prognostic information. Dynamic changes in cardiac structure and function were also prevalent in patients at risk for HF. Adverse remodeling was present in 31% whereas reverse remodeling was present in 18% on LV mass in patients at risk for HF which was similar to patients with HFpEF. However, as expected, patients at risk for HF had a substantially lower burden of co-morbid disease, lower serum NT-proBNP and much fewer events of adverse outcome compared to patients with HFpEF.

Study limitations

This study's sample size limit subgroup analyses of survival. However, due to the high reproducibility of CMR for cardiac volumes and function and the number of events in the overall cohort during 4-year follow-up, we were able to build comprehensive predictive models of outcome that included both clinical, biomarker and imaging parameters. In our study, late gadolinium enhancement was not available in 31% of patients at both time points, thus limiting the evaluation of scar remodeling in HF. Our cohort included diverse HF etiologies and thus these results may not apply to specific cardiomyopathy subtypes. Similarly, patients with cardiac electronic implantable devices are common in patients with HF and were an exclusion criterion for CMR in our study. Hence patients with severe LV dysfunction and ischemic cardiomyopathy were potentially under-represented in our HFrEF group. The relatively high prevalence of cardiac remodeling in patients at risk for HF is an intriguing result however its relationship to

downstream incident heart failure is beyond the scope of our study. Ultimately, the utility of routine surveillance imaging for ambulatory patients with HF (and those at risk) should be evaluated in a randomized controlled trial.

3.5 CONCLUSION

Our study confirms that cardiac remodeling is common in patients with chronic HF, even with apparent good disease control. One-year change in LV mass and/or global longitudinal strain strongly predict outcome, even after adjustment for baseline clinical risk, whereas change in LVEF was not predictive. This suggests that, in patients with chronic HF, the serial imaging surveillance of LV mass and global longitudinal strain is more valuable than LVEF. Future studies should evaluate mechanisms of adverse and reverse remodeling and if surveillance cardiac imaging can guide care and improve outcome for patients with chronic HF.

Chapter 4: Development and validation of a novel imaging predicting model beyond traditional risk profile in patients with chronic heart failure: a cardiac magnetic resonance study

4.1 INTRODUCTION

Numerous risk models have been established[126] to identify patients with heart failure (HF) at high risk for adverse events, however only a few of them have been external validated and the majority of the validated models have been predominately based on traditional risk factors. For instance, the Meta-Analysis Global Group in Chronic (MAGGIC) Heart Failure Risk Score[62] is a well-validated HF risk prediction model.[65, 127] This model utilizes data from demographics, disease status, cardiovascular risk factors, serum biomarkers, medication usage however it only includes one cardiac imaging parameter, left ventricular ejection fraction (LVEF). Furthermore, LVEF has been shown to have poor prognostic value in patients with HF.[7, 45] The MAGGIC risk score also performed modestly in external validation studies. The addition of serum BNP has been shown to enhance the predictive performance of the MAGGIC risk score[65] but this has not been studied in combination with cardiac imaging. Similar to the MAGGIC risk score, other HF risk models[64-70] are predominantly driven by patient demographics and medical history. To the best of our knowledge, there have been no well-validated risk models in HF comprehensively evaluating and incorporating cardiac imaging measures.

Cardiac magnetic resonance (CMR) is an accurate and highly reproducible cardiac imaging test. It enables us to comprehensively collect state-of-the-art information on cardiac function, volume, and tissue characterization as a one-stop scan. Unlike echocardiography, biventricular volumes and mass are acquired as true volumetric data acquisitions and is considered as the gold standard evaluation for cardiac structure and function. Current guidelines provide a recommendation for CMR in the diagnosis of patients with HF and are increasingly used in clinical practice. Therefore, the aims of this study were to 1) evaluate the incremental

value of CMR derived parameters of cardiac function and structure on clinical risk prediction models of HF; and 2) evaluate its applicability and validity in an external HF cohort.

4.2 METHODS

4.2.1 Patient identification

The derivation cohort was retrospectively identified from a clinical database at a high volume CMR facility (>1500 cases/year) and included patients referred for assessment of cardiomyopathy and/or heart failure. Medical history and cardiovascular risk factors were identified from electronic health records using the International Classification of Diseases codes version 10 (ICD version10). Cardiovascular medication use was also identified from electronic health record using drug identification number according to the Drug Product Database online query from Health Canada. The retrospective study of the derivation cohort obtained approval from the health ethics research committee of the University of Alberta.

Patients from the validation cohort were prospectively recruited in the Alberta HEART study, a multicenter study of heart failure.[71] In brief, patients with HF and those at-risk for HF were recruited from ambulatory clinics and underwent comprehensive phenotyping that included a detailed history and physical examination and a multi-parametric cardiovascular MRI exam. The Alberta HEART study obtained approval from the health research ethics committees of the Universities of Alberta and Calgary. All patients from the validation cohort provided written informed consent.

The primary composite outcome of both the derivation and validation cohorts consisted of all-cause mortality and cardiovascular disease related hospitalization, which were identified from direct patient contact, vital statistics and electronic health record (Analytics, Data Integration, Measurement and Reporting, Alberta Health Services) during 5 year follow up. Clinical events within 30 days from the CMR were excluded given the likelihood of not being indicative of a new event.

4.2.2 Cardiovascular MRI Protocol

Each subject underwent a comprehensive CMR scan on a 1.5 T magnet (Sonata or Avanto, Siemens, Erlangen, Germany). Imaging sequences included localizers, steady-state free precession (SSFP) cine imaging in long-axis and short-axis projections to determine cardiac volumes and function as well as late enhancement imaging with 0.15mmol/kg of gadolinium contrast to assess for the presence of myocardial scar. Typical imaging parameters for SSFP included a 380x300 mm^2 field of view, 256x162 matrix, 8 mm slice thickness, TE 1.24 ms, TR 2.48 ms, flip angle 51°, 10-14 views/segment and 25-30 phases/cardiac cycle and for LGE imaging: 380 x 285mm field of view, 256 x 173 matrix, repetition time/echo time 14.7ms/4.2ms, flip angle 25° and inversion time of 300ms. All cardiac images were acquired with ECG gating within an 8-12 second breath-hold per slice.

4.2.3 Image analysis

Ventricular volumes and mass were measured using commercially available software (Syngo Argus, Siemens, Erlangen, Germany) or CVI42 (Circle, Calgary, Canada) by three experienced CMR interpreters (DIP, LX and YM). Right and left ventricular volumes were traced from short-axis SSFP cines and indexed to body surface area. Myocardial trabeculations were included in RV and LV end-diastolic volumes but were excluded from LV mass. Left atrial volume was calculated by the area-length biplane method.

Strain was measured from SSFP short and long axis cine images using a custom feature tracking approach similar to other reported.[86, 87] Endocardial and epicardial borders were manually traced only on the end-diastolic image frame by an experienced interpreter for all subjects (LX). A mid-wall contour was generated as the mid-point of the endocardial and epicardial tracings. Subsequently, the end-diastolic contours were automatically propagated to all image frames over the full cardiac cycle using the calculated feature tracking displacement fields. Strain in each slice was calculated for the mid-wall contours as the fractional change in length of the contour from end-diastole to end-systole relative to end-diastolic length, reported as a percentage. Global longitudinal systolic strain (GLS) was calculated as the average of the peak strains from the three long-axis slices. Similarly, global circumferential systolic strain (GCS) was calculated as the average of the peak strains from two mid-ventricular short-axis slices.

Myocardial scar pattern was identified from the magnitude dataset of late gadolinium enhancement (LGE) images by two interpreters (DIP & LX). Myocardial scar was classified into 4 patterns: no presence of scar, ischemic scar, major non-ischemic scar (well-established, classic patterns, e.g., diffuse scar, mid-wall scar, subepicardial, and patchy/immediate scar), minor non-ischemic scar (remaining localized patterns not meeting major criteria, e.g., scar close to aortic root, close to mitral annulus, at the RV insertion point without LV hypertrophy, intermediate basal inferolateral scar).[40] Patients not receiving gadolinium contrast were classified as no LGE image.

4.2.4 Statistics and Outcomes

The normal distribution of continuous variables was tested by Shapiro-Wilk normality test. Continuous variables were expressed as mean ± standard deviation or median (25^{th}, 75^{th} percentile), as appropriate. Categorical variables were expressed as frequency and percentage. Two sample t-test (or Mann-Whitney U test) or Chi-square test were used to compare variables between derivation and validation cohorts, as appropriate.

The analysis consisted of two parts. First part was developing the predictive model (imaging parameters plus base model) from derivation cohort; the second part was externally validating the predictive model in the validation cohort.

4.2.4.1 Developing candidate models from the derivation cohort

The process for establishing the final predictive model is outlined in Figure 1. First, we constructed a multivariable Cox model in the derivation cohort and the proportional odds assumption of every baseline characteristic was tested. Univariable Cox proportional regression was performed in all demographic parameters, cardiovascular risk factors, cardiovascular disease history, and concomitant diseases. The forward selection approach based on Akaike Information Criterion (AIC) was used to build the optimal set of clinical predictors for the base model. In the multivariable Cox proportional hazard analysis, each cardiac MRI parameters was adjusted with the base model to test their independent association with composite outcome. Significant imaging predictors were also tested for multicollinearity using conditioning diagnostics.[128] Multicollinearity was identified either as condition index > 30, or a large variance-decomposition proportions > 50%. The significant imaging parameters with no multicollinearity were added stepwise added to build primary candidate models. Likelihood ratio testing was used to identify

the best secondary candidate models from subgroups of primary candidate models. Finally, Akaike Information Criterion (AIC) analysis and continuous net reclassification improvement (NRI) were used to identify the final predictive model from secondary candidate models. For AIC, the model with lowest score ($AIC_{minimum}$) indicates the best model and Δ_i >10 indicating a significant difference between models.[89] Continuous NRI was used to identify superior outcome predictors among imaging parameters with multicollinearity.

4.2.4.2 External validation of the original predicting model in the validation cohort

We externally validated the final predictive model in the Alberta HEART cohort. The assessment of the external validation included discrimination and calibration.[129] Discrimination evaluated the ability of the final predictive model to distinguish patients experiencing clinical outcome and from those who did not in the validation dataset. The C-statistics was used to assess the discrimination performance with a score 0.7 or more considered to be sufficiently accurate.[130]

Calibration evaluated the agreement between the predicted rate and observed rate of clinical outcome and was checked in Cox regression modeling.[131] First, calibration in-the-large systemically compared the mean predicted event rate and the observed event rate by using the final predictive model in the validation cohort, with a perfect intercept of 0. Calibration slope represented the magnitude of miscalibration, which is the regression slope of the linear predictor, with a perfect slope coefficient of 1.[129, 132] The calibration was performed based on a single time point (5-year composite outcome) and multiple time-points (each year according to 5-year follow-up),[133] respectively. A non-significant difference ($p > 0.05$) between predicted and observed outcomes indicates good calibration.

A p value less than 0.05 was considered significant for all other tests. Statistical analyses were performed using STATA version 16.0 software (StataCorp LP, College Station, Texas).

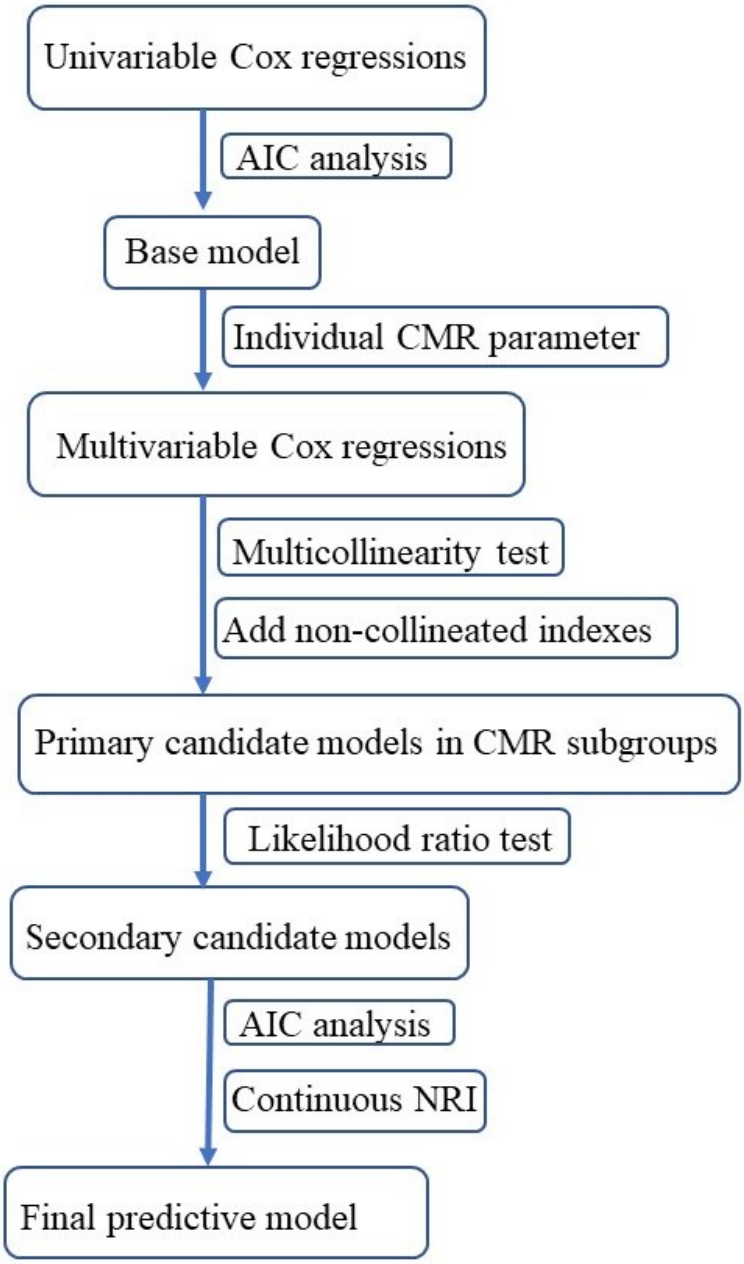

Figure 4.1. Flow chart for the development of the final predictive model. Abbreviations: AIC=Akaike Information Criterion; CMR=cardiac magnetic resonance; NRI=net reclassification improvement.

4.3. RESULTS

4.3.1 Basic characteristics and CMR imaging in derivation cohort.

In derivation cohort, 4400 consecutive scans were screened from 2006-2013 and 766 patients fulfilled study entry criteria. A further 121 patients were excluded including 28 patients with incomplete follow-up and 92 patients with missing clinical information, and 1 patient due to early demise on the day of the scan. Finally, 645 patients with complete clinical, follow-up and imaging data were included in the derivation cohort. In validation cohort, 389 patients underwent a CMR examination however 13 were excluded due to unanalyzable images. The two cohorts had a similar proportion of patients at risk for heart failure (43% vs 38%) and patients with heart failure (57% vs. 62%). The derivation cohort was younger and had a lower incidence of HTN, AF, DM and COPD, but more impaired cardiac function (LVEF, RVEF and GLS), more cardiac remodeling and a higher incidence of major non-ischemic scar. Notably, the derivation cohort also had significant higher incidence of cardiovascular disease- related hospitalization 90 days prior to the CMR scan. (Table 1)

Table 4.1. Comparison of baseline characteristics				
		Derivation cohort (n=645)	Validation cohort (n=376)	P-value
Age, years		53 (40, 65)	68 (61,76)	<0.001
Male gender		429 (67%)	175 (47%)	<0.001
Body mass index, kg/m^2		28.1 (25, 32)	29 (26,33)	<0.001
Prior heart failure		369 (57%)	233 (62%)	0.14
Coronary artery disease		244 (38%)	133 (35%)	0.43
Atrial fibrillation		111 (17%)	116 (31%)	<0.001
Hypertension		200 (31%)	279 (74%)	<0.001
Diabetes mellitus		94 (15%)	131 (35%)	<0.001
Current smoker		108 (17%)	42 (11%)	0.02
Chronic obstructive pulmonary disease		51 (8%)	55 (15%)	<0.001
Chronic kidney disease		90 (14%)	58 (15%)	0.52
CV admission within last 90 days		245 (38%)	10 (3%)	<0.001
Beta blocker		246 (38%)	239 (64%)	<0.001
ACEI/ARB		213 (33%)	300 (80%)	<0.001
LV ejection fraction, %		50 (32,61)	58 (46,66)	<0.001
LV end-diastolic volume index, ml/m^2		90 (71,121)	72 (61,95)	<0.001
LV end-systolic volume index, ml/m^2		44 (28,79)	30 (22,48)	<0.001
LV mass index, g/m^2		71 (58,88)	60 (49,73)	<0.001
RV ejection fraction, %		52 (42,58)	57 (49,64)	<0.001
RV end-diastolic volume index, ml/m^2		81 (67,98)	68 (55,81)	<0.001
RV end-systolic volume index, ml/m^2		38 (30,51)	29 (22,37)	<0.001
Left atrial volume index, ml/m^2		44 (34,60)	45 (32,60)	0.92
Global longitudinal strain, %		14.9±5.8	16.4±4.7	<0.001
Global circumferential strain, %		17.5±7.8	16.6±5.2	0.03
Scar pattern				<0.001
	No scar	165 (26%)	179 (48%)	
	Ischemic	161 (25%)	47 (13%)	
	Minor-nonischemic	99 (15%)	46 (12%)	
	Major-nonischemic	167 (26%)	25 (7%)	
	No contrast given	53 (8%)	79 (21%)	

Values are given as median (95% confidence intervals) or total count (percentage) as appropriate. Abbreviations: CV = cardiovascular, ACEI = angiotensin converting enzyme inhibitor, ARB = angiotensin receptor blocker, LV = left ventricular, RV = right ventricular.

4.3.2 Developing the final predictive model from the derivation cohort

During a mean follow-up of 1456 ± 638 days, 179 of 645 (27.8%) patients in the derivation cohort had a clinical event including 58 deaths and 157 cardiovascular disease related hospitalizations. Following univariable analysis and stepwise forward selection of AIC analysis, clinical characteristics associated with outcome included age, prior HF, CAD, DM, CKD, COPD, and CV hospitalization 90 days prior to CMR scan (Table 2). In the multivariable analysis, after adjustment with the base model, significant CMR predictors of outcome included LVEDVi, LVESVi, LVmassi, LAVi, GLS, and major non-ischemic (MNI) scar (Table 3). Testing for multicollinearity among these 6 CMR parameters yieled a condition index of 34.8 with > 50% for the variance-decomposition proportions of LVEDVi, LVESVi, LVmassi and GLS. Therefore only one of these four parameters were included in each candidate model. Four subgroups of models were built based on these 4 imaging parameters. The remaining two imaging parameters LAVi and presence of MNI scar were added stepwise to LVEDVi, LVESVi, LVmassi or GLS, along with the base model. Consequently, twelve primary candidate models of clinical and CMR parameters were identified (Table 4). Following likelihood ratio testing, four secondary candidate models were identified (Table 5): (i) base model + LVEDVi + MNI scar; (ii) base model + LVESVi + MNI scar; (iii) base model + LAVi + LVmassi; (iv) base model + LAVi + GLS+ MNI scar (Table 6). Finally, AIC analysis identified the best model as base model + LAVi + GLS+ MNI scar with consistently lower AIC score than the base model alone, ΔAIC 12.7. Importantly, GLS had incremental predicting value over LVEDVi (continuous NRI 23.3%, P=0.008) LVESVi (continuous NRI 18.4%, P=0.009) and LV massi (continuous NRI 35.4%, P<0.001).

We applied 2 additional statistical analyses to assess the superiority of the prognostic performance of the final model (base model + LAVi + GLS+ MNI scar) over the base model. The area under the curve of receiver operating characteristics for predicting the composite outcome was higher in the final model than the base model (0.739±0.021 vs. 0.705±0.023, p=0.005). The likelihood ratio test showed that the final predictive model was significantly better than the base model, with Model χ^2 96.5 vs. 77.8, p<0.001.

Table 4.2. Cox Regression of Clinical Parameters for Composite Outcome in the Derivation Cohort (N = 179 events)		
	Univariable analysis	
	Hazard Ratio (95% CI)	p-value
Age, per 10 year increase	1.03 (1.02, 1.04)	<0.001
Male gender	0.96 (0.70, 1.31)	0.81
Body mass index, per 1 kg/m^2 increase	0.98 (0.96, 1.01)	0.21
Prior heart failure	2.21 (1.59, 3.06)	<0.001
Coronary artery disease	1.80 (1.34, 2.41)	<0.001
Atrial fibrillation	1.77 (1.21, 2.61)	0.004
Hypertension	1.80 (1.34, 2.43)	<0.001
Diabetes mellitus	2.35 (1.69, 3.26)	<0.001
Current smoker	1.50 (1.05, 2.13)	0.03
Chronic obstructive pulmonary disease	1.78 (1.21, 2.60)	0.003
Chronic kidney disease	2.47 (1.76, 3.46)	<0.001
CV admission within last 90 days	1.58 (1.18, 2.11)	0.002
Beta blocker	1.43 (1.07, 1.93)	0.02
ACEI/ARB	1.31 (0.97, 1.77)	0.08

Values are given as median (95% confidence intervals).

Abbreviations: CV = cardiovascular, ACEI = angiotensin converting enzyme inhibitor, ARB = angiotensin receptor blocker.

Table 4.3. Cox Regression of Cardiac Magnetic Resonance Parameters for Composite Outcome in the Derivation Cohort (N = 179 events)		
	Multivariable analysis	
	Hazard Ratio (95% CI)	p-value
LV ejection fraction, per 10% decrease	1.03 (0.92,1.15)	0.60
LV end-diastolic volume index, per 10 ml/m^2 increase	1.06 (1.02,1.10)	0.005
LV end-systolic volume index, per 10 ml/m^2 increase	1.05 (1.01,1.09)	0.02
LV mass index, per 10 g/m^2 increase	1.10 (1.04, 1.16)	<0.001
RV ejection fraction, per 10% decrease	1.04 (0.93,1.16)	0.51
RV end-diastolic volume index, per 10 ml/m^2 increase	1.00 (0.95,1.06)	0.98
RV end-systolic volume index, per 10 ml/m^2 increase	0.98 (0.93,1.05)	0.64
Left atrial volume index, per 10 ml/m^2 increase	1.08 (1.03,1.14)	0.003
Global longitudinal strain, per 1% increase	0.95 (0.91,0.98)	0.003
Global circumferential strain, per 1% increase	1.00 (0.98,1.02)	0.92
Major non-ischemic scar	1.09 (1.01,1.19)	0.04

Values are given as median (95% confidence intervals).

Abbreviations: LV = left ventricular, RV = right ventricular.

Table 4.4. **List of primary candidate models tested**	
CMR parameter	**Model permutation**
LVEDVi	Base model + LVEDVi + LAVi
	Base model + LVEDVi + major non-ischemic scar
	Base model + LVEDVi + LAVi + major non-ischemic scar
LVESVi	Base model + LVESVi + LAVi
	Base model + LVESVi + major non-ischemic scar
	Base Model + LVESVi + LAVi + major non-ischemic scar
LV massi	Base model + LVmassi + LAVi
	Base model + LVmassi + major non-ischemic scar
	Base model + LVmassi + LAVi + major non-ischemic scar
GLS	Base model + GLS + LAVi
	Base model + GLS + major non-ischemic scar
	Base model + GLS + LAVi + major non-ischemic scar

Abbreviations: BM = base model including age, prior HF, CAD, DM, CKD, COPD, and CV hospitalization 90 days prior to CMR scan; LVEDVi = left ventricular end-diastolic volume index; LVESVi = left ventricular end-systolic volume index; LV massi = left ventricular mass index; LAVi = left atrial volume index; GLS = global longitudinal strain;

Table 4.5. Predictive performance of secondary candidate models for each CMR parameter			
CMR parameter	Candidate model	AIC	ΔAIC_i
None	Base model	2197.5	0
LVEDVi	Base model + LVEDVi + major non-ischemic scar	2189.5	-8.0
LVESVi	Base model + LVESVi + major non-ischemic scar	2191.7	-5.8
LVmassi	Base model + LVmassi + LAVi	2185.7	-11.8
GLS	Base model + GLS + LAVi + major non-ischemic scar	2184.8	-12.7

Abbreviations: BM = base model including age, prior HF, CAD, DM, CKD, COPD, and CV hospitalization 90 days prior to CMR scan; LVEDVi = left ventricular end-diastolic volume index; LVESVi = left ventricular end-systolic volume index; LV massi = left ventricular mass index; LAVi = left atrial volume index; GLS = global longitudinal strain;

4.3.3 External validation of the final predictive model in the validation cohort

During a mean follow-up of 1535±552 days, 97 of 376 patients (25.8%) in the validation cohort had a clinical event including 33 deaths and 83 cardiovascular hospitalizations. The event rate was similar to the derivation cohort (p=0.50).

The base model had relatively poor performance for calibration in the large, with Chi^2 12.6, p<0.001, but excellent performance in calibration slope, with Chi^2 0.3, p=0.59, indicating the mean predicted event rate was significantly overestimated, but no support of miscalibration (Figure 2A).

The final predictive model, base model + LAVi + GLS+ MNI scar, had excellent discrimination performance with area under the curve 0.779 (95% CI 0.727-0.830), versus 0.731 (95% CI 0.693-0.779) for the base model in the derivation cohort. At 5 years, it also had good Calibration in the large, with Chi^2 3.3, with p=0.07, indicating that the mean observed event rate was similar with the mean predicted event rate, and had excellent calibration slope, p=0.08, indicating no support of miscalibration (Figure 2B). In the multiple time points of every year over 5 year follow-up, the final predictive model had excellent calibration in the large and calibration slope over every year except patients with high event rates in the first year l (Figure 2C).

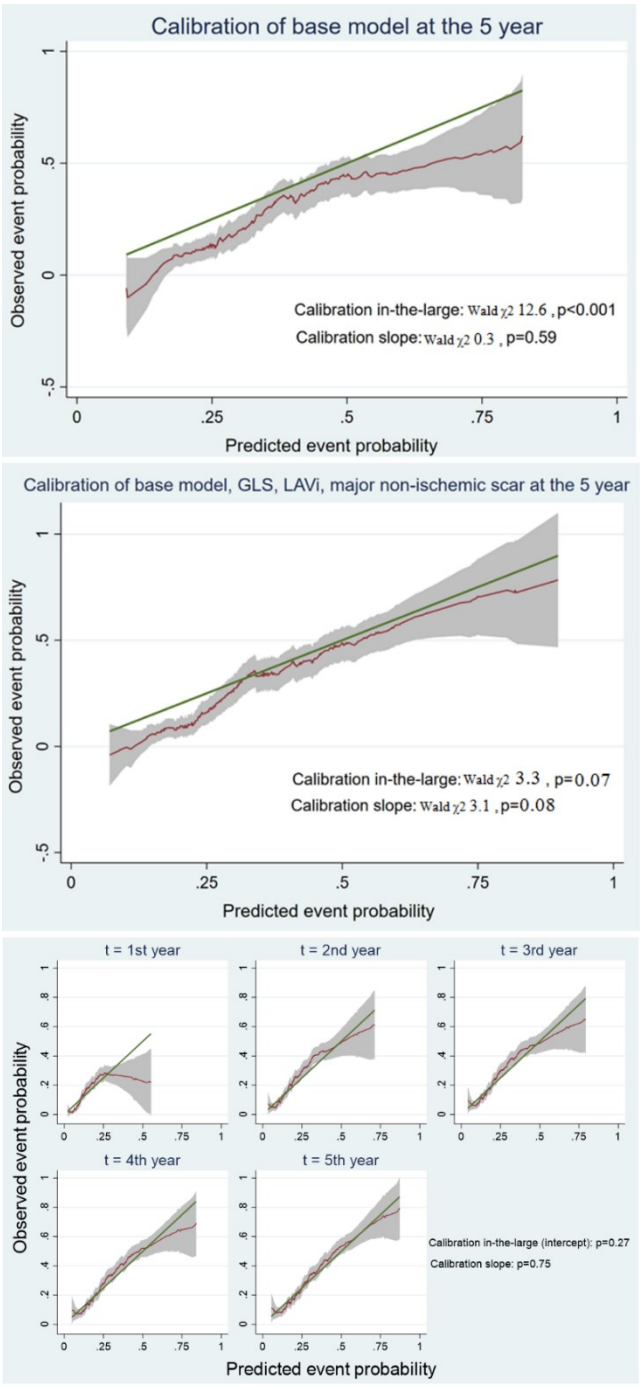

Figure 4.2. Observed event probabilities (red dashed lines) with pointwise 95% CI plotted against predicted event probabilities (green solid line) for validation cohort at 5 years. The solid line is the line of identity, denoting perfect calibration. Calibration plot of the *base model* (2A); Calibration plot of the *base model + LAVi + major non-ischemic scar + GLS (Model 4)* at 5 years (2B) and in each year over five years of follow-up (2C).

4.4 DISCUSSION

The major findings of this study are the following: 1) the optimal combination of CMR-derived imaging parameters (LAVi, GLS and major non-ischemic scar), contributed incremental value over clinical risk factors in predicting cardiovascular events for patients with or at risk for heart failure. 2) the prognostic value of this combined clinical and CMR predictive model was externally validated in an independent cohort with good discrimination and calibration performance.

To date, only limited risk predicting model of heart failure have been external validated and are predominately based on traditional risk factors. This is due to 1) difficulties in acquiring cardiac imaging data, especially CMR data, in a large cohort using a consistent acquisition protocol; 2) lack of standardized approach to image analysis and 3) lack of access to independent validation cohorts. LVEF has been included in some models,[62] but, has demonstrated inconsistent predictive value.[7, 45, 72] GLS has been studied more recently and was shown as a better alternative to LVEF.[45] However, thus far no risk models of HF have included a comprehensive evaluation of cardiac imaging parameters with subsequent external validation.

CMR is the most accurate one-stop cardiac imaging modality, capable of providing accurate volumetric, functional and myocardial tissue characterization information.[34] CMR is increasing used in clinical practice to evaluate patients with HF.[134] Our study confirms that CMR imaging parameters provide distinct and prognostically important information on cardiac structure and function. We identified a predictive model that included a functional metric, GLS, a structural metric, LAVi, and a tissue characterization, MNI scar, as having incremental value over clinical risk. The robustness of these results was confirmed by external validation in a second and distinctly different HF cohort.

GLS has been shown to be superior to LVEF in predicting mortality in patients with heart failure.[45] In multivariable analyses, LVEF was not predictive of outcome in our cohort. We also found that GLS was a good predictor of adverse outcome, but it was also collineated with LVEDVi, LVESVi and LV massi. However, net reclassification index and Akaike information criterion analyses demonstrated the superiority of GLS over other risk models incorporating CMR derived LV volumes or mass.

LAVi measured by CMR at the end-systole is the maximum LAV and it represents the left sided preload. It is also a morphological biomarker of left ventricular diastolic dysfunction[135] and has distinct diagnostic and prognostic significance in patients with HF, both HFpEF[136] and HFrEF.[137] The current study demonstrated that LAVi is a good predictor of outcome in patients with or at risk for HF and had incremental prognostic value over LV and myocardial tissue CMR parameters.

Myocardial scar patterns have been proved to powerful predictors of adverse outcome in a community-based cohort. Particularly, the presence of major non-ischemic scar (MNI scar) was superior to no presence of scar, minor non-ischemic scar, and ischemic scar in predicting adverse outcome.[40] In current study, we also consistently showed that MNI scar had superior prognostic value to the other 3 scar patterns. MNI scar represents a severe scar pattern appearing in non-ischemic heart disease (e.g., dilated cardiomyopathy, hypertrophic cardiomyopathy, hypertensive heart disease, myocarditis, infiltrative disease) and it reflects a high risk tissue characterization. Therefore, it is not surprising that this imaging parameter was a significant predictor in our derivation model.

In current study, we evaluated CMR imaging parameters inclusive of the left ventricle, left atrium, and tissue characterization. Collectively, these CMR measures represent systolic function, diastolic function and tissue features of the left ventricle. This combination (Model 4: base model, LAVi, MNI scar, GLS) yielded extraordinary incremental value over the base model, demonstrating that the addition of imaging indexes is worthwhile for evaluating patient risk. This model was well validated in the validation cohort with excellent discrimination and calibration performance.

Study limitations

The participants from the derivation cohort were retrospectively identified and thus we had incomplete information on vital signs and serum biomarkers such as creatinine and B-type natriuretic peptide. Nevertheless, the clinical risk model had good predictive value and was comparable in performance to previously published risk models for patients with HF. Most risk models to date have not incorporated BNP and its role in the surveillance of patients with chronic HF is not well defined.[112, 125] The clinical characteristics between the derivation and validation cohort were quite different. However, these differences allowed us to demonstrate the robustness of the predictive model. While we found good calibration overall for our risk model, it performed less well in the first year after the index CMR. This suggests that other HF biomarkers of early risk such as BNP and MRI derived lung water[138] may provide additional value to our model. This hypothesis will need to be confirmed in future validation studies. Myocardial T1 mapping, a new CMR method for tissue characterization,[139] was not available in the majority of patients in the derivation cohort and was thus not evaluated in our analyses. However, the role for T1 mapping has not been well established in heart failure and is thus far only recommended for suspected myocardial inflammation and infiltration. Lastly, although our risk model performed well in external validation, it should still be confirmed in a larger independent cohort.

4.5 CONCLUSIONS

CMR derived global longitudinal strain, indexed left atrium volume and myocardial scar characteristics, are predictive of adverse outcomes in patients with chronic heart failure, even after adjusting for clinical risk. The additive prognostic value of these CMR parameters was validated in a distinct and independent cohort, demonstrating its generalizability to other patients with chronic HF.

Chapter 5 Discussion

5.1 Limitations

5.1.1 Project summaries and technical limitation

We demonstrated that layer-specific strains have distinct signatures in the diagnosis and prognosis of patients at risk or with HF. Particularly, GLS measured at the epicardium was capable of differentiating the three groups of patients with preserved LVEF, including healthy controls, patients at risk for HF and patients with HFpEF; GLS averaged across the myocardium and global radial strain were the only independent predictor of 5-year all-cause mortality in patients at risk or with HF. However, three layer-specific GLSs are highly correlated with each other and have moderate to strong correlation with LVEF. Furthermore, layer-specific GLSs are still load dependent[140]. In conclusion, GLSs are still correlated with LVEF and LV volume, and are not a fully independent imaging biomarker of systolic dysfunction. While GLS_EPI is capable of differentiating patients with HFpEF from patients at risk for HF and healthy controls, there is tremendous overlap of GLS_EPI among the three groups. Therefore, imaging biomarkers which more accurately identify systolic and/or diastolic dysfunction, should be further developed to better differentiate these three groups of subjects with preserved LVEF.

In the Chapter 3 and Chapter 4, the presence of major non-ischemic scar was identified as a robust predictor of adverse outcome, but there were only 25 (7%) patients with this scar pattern in the Alberta HEART study. However, in Chapter 4, the derivation cohort had 167(26%) patients with major non-ischemic scar and it was still identified as an independent predictor of outcome. Additionally, an ischemic scar pattern had poor predictive value, as previously shown.[40] While the presence of ischemic scar appears insensitive to prognosis, other characteristics such as location, transmurality, heterogeneity and perfusion may provide important information that we did not consider in our analysis.

We also quantified the myocardial scar mass in Chapter 3. A common threshold of mean plus 5 standard deviation (SD) of the region of interest in remote myocardium was used to identify and quantitatively measure the myocardial scar volume. However, for the assessment of non-ischemic scar volume, a threshold of mean ± 3 SD of the remote myocardium is recommended.[116] To be consistent with recommendations for ischemic scar volume assessment,

we only used the threshold of mean ± 5 SD. Thus, we may have underestimated non-ischemic scar volume in our cohort.

In Chapter 3, there were still 57 patients having no LGE image due to renal dysfunction or personal preference. Therefore, the serial change of myocardial scar mass over 1 year was only available in 183 patients and was not able to evaluate its incremental value over other serial CMR assessment in predicting adverse outcome.

In Chapter 4, the CMR-derived imaging biomarker of our final predictive model included LAVi, GLS, and presence of the major non-ischemic scar. While we considered a comprehensive list of CMR metrics related to cardiac geometry, function and myocardial tissue characterization, we did not include myocardial T1 mapping due to lack of available data.

5.1.2 Limitations of the study cohort

The thesis work was predominantly based on the Alberta HEART study, which comprised 453 subjects undergoing cardiac imaging and clinical evaluation including assessment of outcome. However only 262 patients had both baseline and 1-year CMR acquisitions. Furthermore, the sample size for each HF subgroup (e.g. HFrEF, HFmrEF and HFpEF) was also modest. Thus, subgroup comparisons were not possible, particularly in analyses of prognosis. The number of events in the Alberta HEART study was also modest, with 33 all-cause mortality and 83 cardiovascular hospitalization during 5-year follow up, but it did not prevent us from achieving significance in survival analysis. Nevertheless, our results should be further validated in larger HF cohorts with higher event rates, especially all-cause mortality which is the most common outcome used. Furthermore, as the Alberta HEART study was mainly focused on developing diagnostic, therapeutic and prognostic approaches to patients with HFpEF,[71] the number of patients with HFrEF and HFmrEF was limited. Therefore, the results still need to be validated in HF cohort with bigger and more equal same size of the three subgroups of HF. Finally, the Alberta HEART cohort also included patients with AHA/ACC Stage A/B HF (i.e. preclinical). While prior HF was included in the stepwise selection of the base model in Chapter 4, and the results should still be verified in a HF only cohort (i.e. AHA/ACC Stage C).

In Chapter 4, we have developed a comprehensive model using available clinical information and CMR parameters, but the clinical data in the derivation cohort did not include New York Heart

Function Classification, systolic blood pressure and serum creatinine, 3 well established predictors of HF outcome. Therefore, we were not able to build the base model using the MAGGIC risk score. Furthermore, the cardiac phenotypes were different between two cohorts and the derivation cohorts tended to have more severe disease. Consequently, the validation cohort is not an ideal cohort for external validation.

5.2 Future direction

Based on the Alberta HEART study, we are interested to investigate the diagnostic and prognostic approaches by assessing the strain or strain rate at different cardiac phase from the LA, RV and RA in patients at risk or with HF. This may help us understand the functional status of these three cardiac chambers in HF. LA strain may help us better understand the diastolic function of the LV and filling pressure; RV strain is potentially useful, especially when the geometry of the LV remaining relatively normal in HF.

For tissue characterization of LV, a bigger sample size of HF cohort will be needed, especially a bigger cohort of patients with HFpEF. This will help us better understand the myocardial scar patterns and the temporal change of the scar volume in this subgroup. Alternatively, quantifying the myocardial scar volume in non-contrast images[141, 142] is more applicable to the majority of patients, even to patients with renal dysfunction, and more feasible for serial evaluation.

A comprehensive imaging model can be developed incorporating more detailed information including NYHA, more serum biomarkers (i.e. BNP, creatinine, C-reactive protein) and vital signs. And the imaging risk model should also be validated in a bigger cohort.

Finally, the impact of T1 mapping on diagnosis and prognosis in HF should be further explored. Also, more prospective studies and randomized controlled trials in HF are needed to evaluate the prognostic impact of routine CMR in managing patients with HF.

5.3 Conclusion

This thesis has focuses on the early diagnosis and prognosis of patients with HF. Notably, we found that the baseline global longitudinal strain of the average myocardium is a significant

predictor of all-cause mortality, which is informative to understand the patients' prognosis from the baseline and therefore initiate more intensive management strategy from the beginning. Secondly, we found that cardiac remodeling is prevalent in patients with chronic heart failure and that a temporal change in LV massi, and GLS were robust predictors of outcome. Finally, we established a comprehensive predictive model incorporating multiparametric imaging biomarkers of the cardiac structure and function, including LAVi, GLS and presence of major non-ischemic scar, as well as key clinical factors. This model yielded excellent discrimination and calibration performance in external validation. This modelling and validations identified CMR-derived imaging biomarkers that are consistently associated with prognosis and thus potentially allowing treating clinicians to better distinguish low and high risk patients with HF.

Reference

1. Yancy CW, Jessup M, Bozkurt B, Butler J, Casey DE, Jr., Drazner MH, Fonarow GC, Geraci SA, Horwich T, Januzzi JL, Johnson MR, Kasper EK, Levy WC, Masoudi FA, McBride PE, McMurray JJ, Mitchell JE, Peterson PN, Riegel B, Sam F, Stevenson LW, Tang WH, Tsai EJ and Wilkoff BL. 2013 ACCF/AHA guideline for the management of heart failure: executive summary: a report of the American College of Cardiology Foundation/American Heart Association Task Force on practice guidelines. *Circulation*. 2013;128:1810-52.

2. Ezekowitz JA, O'Meara E, McDonald MA, Abrams H, Chan M, Ducharme A, Giannetti N, Grzeslo A, Hamilton PG, Heckman GA, Howlett JG, Koshman SL, Lepage S, McKelvie RS, Moe GW, Rajda M, Swiggum E, Virani SA, Zieroth S, Al-Hesayen A, Cohen-Solal A, D'Astous M, De S, Estrella-Holder E, Fremes S, Green L, Haddad H, Harkness K, Hernandez AF, Kouz S, LeBlanc MH, Masoudi FA, Ross HJ, Roussin A and Sussex B. 2017 Comprehensive Update of the Canadian Cardiovascular Society Guidelines for the Management of Heart Failure. *Can J Cardiol*. 2017;33:1342-1433.

3. Banke A, Fosbol EL, Ewertz M, Videbaek L, Dahl JS, Poulsen MK, Cold S, Jensen MB, Gislason GH, Schou M and Moller JE. Long-Term Risk of Heart Failure in Breast Cancer Patients After Adjuvant Chemotherapy With or Without Trastuzumab. *JACC Heart Fail*. 2019;7:217-224.

4. Goel S, Liu J, Guo H, Barry W, Bell R, Murray B, Lynch J, Bastick P, Chantrill L, Kiely BE, Abdi E, Rutovitz J, Asghari R, Sullivan A, Harrison M, Kohonen-Corish M and Beith J. Decline in Left Ventricular Ejection Fraction Following Anthracyclines Predicts Trastuzumab Cardiotoxicity. *JACC Heart Fail*. 2019;7:795-804.

5. Heidenreich PA, Albert NM, Allen LA, Bluemke DA, Butler J, Fonarow GC, Ikonomidis JS, Khavjou O, Konstam MA, Maddox TM, Nichol G, Pham M, Pina IL, Trogdon JG, American Heart Association Advocacy Coordinating C, Council on Arteriosclerosis T, Vascular B, Council on Cardiovascular R, Intervention, Council on Clinical C, Council on E, Prevention and Stroke C. Forecasting the impact of heart failure in the United States: a policy statement from the American Heart Association. *Circ Heart Fail*. 2013;6:606-19.

6. Ponikowski P, Voors AA, Anker SD, Bueno H, Cleland JG, Coats AJ, Falk V, Gonzalez-Juanatey JR, Harjola VP, Jankowska EA, Jessup M, Linde C, Nihoyannopoulos P, Parissis JT, Pieske B, Riley JP, Rosano GM, Ruilope LM, Ruschitzka F, Rutten FH, van der Meer P,

Authors/Task Force M and Document R. 2016 ESC Guidelines for the diagnosis and treatment of acute and chronic heart failure: The Task Force for the diagnosis and treatment of acute and chronic heart failure of the European Society of Cardiology (ESC). Developed with the special contribution of the Heart Failure Association (HFA) of the ESC. *Eur J Heart Fail*. 2016;18:891-975.

7. Shah KS, Xu H, Matsouaka RA, Bhatt DL, Heidenreich PA, Hernandez AF, Devore AD, Yancy CW and Fonarow GC. Heart Failure With Preserved, Borderline, and Reduced Ejection Fraction: 5-Year Outcomes. *J Am Coll Cardiol*. 2017;70:2476-2486.

8. Nadar SK and Tariq O. What is Heart Failure with Mid-range Ejection Fraction? A New Subgroup of Patients with Heart Failure. *Card Fail Rev*. 2018;4:6-8.

9. Hsu JJ, Ziaeian B and Fonarow GC. Heart Failure With Mid-Range (Borderline) Ejection Fraction: Clinical Implications and Future Directions. *JACC Heart Fail*. 2017;5:763-771.

10. Butrous H and Hummel SL. Heart Failure in Older Adults. *Can J Cardiol*. 2016;32:1140-7.

11. Ponikowski P, Anker SD, AlHabib KF, Cowie MR, Force TL, Hu S, Jaarsma T, Krum H, Rastogi V, Rohde LE, Samal UC, Shimokawa H, Budi Siswanto B, Sliwa K and Filippatos G. Heart failure: preventing disease and death worldwide. *ESC Heart Fail*. 2014;1:4-25.

12. Crespo-Leiro MG, Anker SD, Maggioni AP, Coats AJ, Filippatos G, Ruschitzka F, Ferrari R, Piepoli MF, Delgado Jimenez JF, Metra M, Fonseca C, Hradec J, Amir O, Logeart D, Dahlstrom U, Merkely B, Drozdz J, Goncalvesova E, Hassanein M, Chioncel O, Lainscak M, Seferovic PM, Tousoulis D, Kavoliuniene A, Fruhwald F, Fazlibegovic E, Temizhan A, Gatzov P, Erglis A, Laroche C, Mebazaa A and Heart Failure Association of the European Society of C. European Society of Cardiology Heart Failure Long-Term Registry (ESC-HF-LT): 1-year follow-up outcomes and differences across regions. *Eur J Heart Fail*. 2016;18:613-25.

13. Lee R, Chan SP, Chan YH, Wong J, Lau D and Ng K. Impact of race on morbidity and mortality in patients with congestive heart failure: a study of the multiracial population in Singapore. *Int J Cardiol*. 2009;134:422-5.

14. Konstam MA, Patten RD, Thomas I, Ramahi T, La Bresh K, Goldman S, Lewis W, Gradman A, Self KS, Bittner V, Rand W, Kinan D, Smith JJ, Ford T, Segal R and Udelson JE. Effects of losartan and captopril on left ventricular volumes in elderly patients with heart failure: results of the ELITE ventricular function substudy. *Am Heart J*. 2000;139:1081-7.

15. Hernandez AF, Hammill BG, O'Connor CM, Schulman KA, Curtis LH and Fonarow GC. Clinical effectiveness of beta-blockers in heart failure: findings from the OPTIMIZE-HF (Organized Program to Initiate Lifesaving Treatment in Hospitalized Patients with Heart Failure) Registry. *J Am Coll Cardiol*. 2009;53:184-92.
16. Wong M, Staszewsky L, Latini R, Barlera S, Volpi A, Chiang YT, Benza RL, Gottlieb SO, Kleemann TD, Rosconi F, Vandervoort PM, Cohn JN and Val-He FTHFTI. Valsartan benefits left ventricular structure and function in heart failure: Val-HeFT echocardiographic study. *J Am Coll Cardiol*. 2002;40:970-5.
17. Groenning BA, Nilsson JC, Sondergaard L, Fritz-Hansen T, Larsson HB and Hildebrandt PR. Antiremodeling effects on the left ventricle during beta-blockade with metoprolol in the treatment of chronic heart failure. *J Am Coll Cardiol*. 2000;36:2072-80.
18. Taylor AL, Ziesche S, Yancy C, Carson P, D'Agostino R, Jr., Ferdinand K, Taylor M, Adams K, Sabolinski M, Worcel M, Cohn JN and African-American Heart Failure Trial I. Combination of isosorbide dinitrate and hydralazine in blacks with heart failure. *N Engl J Med*. 2004;351:2049-57.
19. Muto C, Solimene F, Gallo P, Nastasi M, La Rosa C, Calvanese R, Iengo R, Canciello M, Sangiuolo R, Diemberger I, Ciardiello C and Tuccillo B. A randomized study of cardiac resynchronization therapy defibrillator versus dual-chamber implantable cardioverter-defibrillator in ischemic cardiomyopathy with narrow QRS: the NARROW-CRT study. *Circ Arrhythm Electrophysiol*. 2013;6:538-45.
20. Gerber Y, Weston SA, Redfield MM, Chamberlain AM, Manemann SM, Jiang R, Killian JM and Roger VL. A contemporary appraisal of the heart failure epidemic in Olmsted County, Minnesota, 2000 to 2010. *JAMA Intern Med*. 2015;175:996-1004.
21. Savarese G and Lund LH. Global Public Health Burden of Heart Failure. *Card Fail Rev*. 2017;3:7-11.
22. Owan TE, Hodge DO, Herges RM, Jacobsen SJ, Roger VL and Redfield MM. Trends in prevalence and outcome of heart failure with preserved ejection fraction. *N Engl J Med*. 2006;355:251-9.
23. Cleland JG, Tendera M, Adamus J, Freemantle N, Polonski L, Taylor J and Investigators P-C. The perindopril in elderly people with chronic heart failure (PEP-CHF) study. *Eur Heart J*. 2006;27:2338-45.

24. Massie BM, Carson PE, McMurray JJ, Komajda M, McKelvie R, Zile MR, Anderson S, Donovan M, Iverson E, Staiger C, Ptaszynska A and Investigators IP. Irbesartan in patients with heart failure and preserved ejection fraction. *N Engl J Med*. 2008;359:2456-67.
25. Mahmood SS and Wang TJ. The epidemiology of congestive heart failure: the Framingham Heart Study perspective. *Glob Heart*. 2013;8:77-82.
26. Marantz PR, Tobin JN, Wassertheil-Smoller S, Steingart RM, Wexler JP, Budner N, Lense L and Wachspress J. The relationship between left ventricular systolic function and congestive heart failure diagnosed by clinical criteria. *Circulation*. 1988;77:607-12.
27. Liu L and Eisen HJ. Epidemiology of heart failure and scope of the problem. *Cardiol Clin*. 2014;32:1-8, vii.
28. Wong CY, Chaudhry SI, Desai MM and Krumholz HM. Trends in comorbidity, disability, and polypharmacy in heart failure. *Am J Med*. 2011;124:136-43.
29. Baron-Franco B, McLean G, Mair FS, Roger VL, Guthrie B and Mercer SW. Comorbidity and polypharmacy in chronic heart failure: a large cross-sectional study in primary care. *Br J Gen Pract*. 2017;67:e314-e320.
30. Kirkpatrick JN, Vannan MA, Narula J and Lang RM. Echocardiography in heart failure: applications, utility, and new horizons. *J Am Coll Cardiol*. 2007;50:381-96.
31. Harinstein ME and Soman P. Radionuclide Imaging Applications in Cardiomyopathies and Heart Failure. *Curr Cardiol Rep*. 2016;18:23.
32. Mangalat D, Kalogeropoulos A, Georgiopoulou V, Stillman A and Butler J. Value of Cardiac CT in Patients With Heart Failure. *Curr Cardiovasc Imaging Rep*. 2009;2:410-417.
33. Uretsky S, Gillam L, Lang R, Chaudhry FA, Argulian E, Supariwala A, Gurram S, Jain K, Subero M, Jang JJ, Cohen R and Wolff SD. Discordance between echocardiography and MRI in the assessment of mitral regurgitation severity: a prospective multicenter trial. *J Am Coll Cardiol*. 2015;65:1078-88.
34. American College of Cardiology Foundation Task Force on Expert Consensus D, Hundley WG, Bluemke DA, Finn JP, Flamm SD, Fogel MA, Friedrich MG, Ho VB, Jerosch-Herold M, Kramer CM, Manning WJ, Patel M, Pohost GM, Stillman AE, White RD and Woodard PK. ACCF/ACR/AHA/NASCI/SCMR 2010 expert consensus document on cardiovascular magnetic resonance: a report of the American College of Cardiology Foundation Task Force on Expert Consensus Documents. *J Am Coll Cardiol*. 2010;55:2614-62.

35. Kancharla K, Weissman G, Elagha AA, Kancherla K, Samineni S, Hill PC, Boyce S and Fuisz AR. Scar quantification by cardiovascular magnetic resonance as an independent predictor of long-term survival in patients with ischemic heart failure treated by coronary artery bypass graft surgery. *J Cardiovasc Magn Reson*. 2016;18:45.

36. Castelvecchio S, Careri G, Ambrogi F, Camporeale A, Menicanti L, Secchi F and Lombardi M. Myocardial scar location as detected by cardiac magnetic resonance is associated with the outcome in heart failure patients undergoing surgical ventricular reconstruction. *Eur J Cardiothorac Surg*. 2018;53:143-149.

37. Ekstrom K, Nepper-Christensen L, Ahtarovski KA, Kyhl K, Goransson C, Bertelsen L, Ghotbi AA, Kelbaek H, Helqvist S, Hofsten DE, Kober L, Schoos MM, Vejlstrup N, Lonborg J and Engstrom T. Impact of Multiple Myocardial Scars Detected by CMR in Patients Following STEMI. *JACC Cardiovasc Imaging*. 2019;12:2168-2178.

38. Musa TA, Treibel TA, Vassiliou VS, Captur G, Singh A, Chin C, Dobson LE, Pica S, Loudon M, Malley T, Rigolli M, Foley JRJ, Bijsterveld P, Law GR, Dweck MR, Myerson SG, McCann GP, Prasad SK, Moon JC and Greenwood JP. Myocardial Scar and Mortality in Severe Aortic Stenosis. *Circulation*. 2018;138:1935-1947.

39. Volpe GJ, Moreira HT, Trad HS, Wu KC, Braggion-Santos MF, Santos MK, Maciel BC, Pazin-Filho A, Marin-Neto JA, Lima JAC and Schmidt A. Left Ventricular Scar and Prognosis in Chronic Chagas Cardiomyopathy. *J Am Coll Cardiol*. 2018;72:2567-2576.

40. Shanbhag SM, Greve AM, Aspelund T, Schelbert EB, Cao JJ, Danielsen R, Thornorgeirsson G, Sigurethsson S, Eiriksdottir G, Harris TB, Launer LJ, Guethnason V and Arai AE. Prevalence and prognosis of ischaemic and non-ischaemic myocardial fibrosis in older adults. *Eur Heart J*. 2019;40:529-538.

41. Suksaranjit P, McGann CJ, Akoum N, Biskupiak J, Stoddard GJ, Kholmovski EG, Navaravong L, Rassa A, Bieging E, Chang L, Haider I, Marrouche NF and Wilson BD. Prognostic Implications of Left Ventricular Scar Determined by Late Gadolinium Enhanced Cardiac Magnetic Resonance in Patients With Atrial Fibrillation. *Am J Cardiol*. 2016;118:991-7.

42. Li F, Xu M, Fan Y, Wang Y, Song Y, Cui X, Fu M, Qi B, Han X, Zhou J and Ge J. Diffuse myocardial fibrosis and the prognosis of heart failure with reduced ejection fraction in Chinese patients: a cohort study. *Int J Cardiovasc Imaging*. 2020.

43. Patel RB, Li E, Benefield BC, Swat SA, Polsinelli VB, Carr JC, Shah SJ, Markl M, Collins JD and Freed BH. Diffuse right ventricular fibrosis in heart failure with preserved ejection fraction and pulmonary hypertension. *ESC Heart Fail*. 2020.
44. Nitsche C, Kammerlander AA, Binder C, Duca F, Aschauer S, Koschutnik M, Snidat A, Beitzke D, Loewe C, Bonderman D, Hengstenberg C and Mascherbauer J. Native T1 time of right ventricular insertion points by cardiac magnetic resonance: relation with invasive haemodynamics and outcome in heart failure with preserved ejection fraction. *Eur Heart J Cardiovasc Imaging*. 2019.
45. Park JJ, Park JB, Park JH and Cho GY. Global Longitudinal Strain to Predict Mortality in Patients With Acute Heart Failure. *J Am Coll Cardiol*. 2018;71:1947-1957.
46. Reindl M, Tiller C, Holzknecht M, Lechner I, Beck A, Plappert D, Gorzala M, Pamminger M, Mayr A, Klug G, Bauer A, Metzler B and Reinstadler SJ. Prognostic Implications of Global Longitudinal Strain by Feature-Tracking Cardiac Magnetic Resonance in ST-Elevation Myocardial Infarction. *Circ Cardiovasc Imaging*. 2019;12:e009404.
47. Prakken NH, Teske AJ, Cramer MJ, Mosterd A, Bosker AC, Mali WP, Doevendans PA and Velthuis BK. Head-to-head comparison between echocardiography and cardiac MRI in the evaluation of the athlete's heart. *Br J Sports Med*. 2012;46:348-54.
48. Rastogi A, Novak E, Platts AE and Mann DL. Epidemiology, pathophysiology and clinical outcomes for heart failure patients with a mid-range ejection fraction. *Eur J Heart Fail*. 2017;19:1597-1605.
49. Kraigher-Krainer E, Shah AM, Gupta DK, Santos A, Claggett B, Pieske B, Zile MR, Voors AA, Lefkowitz MP, Packer M, McMurray JJ, Solomon SD and Investigators P. Impaired systolic function by strain imaging in heart failure with preserved ejection fraction. *J Am Coll Cardiol*. 2014;63:447-56.
50. Greenbaum RA, Ho SY, Gibson DG, Becker AE and Anderson RH. Left ventricular fibre architecture in man. *Br Heart J*. 1981;45:248-63.
51. Bloom MW, Hamo CE, Cardinale D, Ky B, Nohria A, Baer L, Skopicki H, Lenihan DJ, Gheorghiade M, Lyon AR and Butler J. Cancer Therapy-Related Cardiac Dysfunction and Heart Failure: Part 1: Definitions, Pathophysiology, Risk Factors, and Imaging. *Circ Heart Fail*. 2016;9:e002661.

52. Pfeffer MA, Lamas GA, Vaughan DE, Parisi AF and Braunwald E. Effect of captopril on progressive ventricular dilatation after anterior myocardial infarction. *N Engl J Med*. 1988;319:80-6.
53. Hoshikawa E, Matsumura Y, Kubo T, Okawa M, Yamasaki N, Kitaoka H, Furuno T, Takata J and Doi YL. Effect of left ventricular reverse remodeling on long-term prognosis after therapy with angiotensin-converting enzyme inhibitors or angiotensin II receptor blockers and beta blockers in patients with idiopathic dilated cardiomyopathy. *Am J Cardiol*. 2011;107:1065-70.
54. Treibel TA, Kozor R, Schofield R, Benedetti G, Fontana M, Bhuva AN, Sheikh A, Lopez B, Gonzalez A, Manisty C, Lloyd G, Kellman P, Diez J and Moon JC. Reverse Myocardial Remodeling Following Valve Replacement in Patients With Aortic Stenosis. *J Am Coll Cardiol*. 2018;71:860-871.
55. Rodriguez-Palomares JF, Gavara J, Ferreira-Gonzalez I, Valente F, Rios C, Rodriguez-Garcia J, Bonanad C, Garcia Del Blanco B, Minana G, Mutuberria M, Nunez J, Barrabes J, Evangelista A, Bodi V and Garcia-Dorado D. Prognostic Value of Initial Left Ventricular Remodeling in Patients With Reperfused STEMI. *JACC Cardiovasc Imaging*. 2019.
56. Menet A, Guyomar Y, Ennezat PV, Graux P, Castel AL, Delelis F, Heuls S, Cuvelier E, Gevaert C, Le Goffic C, Tribouilloy C and Marechaux S. Prognostic value of left ventricular reverse remodeling and performance improvement after cardiac resynchronization therapy: A prospective study. *Int J Cardiol*. 2016;204:6-11.
57. Martens P, Nijst P, Verbrugge FH, Dupont M, Tang WHW and Mullens W. Profound differences in prognostic impact of left ventricular reverse remodeling after cardiac resynchronization therapy relate to heart failure etiology. *Heart Rhythm*. 2018;15:130-136.
58. Lee WC, Chen HC, Chen YL, Tsai TH, Pan KL, Lin YS and Chen MC. Left ventricle remodeling predicts the recurrence of ventricular tachyarrhythmias in implantable cardioverter defibrillator recipients for secondary prevention. *BMC Cardiovasc Disord*. 2016;16:231.
59. Sabbah HN. Silent disease progression in clinically stable heart failure. *Eur J Heart Fail*. 2017;19:469-478.
60. Breathett K, Allen LA, Udelson J, Davis G and Bristow M. Changes in Left Ventricular Ejection Fraction Predict Survival and Hospitalization in Heart Failure With Reduced Ejection Fraction. *Circ Heart Fail*. 2016;9.

61. Solomon SD, Anavekar N, Skali H, McMurray JJ, Swedberg K, Yusuf S, Granger CB, Michelson EL, Wang D, Pocock S, Pfeffer MA and Candesartan in Heart Failure Reduction in Mortality I. Influence of ejection fraction on cardiovascular outcomes in a broad spectrum of heart failure patients. *Circulation*. 2005;112:3738-44.
62. Pocock SJ, Ariti CA, McMurray JJ, Maggioni A, Kober L, Squire IB, Swedberg K, Dobson J, Poppe KK, Whalley GA, Doughty RN and Meta-Analysis Global Group in Chronic Heart F. Predicting survival in heart failure: a risk score based on 39 372 patients from 30 studies. *Eur Heart J*. 2013;34:1404-13.
63. Konstam MA, Kramer DG, Patel AR, Maron MS and Udelson JE. Left ventricular remodeling in heart failure: current concepts in clinical significance and assessment. *JACC Cardiovasc Imaging*. 2011;4:98-108.
64. Sepehrvand N, Alemayehu W, Dyck GJB, Dyck JRB, Anderson T, Howlett J, Paterson I, McAlister FA and Ezekowitz JA. External Validation of the H2F-PEF Model in Diagnosing Patients With Heart Failure and Preserved Ejection Fraction. *Circulation*. 2019;139:2377-2379.
65. Sawano M, Shiraishi Y, Kohsaka S, Nagai T, Goda A, Mizuno A, Sujino Y, Nagatomo Y, Kohno T, Anzai T, Fukuda K and Yoshikawa T. Performance of the MAGGIC heart failure risk score and its modification with the addition of discharge natriuretic peptides. *ESC Heart Fail*. 2018;5:610-619.
66. Upshaw JN, Konstam MA, Klaveren D, Noubary F, Huggins GS and Kent DM. Multistate Model to Predict Heart Failure Hospitalizations and All-Cause Mortality in Outpatients With Heart Failure With Reduced Ejection Fraction: Model Derivation and External Validation. *Circ Heart Fail*. 2016;9.
67. Kasahara S, Sakata Y, Nochioka K, Tay WT, Claggett BL, Abe R, Oikawa T, Sato M, Aoyanagi H, Miura M, Shiroto T, Takahashi J, Sugimura K, Teng TK, Miyata S and Shimokawa H. The 3A3B score: The simple risk score for heart failure with preserved ejection fraction - A report from the CHART-2 Study. *Int J Cardiol*. 2019;284:42-49.
68. Lagu T, Pekow PS, Shieh MS, Stefan M, Pack QR, Kashef MA, Atreya AR, Valania G, Slawsky MT and Lindenauer PK. Validation and Comparison of Seven Mortality Prediction Models for Hospitalized Patients With Acute Decompensated Heart Failure. *Circ Heart Fail*. 2016;9.

69. Voors AA, Ouwerkerk W, Zannad F, van Veldhuisen DJ, Samani NJ, Ponikowski P, Ng LL, Metra M, Ter Maaten JM, Lang CC, Hillege HL, van der Harst P, Filippatos G, Dickstein K, Cleland JG, Anker SD and Zwinderman AH. Development and validation of multivariable models to predict mortality and hospitalization in patients with heart failure. *Eur J Heart Fail*. 2017;19:627-634.
70. Wessler BS, Ruthazer R, Udelson JE, Gheorghiade M, Zannad F, Maggioni A, Konstam MA and Kent DM. Regional Validation and Recalibration of Clinical Predictive Models for Patients With Acute Heart Failure. *J Am Heart Assoc*. 2017;6.
71. Ezekowitz JA, Becher H, Belenkie I, Clark AM, Duff HJ, Friedrich MG, Haykowsky MJ, Howlett JG, Kassiri Z, Kaul P, Kim DH, Knudtson ML, Light PE, Lopaschuk GD, McAlister FA, Noga ML, Oudit GY, Paterson DI, Quan H, Schulz R, Thompson RB, Weeks SG, Anderson TJ and Dyck JR. The Alberta Heart Failure Etiology and Analysis Research Team (HEART) study. *BMC Cardiovasc Disord*. 2014;14:91.
72. Aimo A, Januzzi JL, Jr., Vergaro G, Petersen C, Pasanisi EM, Molinaro S, Passino C and Emdin M. Left ventricular ejection fraction for risk stratification in chronic systolic heart failure. *Int J Cardiol*. 2018;273:136-140.
73. Shi J, Pan C, Kong D, Cheng L and Shu X. Left Ventricular Longitudinal and Circumferential Layer-Specific Myocardial Strains and Their Determinants in Healthy Subjects. *Echocardiography*. 2016;33:510-8.
74. Tanacli R, Hashemi D, Lapinskas T, Edelmann F, Gebker R, Pedrizzetti G, Schuster A, Nagel E, Pieske B, Dungen HD and Kelle S. Range Variability in CMR Feature Tracking Multilayer Strain across Different Stages of Heart Failure. *Sci Rep*. 2019;9:16478.
75. Shah AM, Claggett B, Sweitzer NK, Shah SJ, Anand IS, Liu L, Pitt B, Pfeffer MA and Solomon SD. Prognostic Importance of Impaired Systolic Function in Heart Failure With Preserved Ejection Fraction and the Impact of Spironolactone. *Circulation*. 2015;132:402-14.
76. Iacoviello M, Puzzovivo A, Guida P, Forleo C, Monitillo F, Catanzaro R, Lattarulo MS, Antoncecchi V and Favale S. Independent role of left ventricular global longitudinal strain in predicting prognosis of chronic heart failure patients. *Echocardiography*. 2013;30:803-11.
77. Sarvari SI, Haugaa KH, Zahid W, Bendz B, Aakhus S, Aaberge L and Edvardsen T. Layer-specific quantification of myocardial deformation by strain echocardiography may reveal

significant CAD in patients with non-ST-segment elevation acute coronary syndrome. *JACC Cardiovasc Imaging*. 2013;6:535-44.

78. Scharrenbroich J, Hamada S, Keszei A, Schroder J, Napp A, Almalla M, Becker M and Altiok E. Use of two-dimensional speckle tracking echocardiography to predict cardiac events: Comparison of patients with acute myocardial infarction and chronic coronary artery disease. *Clin Cardiol*. 2018;41:111-118.

79. Hamada S, Schroeder J, Hoffmann R, Altiok E, Keszei A, Almalla M, Napp A, Marx N and Becker M. Prediction of Outcomes in Patients with Chronic Ischemic Cardiomyopathy by Layer-Specific Strain Echocardiography: A Proof of Concept. *J Am Soc Echocardiogr*. 2016;29:412-20.

80. Skaarup KG, Iversen A, Jorgensen PG, Olsen FJ, Grove GL, Jensen JS and Biering-Sorensen T. Association between layer-specific global longitudinal strain and adverse outcomes following acute coronary syndrome. *Eur Heart J Cardiovasc Imaging*. 2018;19:1334-1342.

81. Lee WH, Liu YW, Yang LT and Tsai WC. Prognostic value of longitudinal strain of subepicardial myocardium in patients with hypertension. *J Hypertens*. 2016;34:1195-200.

82. Caspar T, Fichot M, Ohana M, El Ghannudi S, Morel O and Ohlmann P. Late Detection of Left Ventricular Dysfunction Using Two-Dimensional and Three-Dimensional Speckle-Tracking Echocardiography in Patients with History of Nonsevere Acute Myocarditis. *J Am Soc Echocardiogr*. 2017;30:756-762.

83. Kuznetsova T, Cauwenberghs N, Knez J, Yang WY, Herbots L, D'Hooge J, Haddad F, Thijs L, Voigt JU and Staessen JA. Additive Prognostic Value of Left Ventricular Systolic Dysfunction in a Population-Based Cohort. *Circ Cardiovasc Imaging*. 2016;9.

84. Robinson JD, Lupkiewicz SM, Palenik L, Lopez LM and Ariet M. Determination of ideal body weight for drug dosage calculations. *Am J Hosp Pharm*. 1983;40:1016-9.

85. Klein S, Staring M, Murphy K, Viergever MA and Pluim JPW. elastix: A Toolbox for Intensity-Based Medical Image Registration. *Ieee T Med Imaging*. 2010;29:196-205.

86. Pedrizzetti G, Claus P, Kilner PJ and Nagel E. Principles of cardiovascular magnetic resonance feature tracking and echocardiographic speckle tracking for informed clinical use. *J Cardiovasc Magn Reson*. 2016;18:51.

87. Taylor RJ, Moody WE, Umar F, Edwards NC, Taylor TJ, Stegemann B, Townend JN, Hor KN, Steeds RP, Mazur W and Leyva F. Myocardial strain measurement with feature-

tracking cardiovascular magnetic resonance: normal values. *Eur Heart J Cardiovasc Imaging*. 2015;16:871-81.

88. Royston P and White IR. Multiple Imputation by Chained Equations (MICE): Implementation in Stata. *J Stat Softw*. 2011;45:1-20.

89. Burnham KP and Anderson DR. Multimodel inference - understanding AIC and BIC in model selection. *Sociol Method Res*. 2004;33:261-304.

90. Alcidi GM, Esposito R, Evola V, Santoro C, Lembo M, Sorrentino R, Lo Iudice F, Borgia F, Novo G, Trimarco B, Lancellotti P and Galderisi M. Normal reference values of multilayer longitudinal strain according to age decades in a healthy population: A single-centre experience. *Eur Heart J Cardiovasc Imaging*. 2018;19:1390-1396.

91. Nagata Y, Wu VC, Otsuji Y and Takeuchi M. Normal range of myocardial layer-specific strain using two-dimensional speckle tracking echocardiography. *PLoS One*. 2017;12:e0180584.

92. He KL, Burkhoff D, Leng WX, Liang ZR, Fan L, Wang J and Maurer MS. Comparison of ventricular structure and function in Chinese patients with heart failure and ejection fractions >55% versus 40% to 55% versus <40%. *Am J Cardiol*. 2009;103:845-51.

93. Ueda T, Kawakami R, Nishida T, Onoue K, Soeda T, Okayama S, Takeda Y, Watanabe M, Kawata H, Uemura S and Saito Y. Left Ventricular Ejection Fraction (EF) of 55% as Cutoff for Late Transition From Heart Failure (HF) With Preserved EF to HF With Mildly Reduced EF. *Circ J*. 2015;79:2209-15.

94. Buggey J, Alenezi F, Yoon HJ, Phelan M, DeVore AD, Khouri MG, Schulte PJ and Velazquez EJ. Left ventricular global longitudinal strain in patients with heart failure with preserved ejection fraction: outcomes following an acute heart failure hospitalization. *ESC Heart Fail*. 2017;4:432-439.

95. Myhre PL, Vaduganathan M, Claggett BL, Anand IS, Sweitzer NK, Fang JC, O'Meara E, Shah SJ, Desai AS, Lewis EF, Rouleau J, Pitt B, Pfeffer MA and Solomon SD. Association of Natriuretic Peptides With Cardiovascular Prognosis in Heart Failure With Preserved Ejection Fraction: Secondary Analysis of the TOPCAT Randomized Clinical Trial. *JAMA Cardiol*. 2018;3:1000-1005.

96. York MK, Gupta DK, Reynolds CF, Farber-Eger E, Wells QS, Bachmann KN, Xu M, Harrell FE, Jr. and Wang TJ. B-Type Natriuretic Peptide Levels and Mortality in Patients With and Without Heart Failure. *J Am Coll Cardiol*. 2018;71:2079-2088.

97. Stokke TM, Hasselberg NE, Smedsrud MK, Sarvari SI, Haugaa KH, Smiseth OA, Edvardsen T and Remme EW. Geometry as a Confounder When Assessing Ventricular Systolic Function: Comparison Between Ejection Fraction and Strain. *J Am Coll Cardiol*. 2017;70:942-954.
98. MacIver DH, Adeniran I and Zhang H. Left ventricular ejection fraction is determined by both global myocardial strain and wall thickness. *Int J Cardiol Heart Vasc*. 2015;7:113-118.
99. Aurigemma GP, Silver KH, Priest MA and Gaasch WH. Geometric changes allow normal ejection fraction despite depressed myocardial shortening in hypertensive left ventricular hypertrophy. *J Am Coll Cardiol*. 1995;26:195-202.
100. Schillaci G, Verdecchia P, Porcellati C, Cuccurullo O, Cosco C and Perticone F. Continuous relation between left ventricular mass and cardiovascular risk in essential hypertension. *Hypertension*. 2000;35:580-6.
101. Armstrong AC, Gidding S, Gjesdal O, Wu C, Bluemke DA and Lima JA. LV mass assessed by echocardiography and CMR, cardiovascular outcomes, and medical practice. *JACC Cardiovasc Imaging*. 2012;5:837-48.
102. Kuetting DLR, Feisst A, Dabir D, Homsi R, Sprinkart AM, Luetkens J, Schild HH and Thomas DK. Comparison of magnetic resonance feature tracking with CSPAMM HARP for the assessment of global and regional layer specific strain. *Int J Cardiol*. 2017;244:340-346.
103. Maciver DH. The relative impact of circumferential and longitudinal shortening on left ventricular ejection fraction and stroke volume. *Exp Clin Cardiol*. 2012;17:5-11.
104. Erley J, Genovese D, Tapaskar N, Alvi N, Rashedi N, Besser SA, Kawaji K, Goyal N, Kelle S, Lang RM, Mor-Avi V and Patel AR. Echocardiography and cardiovascular magnetic resonance based evaluation of myocardial strain and relationship with late gadolinium enhancement. *J Cardiovasc Magn Reson*. 2019;21:46.
105. Vasan RS, Larson MG, Benjamin EJ, Evans JC and Levy D. Left ventricular dilatation and the risk of congestive heart failure in people without myocardial infarction. *N Engl J Med*. 1997;336:1350-5.
106. Cohn JN, Ferrari R and Sharpe N. Cardiac remodeling--concepts and clinical implications: a consensus paper from an international forum on cardiac remodeling. Behalf of an International Forum on Cardiac Remodeling. *J Am Coll Cardiol*. 2000;35:569-82.

107. Pugliese NR, Fabiani I, La Carrubba S, Conte L, Antonini-Canterin F, Colonna P, Caso P, Benedetto F, Santini V, Carerj S, Romano MF, Citro R, Di Bello V and Italian Society of Cardiovascular E. Classification and Prognostic Evaluation of Left Ventricular Remodeling in Patients With Asymptomatic Heart Failure. *Am J Cardiol*. 2017;119:71-77.
108. Lee TH, Hamilton MA, Stevenson LW, Moriguchi JD, Fonarow GC, Child JS, Laks H and Walden JA. Impact of left ventricular cavity size on survival in advanced heart failure. *Am J Cardiol*. 1993;72:672-6.
109. Yu CM, Bleeker GB, Fung JW, Schalij MJ, Zhang Q, van der Wall EE, Chan YS, Kong SL and Bax JJ. Left ventricular reverse remodeling but not clinical improvement predicts long-term survival after cardiac resynchronization therapy. *Circulation*. 2005;112:1580-6.
110. Zhang Q, Fung JW, Auricchio A, Chan JY, Kum LC, Wu LW and Yu CM. Differential change in left ventricular mass and regional wall thickness after cardiac resynchronization therapy for heart failure. *Eur Heart J*. 2006;27:1423-30.
111. Linde C, Gold MR, Abraham WT, St John Sutton M, Ghio S, Cerkvenik J, Daubert C and Group RErRiSlvdS. Long-term impact of cardiac resynchronization therapy in mild heart failure: 5-year results from the REsynchronization reVErses Remodeling in Systolic left vEntricular dysfunction (REVERSE) study. *Eur Heart J*. 2013;34:2592-9.
112. Januzzi JL, Jr., Prescott MF, Butler J, Felker GM, Maisel AS, McCague K, Camacho A, Pina IL, Rocha RA, Shah AM, Williamson KM, Solomon SD and Investigators P-H. Association of Change in N-Terminal Pro-B-Type Natriuretic Peptide Following Initiation of Sacubitril-Valsartan Treatment With Cardiac Structure and Function in Patients With Heart Failure With Reduced Ejection Fraction. *JAMA*. 2019:1-11.
113. Braga JR, Leong-Poi H, Rac VE, Austin PC, Ross HJ and Lee DS. Trends in the Use of Cardiac Imaging for Patients With Heart Failure in Canada. *JAMA Netw Open*. 2019;2:e198766.
114. American College of Cardiology Foundation Appropriate Use Criteria Task F, American Society of E, American Heart A, American Society of Nuclear C, Heart Failure Society of A, Heart Rhythm S, Society for Cardiovascular A, Interventions, Society of Critical Care M, Society of Cardiovascular Computed T, Society for Cardiovascular Magnetic R, Douglas PS, Garcia MJ, Haines DE, Lai WW, Manning WJ, Patel AR, Picard MH, Polk DM, Ragosta M, Ward RP and Weiner RB. ACCF/ASE/AHA/ASNC/HFSA/HRS/SCAI/SCCM/SCCT/SCMR 2011 Appropriate Use Criteria for Echocardiography. A Report of the American College of Cardiology Foundation

Appropriate Use Criteria Task Force, American Society of Echocardiography, American Heart Association, American Society of Nuclear Cardiology, Heart Failure Society of America, Heart Rhythm Society, Society for Cardiovascular Angiography and Interventions, Society of Critical Care Medicine, Society of Cardiovascular Computed Tomography, and Society for Cardiovascular Magnetic Resonance Endorsed by the American College of Chest Physicians. *J Am Coll Cardiol*. 2011;57:1126-66.

115. Aimo A, Gaggin HK, Barison A, Emdin M and Januzzi JL, Jr. Imaging, Biomarker, and Clinical Predictors of Cardiac Remodeling in Heart Failure With Reduced Ejection Fraction. *JACC Heart Fail*. 2019;7:782-794.

116. Mikami Y, Kolman L, Joncas SX, Stirrat J, Scholl D, Rajchl M, Lydell CP, Weeks SG, Howarth AG and White JA. Accuracy and reproducibility of semi-automated late gadolinium enhancement quantification techniques in patients with hypertrophic cardiomyopathy. *J Cardiovasc Magn Reson*. 2014;16:85.

117. Raman B, Ariga R, Spartera M, Sivalokanathan S, Chan K, Dass S, Petersen SE, Daniels MJ, Francis J, Smillie R, Lewandowski AJ, Ohuma EO, Rodgers C, Kramer CM, Mahmod M, Watkins H and Neubauer S. Progression of myocardial fibrosis in hypertrophic cardiomyopathy: mechanisms and clinical implications. *Eur Heart J Cardiovasc Imaging*. 2019;20:157-167.

118. Ozturk OG, Paydas S, Balal M, Sahin G, Karacor ED, Ariyurek SY and Yaman A. Biological variations of some analytes in renal posttransplant patients: a different way to assess routine parameters. *J Clin Lab Anal*. 2013;27:438-43.

119. Collier P, Watson CJ, Waterhouse DF, Dawkins IR, Patle AK, Horgan S, Conlon CM, O'Hanlon R, Baugh JA, Ledwidge MT and McDonald K. Progression of left atrial volume index in a population at risk for heart failure: a substudy of the STOP-HF (St Vincent's Screening TO Prevent Heart Failure) trial. *Eur J Heart Fail*. 2012;14:957-64.

120. Dunlay SM, Roger VL, Weston SA, Jiang R and Redfield MM. Longitudinal changes in ejection fraction in heart failure patients with preserved and reduced ejection fraction. *Circ Heart Fail*. 2012;5:720-6.

121. Shah AM, Cikes M, Prasad N, Li G, Getchevski S, Claggett B, Rizkala A, Lukashevich I, O'Meara E, Ryan JJ, Shah SJ, Mullens W, Zile MR, Lam CSP, McMurray JJV, Solomon SD and Investigators P-H. Echocardiographic Features of Patients With Heart Failure and Preserved Left Ventricular Ejection Fraction. *J Am Coll Cardiol*. 2019;74:2858-2873.

122. Shah AM, Claggett B, Sweitzer NK, Shah SJ, Anand IS, O'Meara E, Desai AS, Heitner JF, Li G, Fang J, Rouleau J, Zile MR, Markov V, Ryabov V, Reis G, Assmann SF, McKinlay SM, Pitt B, Pfeffer MA and Solomon SD. Cardiac structure and function and prognosis in heart failure with preserved ejection fraction: findings from the echocardiographic study of the Treatment of Preserved Cardiac Function Heart Failure with an Aldosterone Antagonist (TOPCAT) Trial. *Circ Heart Fail*. 2014;7:740-51.

123. Ghimire A, Fine N, Ezekowitz JA, Howlett J, Youngson E and McAlister FA. Frequency, predictors, and prognosis of ejection fraction improvement in heart failure: an echocardiogram-based registry study. *Eur Heart J*. 2019;40:2110-2117.

124. Hu K, Liu D, Nordbeck P, Cikes M, Stork S, Kramer B, Gaudron PD, Schneider A, Knop S, Ertl G, Bijnens B, Weidemann F and Herrmann S. Impact of monitoring longitudinal systolic strain changes during serial echocardiography on outcome in patients with AL amyloidosis. *Int J Cardiovasc Imaging*. 2015;31:1401-12.

125. Felker GM, Anstrom KJ, Adams KF, Ezekowitz JA, Fiuzat M, Houston-Miller N, Januzzi JL, Jr., Mark DB, Pina IL, Passmore G, Whellan DJ, Yang H, Cooper LS, Leifer ES, Desvigne-Nickens P and O'Connor CM. Effect of Natriuretic Peptide-Guided Therapy on Hospitalization or Cardiovascular Mortality in High-Risk Patients With Heart Failure and Reduced Ejection Fraction: A Randomized Clinical Trial. *JAMA*. 2017;318:713-720.

126. Ouwerkerk W, Voors AA and Zwinderman AH. Factors influencing the predictive power of models for predicting mortality and/or heart failure hospitalization in patients with heart failure. *JACC Heart Fail*. 2014;2:429-36.

127. Sartipy U, Dahlstrom U, Edner M and Lund LH. Predicting survival in heart failure: validation of the MAGGIC heart failure risk score in 51,043 patients from the Swedish heart failure registry. *Eur J Heart Fail*. 2014;16:173-9.

128. Belsley DA. *Conditioning diagnostics : collinearity and weak data in regression*. New York: J. Wiley; 1991.

129. Steyerberg EW and Vergouwe Y. Towards better clinical prediction models: seven steps for development and an ABCD for validation. *Eur Heart J*. 2014;35:1925-31.

130. Hosmer DW, Lemeshow S and Sturdivant RX. *Applied logistic regression.* Third edition. ed. Hoboken, New Jersey: Wiley; 2013.

131. Royston P and Altman DG. External validation of a Cox prognostic model: principles and methods. *BMC Med Res Methodol*. 2013;13:33.
132. Grant SW, Hickey GL, Carlson ED and McCollum CN. Comparison of three contemporary risk scores for mortality following elective abdominal aortic aneurysm repair. *Eur J Vasc Endovasc Surg*. 2014;48:38-44.
133. Royston P. Tools for checking calibration of a Cox model in external validation: Approach based on individual event probabilities. *Stata J*. 2014;14:738-755.
134. Puntmann VO, Valbuena S, Hinojar R, Petersen SE, Greenwood JP, Kramer CM, Kwong RY, McCann GP, Berry C, Nagel E and Group SCTW. Society for Cardiovascular Magnetic Resonance (SCMR) expert consensus for CMR imaging endpoints in clinical research: part I - analytical validation and clinical qualification. *J Cardiovasc Magn Reson*. 2018;20:67.
135. Thomas L, Marwick TH, Popescu BA, Donal E and Badano LP. Left Atrial Structure and Function, and Left Ventricular Diastolic Dysfunction: JACC State-of-the-Art Review. *J Am Coll Cardiol*. 2019;73:1961-1977.
136. Yoshida C, Nakao S, Goda A, Naito Y, Matsumoto M, Otsuka M, Shimoshikiryo M, Eguchi A, Lee-Kawabata M, Tsujino T and Masuyama T. Value of assessment of left atrial volume and diameter in patients with heart failure but with normal left ventricular ejection fraction and mitral flow velocity pattern. *Eur J Echocardiogr*. 2009;10:278-81.
137. Rossi A, Cicoira M, Bonapace S, Golia G, Zanolla L, Franceschini L and Vassanelli C. Left atrial volume provides independent and incremental information compared with exercise tolerance parameters in patients with heart failure and left ventricular systolic dysfunction. *Heart*. 2007;93:1420-5.
138. Thompson RB, Chow K, Pagano JJ, Sekowski V, Michelakis ED, Tymchak W, Haykowsky MJ, Ezekowitz JA, Oudit GY, Dyck JRB, Kaul P, Savu A and Paterson DI. Quantification of lung water in heart failure using cardiovascular magnetic resonance imaging. *J Cardiovasc Magn Reson*. 2019;21:58.
139. Schelbert EB and Messroghli DR. State of the Art: Clinical Applications of Cardiac T1 Mapping. *Radiology*. 2016;278:658-76.
140. Grapsa J. Left Ventricular Ejection Fraction and Global Longitudinal Strain: Prognostic When Not Load Dependent? *J Am Coll Cardiol*. 2018;72:1065-1066.

141. Stromp TA, Leung SW, Jing LY, Fornwalt BK, Sorrell VL and Vandsburger MH. Clinical Gadolinium-Free Magnetic Resonance Imaging With Magnetization Transfer Contrast Detects Cardiac Fibrosis With High Sensitivity and Specificity Compared to Late Gadolinium Enhanced Imaging. *Circulation*. 2014;130.
142. Stromp TA, Spear TJ, Kidney RM, Andres KN, Kaine JC, Charnigo RJ, Leung SW, Sorrell VL and Vandsburger MH. Differentiating Cardiac Fibrosis From Hypertrophy in Chronic Kidney Disease Hemodialysis Patients Using Gadolinium-Free Imaging and Biomarkers of Extracellular Matrix Turnover. *Circulation*. 2016;134.